

INFORMATION TO USERS

This manuscript has been reproduced from the microfilm master. UMI films the text directly from the original or copy submitted. Thus, some thesis and dissertation copies are in typewriter face, while others may be from any type of computer printer.

The quality of this reproduction is dependent upon the quality of the copy submitted. Broken or indistinct print, colored or poor quality illustrations and photographs, print bleedthrough, substandard margins, and improper alignment can adversely affect reproduction.

In the unlikely event that the author did not send UMI a complete manuscript and there are missing pages, these will be noted. Also, if unauthorized copyright material had to be removed, a note will indicate the deletion.

Oversize materials (e.g., maps, drawings, charts) are reproduced by sectioning the original, beginning at the upper left-hand corner and continuing from left to right in equal sections with small overlaps.

Photographs included in the original manuscript have been reproduced xerographically in this copy. Higher quality 6" x 9" black and white photographic prints are available for any photographs or illustrations appearing in this copy for an additional charge. Contact UMI directly to order.

**ProQuest Information and Learning
300 North Zeeb Road, Ann Arbor, MI 48106-1346 USA
800-521-0600**

UMI[®]





Universit  d'Ottawa • University of Ottawa

Ms. Sc. Thesis, Pharmacology

**The Role of Different Scinderin Domains
In
The Control of Actin Filament Dynamics
And
Regulated Exocytosis**

Teodora Pene Dumitrescu

Department of Cellular and Molecular Medicine

University of Ottawa

Ottawa, Ontario, Canada

Year 2001



**National Library
of Canada**

**Acquisitions and
Bibliographic Services**

**395 Wellington Street
Ottawa ON K1A 0N4
Canada**

**Bibliothèque nationale
du Canada**

**Acquisitions et
services bibliographiques**

**395, rue Wellington
Ottawa ON K1A 0N4
Canada**

Your file Votre référence

Our file Notre référence

The author has granted a non-exclusive licence allowing the National Library of Canada to reproduce, loan, distribute or sell copies of this thesis in microform, paper or electronic formats.

The author retains ownership of the copyright in this thesis. Neither the thesis nor substantial extracts from it may be printed or otherwise reproduced without the author's permission.

L'auteur a accordé une licence non exclusive permettant à la Bibliothèque nationale du Canada de reproduire, prêter, distribuer ou vendre des copies de cette thèse sous la forme de microfiche/film, de reproduction sur papier ou sur format électronique.

L'auteur conserve la propriété du droit d'auteur qui protège cette thèse. Ni la thèse ni des extraits substantiels de celle-ci ne doivent être imprimés ou autrement reproduits sans son autorisation.

0-612-66100-8

Canada

Abstract

In chromaffin cells, cortical F-actin disassembly in response to stimulation allows the movement of secretory vesicles towards exocytotic sites. Scinderin (Sc), a Ca^{2+} -dependent F-actin severing protein, controls F-actin dynamics. The Sc gene has previously been cloned in our laboratory. Sc has six domains with three actin-binding sites in domains 1, 2 and 5, two PIP₂ in domains 1 and 2 and two Ca^{2+} -binding sites. In order to obtain additional data on the role of Sc domains in secretion, we performed experiments with a human growth hormone reporter gene (hGH) system for regulated exocytosis, and different GFP-fusion Sc constructs: Sc1-6, Sc1-2 (the first two domains of Sc), Sc5 (5th domain of Sc), ScL5 (5th domain lacking the third actin binding site of Sc), and ScABS3. Cortical F-actin distribution evaluated by rhodamine-phalloidine staining, in resting and stimulated cells (56 mM K⁺), showed that cells overexpressing Sc1-6 or Sc1-2 had an increased F-actin disassembly upon stimulation, whereas cells overexpressing Sc5 or ScABS3 had a decreased F-actin disassembly. No significant difference in F-actin assembly / disassembly was obtained for cells overexpressing ScL5. Increased hGH release in response to stimulus was found for cells overexpressing Sc1-6 or Sc1-2 when compared to cells transfected with vector alone. Cells overexpressing Sc5 or ScABS3 showed decreased hGH release in response to stimulus. These results suggest that during secretion the N-terminal half of the protein involved in F-actin severing and the C-terminal domains of Sc are responsible for actin polymerization. Thus, it appears that Sc functions as a molecular switch in the control of actin dynamics during secretion.

Acknowledgements

First and foremost, I would especially like to thank Dr. José Mariá Trifaró for accepting me in his laboratory, as well as for supervising and supporting me throughout the course of my graduate studies.

I extend my appreciation to the members of my advisory committee, namely Dr. Stephen Gee and Dr. Paul Albert for their direction and advice.

I am grateful to Dr. Sergio Rosé for his humor and guidance, and for never saying “I am busy now” when I needed his advice.

Special thanks go to Dr. Tatiana Lejen for her advice and support, and for the preparation of chromaffin cell cultures.

I would also like to acknowledge the substantial financial support of the Medical Research Council of Canada.

Abbreviations

- ADP = adenosine diphosphate
- ATP = adenosine triphosphate
- BSA = bovine serum albumin
- cDNA = complementary deoxyribonucleic acid
- DIC = differential interference contrast
- DMEM = Dubelcco's modified Eagle's medium
- DNase = deoxyribonuclease
- EBSS = Eagle's balance salt solution
- ECL = enhanced chemiluminescence
- EDTA = ethylenediaminetetraacetic acid
- EGFP = enhanced green fluorescent protein
- F-actin = filamentous actin
- FITC = fluoresceine iso-thiocyanate
- GFP = green fluorescent protein
- HEPES = N-[2-hydroxyethyl] piperazine-N'-[2-ethanesulfonic acid]
- hGH = human growth hormone
- HRP = horse radish peroxidase
- IgG = immunoglobulin G
- Kb = kilobase pairs
- KDa = kilodaltons
- MCS = multiple cloning site
- mRNA = messenger ribonucleic acid

NA = noradrenaline

PBS = phosphate buffer saline

PCR = polymerase chain reaction

PI = phosphatidyl inositol

PIP2 = phosphatidylinositol 3,4,5-triphosphate

PKC = protein kinase C

RT = room temperature

Sc = scinderin

SDS = sodium dodecyl sulphate

SDS-PAGE = sodium dodecyl sulphate-polyacrylamide gel electrophoresis

TCA = trichloroacetic acid

TEMED = tetramethylene diamine

Table of contents

<u>Abstract</u>	ii
<u>Acknowledgements</u>	iii
<u>Abbreviations</u>	iv
<u>Table of contents</u>	vi
<u>List of figures</u>	xii
<u>List of tables</u>	xvii
<u>1 - Introduction</u>	1
<u>1.1. Adrenal medulla and adrenal chromaffin cells</u>	2
<u>1.2. Cultured chromaffin cells as a model for neurosecretory studies</u>	5
<u>1.3. Chromaffin cell cytoskeleton and exocytosis</u>	9
<u>1.3.1. General Organization of the Cytoskeleton: Actin Microfilaments and Actin — Binding Proteins</u>	9
<u>1.3.2. Chromaffin cell exocytosis and cytoskeleton dynamics during neurotransmitter release</u>	19
<u>1.4. Scinderin characteristics and role in chromaffin cell secretion</u>	26
<u>1.5. Statement of the problem</u>	35
<u>2 – Materials and Methods</u>	37
<u>Materials</u>	38
<u>Methods</u>	39
<u>2.1 Chromaffin cell culture</u>	39
<u>2.1.a Isolation of cells</u>	39
<u>2.1.b. Differential plating of chromaffin cells</u>	40

<u>2.2. Preparation of pEGFP vectors containing full-length Scinderin (Sc) or various Sc deletion constructs</u>	41
<u>2.2.a. Preparation of full-length Scinderin (Sc1-6)</u>	41
<u>2.2.b. Cloning of full-length Scinderin Sc1-6 into pEGFPC3 vector</u>	42
<u>2.2.c. Preparation of various deletion constructs of Sc and cloning into pEGFP-C3 vector</u>	43
<u>2.3. Transient transfection of chromaffin cells</u>	48
<u>2.3.a. Chromaffin cell transient transfection using a liposome-mediated gene transfer system (Lipofectin)</u>	48
<u>2.3.b. Chromaffin cell transient transfection using a non-liposomal lipid-mediated gene transfer system (Effectene method)</u>	50
<u>2.3.c. Chromaffin cell transient transfection using the calcium phosphate method</u>	53
<u>2.3.d. Chromaffin cell transient transfection by electroporation</u>	56
<u>2.4. Determination of chromaffin cell viability following electroporation</u>	58
<u>2.4.a. Determination of chromaffin cell number by counting cells.</u>	58
<u>2.4.b. Determination of chromaffin cell number by measuring total DNA content</u>	60
<u>2.5. Measurement of chromaffin cell transient transfection efficiency</u>	60
<u>2.6. Improvement of hGH labeling of chromaffin cell vesicles using an extensive high K⁺ (56 mM) - induced depolarization</u>	63
<u>2.7. Characterization of chromaffin cells expressing hGH and GFP-fused Sc deletion constructs</u>	63

<u>2.7.a. Determination of protein expression by electrophoresis, immunoblotting and densitometric analysis</u>	63
<u>2.7.b. Analysis of hGH localization in chromaffin vesicles by immunocytochemistry and fluorescence microscopy</u>	64
<u>2.8. Analysis of cortical F-actin distribution in resting and stimulated chromaffin cells</u>	66
<u>2.8.a. Fluorescence microscopy</u>	66
<u>2.8.b. Video-enhanced image processing</u>	66
<u>2.9. Analysis of the effects of Sc1-6 or Sc deletion constructs overexpression on high K⁺- or nicotine- evoked chromaffin cell exocytosis</u>	67
<u>2.10. Statistical analysis</u>	70
<u>3 – results</u>	71
<u>Characterization of the co-transfection gene system</u>	72
<u>3.1. Transient transfection of chromaffin cells</u>	72
<u>3.1.a. Chromaffin cell transient transfection using lipofectin</u>	74
<u>3.1.b. Chromaffin cell transient transfection using effectene</u>	74
<u>3.1.c. Chromaffin cell transient transfection using calcium phosphate</u>	74
<u>3.1.d. Chromaffin cell transient transfection by electroporation</u>	77
<u>3.2. Localization of hGH in chromaffin vesicles</u>	80
<u>3.2.a. hGH localization in chromaffin cells by immunocytochemistry</u>	80
<u>3.2.b. Transiently expressed hGH undergoes secretion from chromaffin cells in response to cell depolarization</u>	82
<u>3.3. Improvement of hGH expression in chromaffin cells</u>	84

<u>3.3.a. Improvement of chromaffin vesicle labeling with hGH</u>	84
<u>3.3.b. hGH release from resting and stimulated chromaffin cells.</u>	86
<u>3.4. Co-transfection of Sc fragments and hGH gene into chromaffin cells and</u> <u>characterization of the double – labeled system</u>	86
<u>3.4.a. Chromaffin cell survival following co – transfection by electroporation</u>	89
<u>3.4.b. Co-expression of Sc fragments and hGH in chromaffin cells</u>	89
<u>3.4.c. Co-transfection efficiency in chromaffin cells.</u>	91
<u>3.4.d. Cortical F-actin network and intracellular localization of GFP-fused Sc</u> <u>constructs using immunofluorescence microscopy</u>	95
<u>Effects of Sc or Sc deletion mutant overexpression on stimulation-induced cortical</u> <u>F-actin disassembly and chromaffin cell exocytosis</u>	97
<u>3.5. Stimulation induced changes in the organization of cortical F-actin</u> <u>cytoskeleton in chromaffin cells overexpressing Sc deletion mutants</u>	97
<u>3.5.a. High potassium-evoked F-actin disassembly</u>	97
<u>3.5.b. Nicotine-induced F-actin disassembly</u>	110
<u>3.6. Stimulation-induced exocytosis in chromaffin cells overexpressing Sc</u> <u>deletion constructs</u>	110
<u>3.6.a. High-potassium evoked chromaffin cell exocytosis</u>	111
<u>3.6.b. Nicotine-induced chromaffin cell exocytosis</u>	117
<u>4 - Discussion</u>	121
<u>4.1. Investigation by transient transfection of the effects of Scinderin or various</u> <u>Scinderin deletion constructs on regulated exocytosis</u>	122
<u>4.1.a. Selection of the transient transfection method for chromaffin cells</u>	124

<u>4.1.b. Human Growth hormone is targeted to the regulated secretory pathway in chromaffin cells</u>	128
<u>4.1.c. Extensive high K⁺ depolarization results in an improvement of chromaffin vesicle labeling with hGH and of hGH signal in release experiments</u>	129
<u>4.1.d. Co-expression in chromaffin cells of pXGH5 and pEGFP carrying Sc construct creates a double – labeled system suitable for the study of the effects of this protein on regulated secretion</u>	131
<u>4.2. Scinderin sequence analysis and three dimensional structure prediction by homology modeling using gelsolin as a template for model building.</u>	134
<u>4.2.a. Molecular structure and active sites of Scinderin</u>	134
<u>4.2.b. Actin binding sites of Scinderin</u>	138
<u>4.2.c. PIP2- binding sites of Scinderin</u>	146
<u>4.3. Role of Scinderin in the control of F-actin disassembly and chromaffin cell exocytosis</u>	147
<u>4.3.a. Effect of full Scinderin (Sc1-6) or of Sc1-2 deletion construct overexpression on high K⁺- or nicotine – induced hGH release from chromaffin cells</u>	148
<u>4.3.b. Effect of Sc56, Sc5, ScL5 or ScABS3 deletion constructs overexpression on high K⁺- or nicotine – induced hGH release from chromaffin cells</u>	150
<u>5 – Summary of contributions to original knowledge</u>	154
<u>6 - References</u>	157

List of figures

<u>Figure 1.1: Spontaneous actin polymerization</u>	13
<u>Figure 1.2: The different roles of actin-binding proteins</u>	15
<u>Figure 1.3: Eight members of the gelsolin family of proteins (mammals only) are modeled</u>	18
<u>Figure 1.4: Electron micrographs of microfilament networks in resting chromaffin cells</u>	22
<u>Figure 1.5: Electron micrographs of microfilament networks of chromaffin cells after nicotinic receptor stimulation</u>	23
<u>Figure 1.6: Schematic representation of scinderin domains</u>	27
<u>Figure 1.7: Regulation of gelsolin and/or scinderin activities by ions and polyphosphoinositides</u>	29
<u>Figure 1.8: Integrated mechanism of actin assembly and disassembly by cell intracellular pH and free Ca²⁺</u>	31
<u>Figure 2.1: Schematic representation of the pEGFP-C3 vector</u>	44
<u>Figure 2.2: Schematic representation of Sc domains and various Sc deletion constructs obtained by PCR</u>	45
<u>Figure 2.3: Schematic representation of the synthesis of the third Sc actin binding site construct (ScABS3)</u>	47
<u>Figure 2.4: Sequence and localization on Sc gene of the primers used for segmental sequencing of Sc cDNA</u>	49
<u>Figure 2.5: Flowchart of lipofectin-mediated transfection</u>	51
<u>Figure 2.6: Flowchart of effectene-mediated transfection</u>	55

<i>Figure 2.7: Electroporation principle</i>	57
<i>Figure 2.8: Flowchart of transfection by electroporation</i>	59
<i>Figure 2.9: β-Gal vector map and the multiple cloning site (MCS)</i>	62
<i>Figure 2.10: Scheme of the hGH reporter system used to study regulated secretion</i>	68
<i>Figure 3.1: pXGH5 vector map</i>	73
<i>Figure 3.2: Lipofectin mediated transfection</i>	75
<i>Figure 3.3: Effectene mediated transfection</i>	76
<i>Figure 3.4: Calcium phosphate – mediated transfection</i>	78
<i>Figure 3.5: Transfection using electroporation</i>	79
<i>Figure 3.6: Immunohistochemical localization of DBH and hGH</i>	81
<i>Figure 3.7: Transiently expressed hGH undergoes secretion from chromaffin cells in response to cell depolarization</i>	83
<i>Figure 3.8: Effects of extensive depolarization of transfected chromaffin cells on the distribution pattern of hGH and DBH staining</i>	85
<i>Figure 3.9: Efficiency of hGH labeling of chromaffin vesicles</i>	87
<i>Figure 3.10: High K^+-stimulated hGH release from control (non-depolarized) and previously depolarized chromaffin cells</i>	88
<i>Figure 3.11: Comparison of cell survival in cultures transfected with various Sc deletion constructs</i>	90
<i>Figure 3.12: Localization of Scinderin deletion constructs and hGH in chromaffin cells</i>	92
<i>Figure 3.13: Intracellular localization of hGH and Scinderin deletion constructs in chromaffin cells</i>	93

<u>Figure 3.14: Co-transfection efficiency for cells transfected with pXGH5 and pEGFP-C3, alone or containing a Sc construct.</u>	94
<u>Figure 3.15: Cortical F-actin network and intracellular localization of GFP-fused Sc constructs.</u>	96
<u>Figure 3.16: Cortical F-actin distribution in resting and High K⁺ stimulated chromaffin cells transfected with pEGFP vector.</u>	99
<u>Figure 3.17: Cortical F-actin distribution in resting and High K⁺ stimulated chromaffin cells transfected with pEGFPSc1-6.</u>	100
<u>Figure 3.18: Cortical F-actin distribution in resting and High K⁺ stimulated chromaffin cells transfected with pEGFPSc1-2.</u>	101
<u>Figure 3.21: Cortical F-actin distribution in resting and High K⁺ stimulated chromaffin cells transfected with pEGFPScL5.</u>	104
<u>Figure 3.22: Cortical F-actin distribution in resting and High K⁺ stimulated chromaffin cells transfected with pEGFPScABS3.</u>	105
<u>Figure 3.23: Cortical F-actin distribution in resting and nicotine stimulated chromaffin cells transfected with pEGFP vector.</u>	107
<u>Figure 3.24: Cortical F-actin distribution in resting and nicotine stimulated chromaffin cells transfected with pEGFPSc1-6.</u>	108
<u>Figure 3.25: Cortical F-actin distribution in resting and nicotine stimulated chromaffin cells transfected with pEGFPSc5-6.</u>	109
<u>Figure 3.26: The effect of Sc1-6 overexpression on high K⁺- evoked chromaffin cell exocytosis.</u>	112
<u>Figure 3.27: The effect of Sc1-2 overexpression on high K⁺- evoked chromaffin cell</u>	

<u>exocytosis</u>	113
<u>Figure 3.28: The effect of Sc5-6 overexpression on high K⁺- evoked chromaffin cell</u>	
<u>exocytosis</u>	114
<u>Figure 3.29: The effect of Sc5 overexpression on high K⁺- evoked chromaffin cell</u>	
<u>exocytosis</u>	115
<u>Figure 3.30: The effect of ScL5 overexpression on high K⁺- evoked chromaffin cell</u>	
<u>exocytosis</u>	116
<u>Figure 3.31: The effect of ScABS3 overexpression on high K⁺- evoked chromaffin cell</u>	
<u>exocytosis</u>	118
<u>Figure 3.32: The effect of Sc1-6 overexpression on nicotine - evoked chromaffin cell</u>	
<u>exocytosis</u>	119
<u>Figure 3.33: The effect of Sc5-6 overexpression on nicotine - evoked chromaffin cell</u>	
<u>exocytosis</u>	120
<u>Figure 4.1. Sequence alignment and domain organization of human plasma gelsolin and bovine scinderin</u>	
	137
<u>Figure 4.2. Comparison of amino acid sequences of two Sc regions with corresponding sequences of known actin-binding domains of gelsolin and villin</u>	
	139
<u>Figure 4.3. Three-dimensional structure and domain arrangement of calcium free gelsolin</u>	
	144

List of tables

Table 1. Optimization of transfection using lipofectin. 52

Table 2. Optimization of transfection efficiency using the effectene reagent. 54

1 - INTRODUCTION

1.1. Adrenal medulla and adrenal chromaffin cells

The adrenal medulla is the core of the adrenal glands (Nagel, 1886). These ductless endocrine glands form part of the sympathetic nervous system, which is one of the two branches of the autonomic nervous system.

The autonomic nervous system is the portion of the nervous system that controls the visceral functions of the body; it is activated mainly by centers located in the spinal cord, brain stem and hypothalamus. The autonomic system transmits signals to the body through its two major subdivisions: the sympathetic and parasympathetic systems.

The sympathetic nerves originate in the spinal cord between the segments T1 and L2 and extend from there to the sympathetic paravertebral chains (containing 22 pairs of ganglia), and then to the organs that are innervated by the sympathetic nerves (DeQuatro, 1979; Guyton, 1987; Keese et al., 1988). Each sympathetic pathway is comprised of two fibers: a preganglionic and a postganglionic neuron. The sympathetic fibers originating in various parts of the spinal cord connect to various organs in the body. Some of the preganglionic sympathetic nerve fibers extend from the intermediolateral horn cells of the spinal cord, through the sympathetic chains, through the splanchnic nerves into the adrenal medullae (in adrenal glands), to special cells that secrete epinephrine / adrenaline, norepinephrine / noradrenaline (catecholamines) and dopamine directly into the blood (Fujita, 1977; Guyton, 1987; Landsberg and Young, 1980). These secretory cells derive embryologically from nervous tissue (from neural crest), and are analogous to postganglionic neurons (Fujita, 1977; Kobayashi and Coupland, 1977; Pearse, 1969:). They also have rudimentary nerve fibers, and it is these fibers that secrete hormones (Prentice and Wood, 1975).

The adrenal glands are paired structures localized anterior or medial to each kidney (In Latin, *adrenal* means *adjacent to the kidney*.) In humans, they might best be referred to as suprarenal glands, because they lie on the top of the kidneys at the level of the 11-th or 12-th vertebra (embedded in adipose tissue and encapsulated by the renal fascia) (DeQuatro, 1979). The medulla (from Latin, meaning *marrow*) is the central part of the gland, and it is surrounded by an adrenal cortex. Its proper anatomical name is glandula suprarenalis medulla (DeQuatro, 1979; Guyton, 1987). As an endocrine gland, the adrenal medulla affects other organs by discharging hormones into the blood. The medulla is also part of the sympathetic nervous system, and its main adrenal hormone, adrenaline, is closely related to noradrenaline, the primary sympathetic neurotransmitter (Benchimol and Cantin, 1977; DeQuatro, 1979; Landsberg, 1980). Furthermore, the adrenal medulla itself secretes noradrenaline, some dopamine and several neuropeptides (Hillarp, 1953; Landsberg, 1980; Unsicker, 1976)

Together, the two human glands weigh about 1 g. The central part of each medulla consists mainly of chromaffin cells (historically, these have been characterized as reacting and producing a color with dichromate salts – (Kohn, 1902), with the coloured tissue resembling an irregularly shaped polyhedron. These cells are surrounded by nerves, connective tissue and blood vessels. Inside the chromaffin cells, the catecholamines are stored in numerous chromaffin vesicles (100-300 nm diameter), which are electron-dense structures resembling the dense core vesicles of sympathetic nerve endings (Blaschko, and Welsch, 1953; Hillarp, and Hofelt, 1953). The cells contain one or the other of the catecholamines in their vesicle stores. There are three main types of chromaffin cells. These are characterized as containing noradrenaline (NA -

representing 15% of the cells), adrenaline (A – representing 85% of the cells) and dopamine (about 1% of the cells) (Benchimol and Cantin, 1977; Hillarp and Hofcfey, 1953; Landsberg, 1980).

The adrenal glands are well served by arteries. The superior adrenal arteries are derived from the inferior phrenic artery, the middle artery comes from the aorta above the origin of the renal artery, and the inferior adrenal artery arises from the renal artery. Their main venous drainage is via the adrenal vein, arising from the central vein within the gland (DeQuatro, 1979; Yeasting, 1986).

The chromaffin cells of the adrenal medulla are arranged in groups, separated by connective tissue, around blood vessels (Carmichael, 1979). Isolated cells are spherical, with a diameter of 10-20 μm and a nucleus of 5 μm . In 1955 Lever was the first to study the adrenal medulla at the electron microscope level. He demonstrated the presence of electron-dense membrane-bound vesicles as a characteristic feature of these cells. The chromaffin vesicles (often called “chromaffin granules”, a term indicating their appearance in the light microscope) were the first secretory organelle to be isolated (Blaschko and Welsch, 1953; Hillarp, 1953). The discovery of these vesicles was the first indication of the mode of storage employed in endocrine systems, a mode now known to be common to most secretory cells. There are between 17,000 and 30,000 vesicles per cell (Nordmann, 1984; Vitale et al, 1995). Eranko (1955) firstly distinguished adrenaline - containing vesicles from the noradrenaline (denser) containing vesicles. In most mammals, A-containing cells comprise 80-90% of the chromaffin cell population, with large species variations (Benchimol and Cantin, 1977).

As mentioned above, biochemical data, together with morphological observations, have

demonstrated the presence of three types of secretory vesicles, subsequently three types of chromaffin cells: A containing cells, NA-containing cells and small granule chromaffin cells (SGC) (Hillarp and Høcfelt, 1953; Unsicker, 1976). The first two types are represented by the large dense-core vesicles (750-1,000 Å), related to the LDCV of the sympathetic neurons, while SGC is comprised of the small dense-core vesicles (400-500 Å), also found in sympathetic nerves (Trifaró et al., 1992). Electron-translucent vesicles have been described in chromaffin cells (Navone et al., 1989) but their function is not clear yet. At the electron microscopy level, SGC (which contain dopamine) look as though they could contain both A and NA (Coupland, 1989)

1.2. Cultured chromaffin cells as a model for neurosecretory studies

A major breakthrough in understanding the neuronal function, endocrine mechanisms and stimulus-secretion coupling of secretory cells was the development of techniques to isolate and culture adrenal chromaffin cells. Once isolated, these cells provide a relatively homogenous population for the study of secretion by morphological, biochemical and electrophysiological methods (Douglas et al., 1967; Trifaró, 1977). Adrenal chromaffin cells store their secretory products in membrane-bound organelles. Upon stimulation by acetylcholine, a cascade of events is triggered in the cell, leading to the secretion of catecholamines and other vesicle components by exocytosis.

Many important aspects of these mechanisms are still poorly understood. Isolation and maintenance of chromaffin cells in culture for long periods of time have provided a better opportunity to study the mechanisms of membrane fusion during exocytosis, site of action of cellular Ca^{2+} , origin and fate of secretory vesicles, turnover of membrane and receptor proteins. (Douglas, 1975; Trifaró and Lee, 1980). For the neuroscientist,

chromaffin cells also have the advantage of sharing their primordial origin with sympathetic neurons. Moreover, they have some common properties with neurons (voltage-dependent Na⁺ and Ca²⁺ channels, neuronal specific proteins, both chromaffin cells and sympathetic neurons synthesize, store and release catecholamines in response to cholinergic stimulation) as well as with the endocrine cells (Fujita, 1977; Kobayashi, and Coupland, 1977). Another advantage of chromaffin cells is their availability in relatively pure form after isolation from the adrenal gland, unlike the sympathetic neurons, which are difficult to isolate and study, because they are scattered through the whole organism. In other words, adrenal chromaffin cells represent a great practical laboratory model for the study of neurons.

Different research groups have described methods for isolating and culturing chromaffin cells of various origins (Douglas et al., 1967; Hochman, and Perlman, 1976; Brooks, 1977; Trifaró et al., 1978, 1980). There are significant species-related differences in chromaffin cells, but most of the work on this type of cell has been based on bovine-derived cultures. This is the best-studied system and most of the literature deals with data derived from it. In our laboratory, we also use a bovine-derived, primary chromaffin cell type of culture developed by Trifaró and Lee (1980). Chromaffin cells change functionally over time in culture. They begin to develop processes (neurite-like in nature) after several days, so they are best used the first days after they are cultured. The lengths of these processes are linearly related to the age of the culture; the axon-like processes display varicosities containing catecholamines (Trifaró and Lee, 1980). Another morphological feature of bovine chromaffin cell culture is the presence of body-body or process-body cell contacts (Trifaró and Lee, 1980). The relevance of this phenomenon to

the formation of new synapses, for instance, remains to be elucidated.

A large number of technical approaches have enabled researchers to examine the mechanisms of exocytosis in chromaffin cells in culture. These include:

- i) single cell membrane capacitance measurements with the patch-clamp method to determine the extent of vesicle-plasma membrane fusion in exocytosis (Neher and Marty, 1982) and / or Ca^{2+} transients measurements (Penner et al., 1988), as well as single cell video imaging of topographical dynamics of Ca^{2+} signal.
- ii) single cell staining with antisera against certain secretory vesicle components appearing at the surface of the cell after exocytosis and membrane fusion (Cheek et al., 1989; Vitale et al., 1991)
- iii) single cell voltametric measurement of catecholamine release from a single chromaffin granule (Leszczyszyn et al., 1990)
- iv) simultaneous, independent measurement of endocytosis (capacitance minus fluorescence) and exocytosis (fluorescence) (Smith and Jonson, 1996).
- v) biochemical and immunocytochemical methods after cell permeabilization (with digitonin, saponin, etc.) and direct manipulation of intracellular factors involved in exocytosis. Permeabilized chromaffin cells have proven to be an excellent model for studying the role of these factors (Knight and Baker, 1982). Digitonin produces membrane holes that are small enough to impede the exit of large molecules while permitting the slow entry or exit of proteins. Electron microscopy has shown that digitonin-permeabilized chromaffin cells release catecholamine by exocytosis, but intact granules are not released, and the morphology of the cells is not changed by permeabilization (Schafer et al., 1987; Ito et al., 1991). In other words, digitonin

permeabilization of the membrane preserves the secretory process (Dunn and Holz, 1983; Wilson and Kirshner, 1983). Following digitonin treatment, soluble, cytosolic proteins and other components are lost at a relative slow rate, the responsiveness to Ca^{2+} challenge decreases with time and the secretory process is slowed down (Ito et al., 1991). Upon addition of the necessary leaked proteins, the exocytosis can be reinstated (Dunn and Holz, 1983). Thus, the constituents vital for exocytosis can be identified and studied.

vi) transient transfection method to measure the effects of specific proteins on regulated exocytosis (Holz et al. 1993). This technique consists of the co-transfection in chromaffin cells of two plasmids, one for human growth hormone (hGH) and one for the protein that is studied for the effects on secretion. It has been shown that transiently expressed growth hormone undergoes Ca^{2+} dependent secretion similarly to endogenous catecholamine (Holz et al. 1993). The ability to cotransfect with two plasmids of the same cell, allows the labeling of vesicles with GH and permits the investigation of the effect on the secretory pathway of the second exogenous protein expressed in the same cell.

The spontaneous release of catecholamines from cultured chromaffin cells is much lower than that of freshly isolated chromaffin cells, possibly due to the experimental conditions during isolation of the cells i.e.: collagenase treatment, Ca^{2+} -free and Mg^{2+} -free media (Trifaró and Lee, 1980). The response to acetylcholine or depolarizing concentration of K^{+} (56 mM) seems to be enhanced in cultured cells compared to freshly isolated cells (Trifaró and Lee, 1980). The cholinergic receptor of bovine cultured chromaffin cells appears to be nicotinic, since catecholamine release is stimulated by nicotine and carbamylcholine but not by pilocarpine (Trifaró and Lee, 1980)

In conclusion, adult bovine chromaffin cells in culture display many of the morphological

and functional characteristics of sympathetic neurons, and constitute an excellent model for studying their secretion.

1.3. Chromaffin cell cytoskeleton and exocytosis

1.3.1. General Organization of the Cytoskeleton: Actin Microfilaments and Actin — Binding Proteins.

The eukaryotic cytoskeleton is a dynamic filamentous network of microfilaments (thin filaments consisting mainly of actin), microtubules (hollow, noncontractile structures assembled from tubulin dimers) and intermediate filaments (built of different peptide polymers) involved in the control of cell shape, motility, intracellular organization and cell division (Darnell et al., 1990). Traditionally, the cytoskeleton was mainly viewed as a supporting web. However, recent findings have shown that this mechanical support and its force-carrying connections which can reach all the way from the membrane to the nucleus, can affect signal transduction, the way some proteins bind to the DNA and even affect the fate of malignant cells (Glanz J., 1997). Its cytocontractile and cytoskeletal elements also play an important role in certain pathological processes such as fibromatosis, liver cirrhosis (and other fibrotic lesions), formation of hypertrophic scars, retinitis pigmentosa, Alzheimer's disease, various muscular dystrophies as well as tumor invasion and metastasis (Rungger-Brandle and Gabbiani, 1983).

It is known that the movement of cells and sub-cellular organelles is regulated by dynamic cytoskeletal proteins such as tubulin, actin, myosin, etc. Proteins responsible for such dynamic changes reside in cells in monomeric states (soluble form) and are capable of polymerization into insoluble or gel form. This sol-gel transformation of linear polymers represents the formation of a giant coherent molecule from dispersed subunits.

Such dynamic changes, resulting in polymerization (with consequences in motility), are tightly regulated by a number of proteins (gelsolin, scinderin, villin, alpha-actinin, etc.) and transduction pathways. One of the most important components of the cytoskeleton is actin in the form of microfilaments (5-7 nm diameter), which are present in all eukaryotic cells (Burgoyne and Cheek, 1987). Bundles of micro-filaments (stress fibers) exert an important structural role by anchoring the cytoplasmic matrix to the substrate, are responsible for the gel-like consistency of the marginal cytoplasm and are characteristic for compartments that display active motility and movement (Rungger-Brandle and Gabbiani, 1983).

ACTIN (MW= 43,000) is the most abundant protein in typical eukaryotic cells (Darnell et al., 1990). In the cytoplasm most of the actin is in the form of a randomly cross-linked network of filaments. These remarkably stable polymers (the concentration of actin in the cytoplasm favors full polymerization) can behave as either gels or liquids, depending on filament length and degree of cross-linking. Rapid interconversions of the polymeric states of actin change the viscoelastic properties of the network; these changes are the structural fundamentals of cell shape, motility and intracellular organelle movement (Burgoyne and Cheek, 1987). The actins in nonmuscle cells are the products of different genes, and therefore differ slightly in some of their properties (Darnell et al., 1990). At least six different actins have been identified in eukaryotes, however many multicellular organisms contain multiple actin genes (maybe not all of them expressed). Moreover, actins are posttranslationally modified by acetylation of the N-terminus and methylation of a histidine, thus, leading to multiple functional species in excess of the actual number of genes (Darnell et al., 1990). Microfilaments, also called F-actin, are polymers of the

globular (G-actin) subunit. Viewed in the electron microscope, they appear as double stranded helices. In the filament, the actin subunit has a certain polarity.

Many signal-transduction mechanisms (e.g. calcium transients, pH changes, protein phosphorylation reactions, phospholipid turnover, GTP-binding proteins, etc.) are proposed to mediate actin assembly, actin disassembly and cell movement (Stossel, review, 1993). The first step in the assembly of actin filaments from subunits is nucleation, a step in which two or three monomers aggregate (a highly unfavourable reaction). The two ends of the microfilament have been referred to as the “pointed” (-end) and the “barbed” (+ end) (Huxley, 1963), as determined by the presence of heavy meromyosin labeled filaments. The next step is based on the “barbed” and “pointed” end polarities of the actin filaments. The overall rates of monomer assembly at the two ends are different, the barbed end is preferred for monomer addition over the pointed end where the disassembly is more favored (Woodrum, 1975). The barbed ends of actin filaments serve as nuclei onto which actin subunits can rapidly add. This occurs at actin monomer concentrations of a few micro-molars (fig. 1.1). A near 10-fold higher actin monomer concentration is required to add subunits to the pointed ends (Sheterline et al., 1994). Polymerization of globular actin monomers is induced by Mg^{2+} and K^{+} , at concentrations similar to those found in the cytosol. The double-helical structure of the actin filament requires that each actin monomer within the filament be in contact with four adjacent monomers (Tellam et al., 1989). Hydrophobic and electrostatic forces contribute to the noncovalent bonds between the actin subunits (Stossel et al., 1985). The extent of polymerization is determined by the thermodynamics of the microenvironment; and average filament length (which is inversely proportional to the number of filaments)

is influenced by the kinetics of polymerization (Stossel et al., 1985). Ionic conditions favorable for polymerization of the actin dimers are thermodynamically unstable so that the dimers dissociate easily. But when aggregates consisting of a critical number of monomers assemble, addition of new monomers is more probable than dissociation, therefore polymerization is enhanced by these "nuclei" (Stossel et al., 1985). Nucleation is viewed as the rate-limiting step in the polymerization reaction (Stossel et al., 1985). Given the ionic environment within cells, one would expect to find most of their actin in filamentous form, but this is not the case. About half their actin is present in the G-form due to the action of various small actin-binding proteins such as profilin and actin depolymerizing factor (ADF), which bind and sequester individual actin monomers (Tellam et al., 1989). In vivo, cell activation does not appear to change the amount of total actin, but leads to an increase in the relative amount of F-actin (Carisson et al., 1979). Associated with actin filaments are a great number of other actin-binding proteins. These bind to actin monomers, cross-link actin filaments into bundles, gel or sever the actin filament and cap its growing ends (fig. 1.2). Actin binding proteins can be placed into families, which share similar properties, but most of the time these proteins share domains with actin-binding proteins of other families; these domains are responsible for actin binding itself and/or for various controlling and structural functions (Stossel et al., 1985).

Chromaffin cells are among the non-muscle cells from which a great number of cytoskeletal proteins have been isolated and characterized, their cellular localization has been determined by immunocytochemical, biochemical and ultra structural techniques.

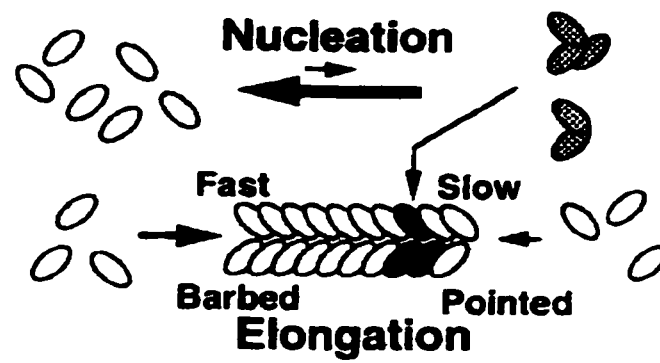


Figure 1.1: Spontaneous actin polymerization.
(From Stossel T., review, 1993)

Actin-binding proteins - (fig. 1.2.). The list of actin-binding proteins continues to increase, but it is now clear that most of them can be placed into the following three main families:

1) *Actin cross-linking proteins* join actin filaments together and possess at least two F-actin-binding sites (Darnell et al., 1990). They have different potencies and are sensitive to pH, Ca²⁺ concentration, temperature and ionic strength. They vary widely in molecular weight, subunit composition, etc., but they all seem to have the shape of long, flexible rods (which probably facilitates cross-linking and rigidity before formation of actin bundles and aggregates takes place) (Craig and Pollard, 1982). Spectrin (fodrin) (Bennet, 1990), villin (Bretscher and Weber, 1980), vinculin (Burrige and Feramisco, 1988), alpha-actinin (Maruyama and Ebashi, 1965) and caldesmon (Sobue, 1988) are just a few of the actin-cross-linking proteins, but other 'non-specific gelation factors are known as well, including histones, RNase, aldolase and lysozyme (Craig and Pollard, 1982).

2) *Actin filament depolymerizing proteins* (ADP) predominantly sequester actin monomers. Examples of these include DNaseI (Lazarides and Lindberg, 1974) and profilin (Carisson et al., 1976). These proteins bind to actin monomers, but do not form stable complexes with the filaments. As a consequence, polymerization in vitro is retarded due to the delay in the incorporation of actin monomers into filaments (Stossel et al., 1985).

These sequestering proteins can bind to the same actin filament end where addition would occur, thus impeding the growth of filament length, and can even extract an actin monomer from the middle of a filament (Stossel et al., 1985).

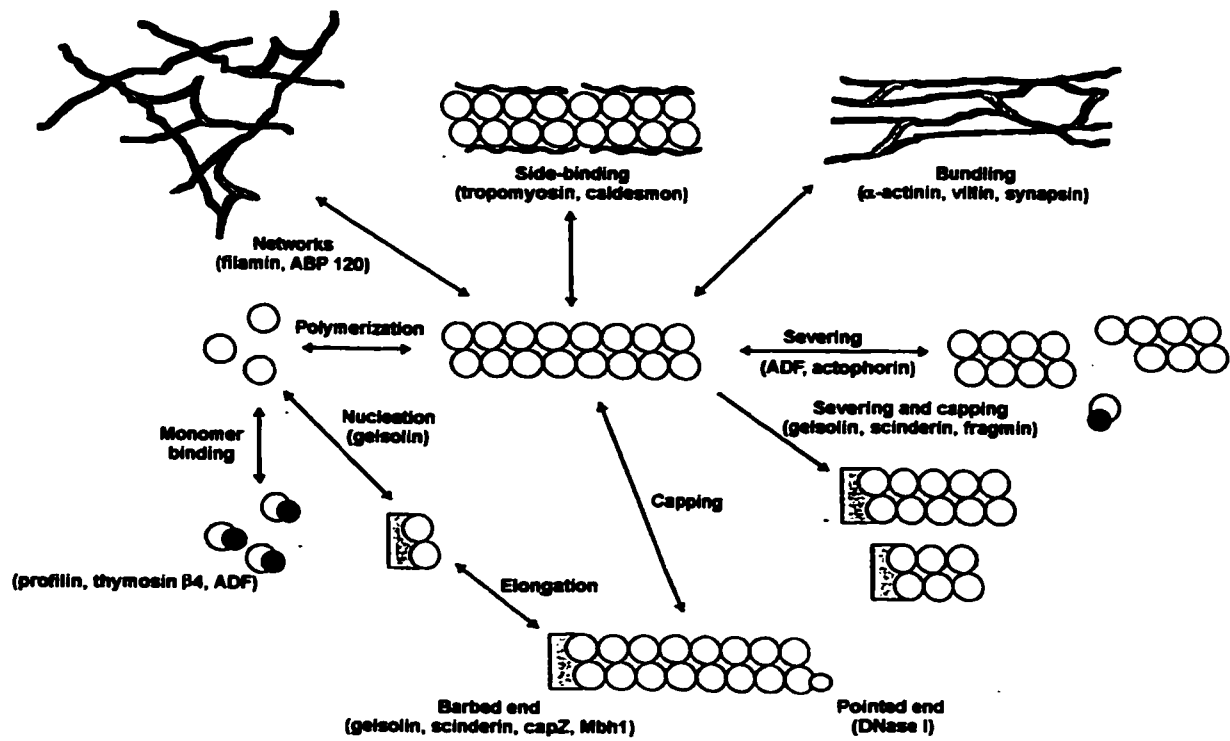


Figure 1.2: The different roles of actin-binding proteins (modified from Way M. & Weeds A., 1990)

Actin depolymerizing proteins decrease the amount of polymer rather than filament length; they bind to monomeric actin with greater affinity than monomeric actin binds to the end of a filament. Therefore monomers dissociate from filament ends in order to restore the equilibrium concentration of free monomers (Craig and Pollard, 1982).

3. Actin filament length regulators and capping proteins These can shorten the length of actin filaments and influence both the nucleation and the elongation steps of actin polymerization through their preferential binding to one of the two polar ends of the filament, thus preventing the exchange of monomers with that end. If actin polymerization (and the effects of these capping proteins) is assayed by shear viscosity, the lag phase of viscosity increase (which is reduced by nucleation) is eliminated in the presence of these proteins; therefore they should be able to favor the nucleation process (Craig and Pollard, 1982). Capping proteins bind to the (+) end of actin filaments, and can bind to one or two actin monomers, thereby accelerating the nucleation process. But when added in vitro to preformed F-actin, these proteins shorten filaments by the mechanical displacement of individual units from neighboring units (Stossel et al., 1985). The end of the filament remains “capped” after binding by a capping protein, so monomer addition is impeded. Severing is a nonenzymatic, nonproteolytic process dependent on Ca^{2+} (Matsudaira and Janmey, 1988). In vitro, severing can be assayed by a number of methods; one of the most frequently used, falling ball viscometry, is based on simple rheologic measurements of the viscosity of F-actin solutions. The apparent viscosity of a solution is proportional to the number, concentration and length of its actin filaments (MacLean Fletcher et al., 1980).

Gelsolin (MW=87,000) was the first protein in this category to be described (Yin and

Stossel, 1979). This group also includes villin (Bretscher and Weber, 1980), fragmin (Hasegawa et al., 1980), β -actinin (Maruyama and Ebashi, 1977) and scinderin (Rodriguez Del Castillo et al., 1990). Gelsolin is built by six domains that originated by a duplicated triplet. No single domains are known but cofilin/ADP have similar fold. Structures of gelsolin family of proteins are very conserved in amoeba, yeast and animals. A schematic representation of the gelsolin family of proteins (mammals only) is represented in Fig. 1.3. Gelsolin is an ubiquitous multi-domain protein with at least three actin-, and two phosphatidylinositol 4,5-bisphosphate - binding sites which can be activated alone or in combination in the course of actin assembly and disassembly (Janmey et al., 1992). Gelsolin binds avidly ($K_D=109$ mol/liter) to the barbed end of F-actin, capping it (Yin and Janmey, 1988), and can also bind to the sides of filaments, breaking their noncovalent actin-to-actin bonds (Yin and Janmey, 1988). The overall effect is the depolymerization of F-actin and an exponential increase in the number of filaments (Yin and Janmey, 1988). Interestingly, a plasma form of gelsolin – brevin plays a vital role in protection against plasma actin filament elongation (by severing). In the absence of such protection, these filaments can reach 10 μ m in length. Consequently, altering microcirculatory flow or even leading to disseminated intravascular coagulation in patients, causing disorders characterized by severe tissue damage, such as: fulminant hepatic necrosis, septic shock, acute respiratory distress, myocardial infarction, etc. (Lee and Galbraith 1992).

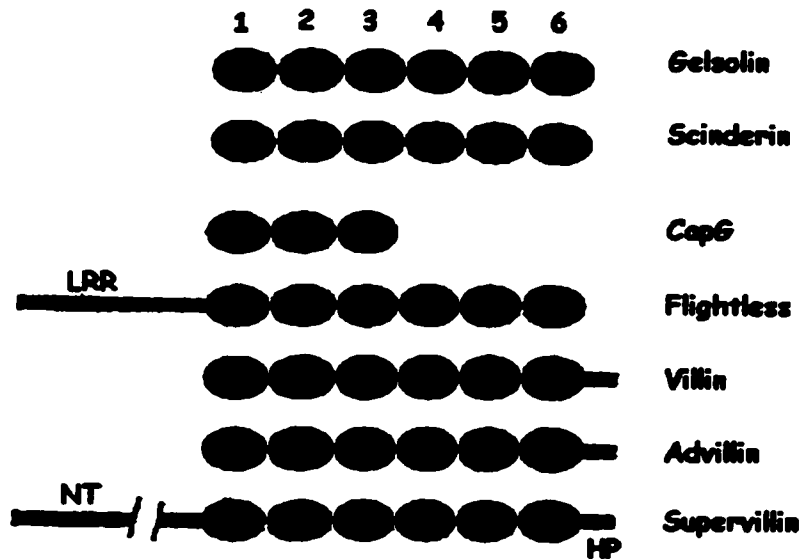


Figure 1.3: Eight members of the gelsolin family of proteins (mammals only) are modeled. The core domain, which is repeated six times is shown. LRR, leucine rich repeat, HP, headpiece, NT, nuclear translocation domain. (modified from Kwiatkowski D., J., 1999)

1.3.2. Chromaffin cell exocytosis and cytoskeleton dynamics during neurotransmitter release.

Over the last few years, remarkable progress has been made in understanding the organization and function of the exocytosis apparatus (*exocytosis* = the fusion of the membrane of an intracellular vesicle with the cell's plasma membrane), with the identification of new protein effectors involved in vesicle transport and fusion (Kelly, 1993; Zucker, 1996). Nevertheless, many questions remain to be answered and little is known about the fundamental mechanisms underlying exocytosis and its regulation by several interacting second-messenger systems.

The ultrastructural and molecular organization of the cytoskeletons of neurons and secretory cells (such as chromaffin cells) differ significantly, but there are also similarities between the two systems (for instance, Ca^{2+} plays a vital role in the control of secretion). Neurons are specialized for the fast release of neurotransmitters, so clusters of synaptic vesicles are closely positioned to the presynaptic membrane where they are readily available for release, and another "reserve" pool can also be recruited for release upon cell stimulation (Hirokawa, 1991)

In secretory cells, the majority of the vesicles are positioned at a distance of about 250 nm from the plasma membrane, a circumstance that might suggest the presence of an impediment (a physical barrier) in the cortical area of these cells (Burgoyne, 1982; Cheek and Burgoyne, 1991; Vitale et al., 1995). In resting chromaffin cells, 1-3% of the total secretory vesicles are either docked to the plasma membrane or within about 50 nm of it (Vitale et al., 1995); this represents the release-ready pool (Neher and Marty, 1993), in contrast to the reserve pool (the remaining 97-99% of the vesicles), which remains behind

the cytoskeletal F-actin barrier (Vitale et al., 1995)

Calcium performs an important role in neurotransmitter release. As was indicated in section 1.2, adrenal chromaffin cells have been extensively studied for many reasons. The main physiological stimulus for release of the secretory material in these cells is a significant rise in $[Ca^{2+}]_i$ entry (Douglas and Rubin., 1961; Douglas and Nemeth, 1982; Llinas et al., 1982) through the nicotinic receptor-associated channel itself and mainly through voltage-dependent Ca^{2+} channels, from a resting level of $0.1 \mu M$ to the range of $0.5-10 \mu M$ (Baker and Knight, 1981). Many researchers have demonstrated that under physiological conditions it is Ca^{2+} entry, rather than its release from internal stores, that activates exocytosis in chromaffin cells (Burgoyne, 1991; O'Sullivan et al., 1988;). A large variety of Ca^{2+} channels (L, N, P, Q, T) have been identified in chromaffin cells, but their precise contribution to the regulation of exocytosis remains to be established (Burgoyne, 1991; Lopez et al., 1994). Activation of any of a number of receptors (such as angiotensin II, ATP, bradykinin, endothelin, muscarinic, nicotinic, etc.) of chromaffin cells will stimulate catecholamine secretion by various mechanisms. For instance, nicotinic stimulation and depolarization with high K^+ leads to the production of $Ins(1,4,5)P_3$ through the Ca^{2+} -dependent activation of PLC (Eberhard and Holz, 1987).

In recent years it has been suggested that in certain secretory systems, such as insulin-secreting cells (Blondel et al., 1995) as well as chromaffin cells (Yoo and Albanesi, 1990), $Ins(1,4,5)P_3$ - elicited Ca^{2+} release from secretory granules can play a role in controlling secretion and neurotransmitter release. In any case, exocytosis requires very high local Ca^{2+} concentrations (Neher and Zucker, 1993). They can be achieved by the clustering of plasma membrane Ca^{2+} channels near the zones where exocytosis occurs

(Llinas et al., 1992) or by Ca^{2+} release from the granules themselves (Blondel et al., 1995; Ravazzola et al., 1996) or by both of these mechanisms. Without a doubt, Calcium also has a pivotal role in secretion due to its second messenger activity (i.e. PKC, calmodulin), control of the cytoskeleton dynamics (actin filament disassembly), and involvement in the vesicle-plasma membrane fusion process, etc.

Fluorescence microscopy using actin antibodies (Lee and Trifaró, 1981) and rhodamine-phalloidin (Cheek and Burgoyne, 1986; Vitale et al. 1991), a probe for filamentous actin (Faulstich et al. 1988), has revealed the presence of a cortical subplasmalemmal network of actin filaments (F-actin) in chromaffin cells. In electron micrographs of resting chromaffin cells, actin filaments were observed running parallel to the plasma membrane, forming a nonuniform network (Fig 1.4) (Tchakarov et al. 1998).

Chromaffin vesicles interact with F-actin through anchoring proteins, such as α -actinin (Jockush et al., 1977; Bader and Aunis 1983; Trifaró et al. 1984) and fodrin (Aunis and Perrin 1984). The cortical actin microfilament network acts as a barrier (negative clamp) to the movement of secretory vesicles by blocking their access to exocytotic sites on the plasma membrane (Burgoyne and Cheek 1987; Burgoyne et al. 1989, Trifaró and Vitale, 1993). Electron micrographs of microfilament networks of chromaffin cells (Fig. 1.5) show that this cortical actin network is disassembled upon Ca^{2+} entry and activation of actin-filament severing proteins such as scinderin (Trifaró and Vitale, 1993; Vitale et al., 1991). Reorganization of actin filaments in certain subplasmalemmal areas leads to the formation of low viscosity cytoplasmic spaces (Fig. 1.5) where chromaffin granules have increased mobility, permitting their movement toward the release sites on the plasma membrane (Trifaró et al., 1998).

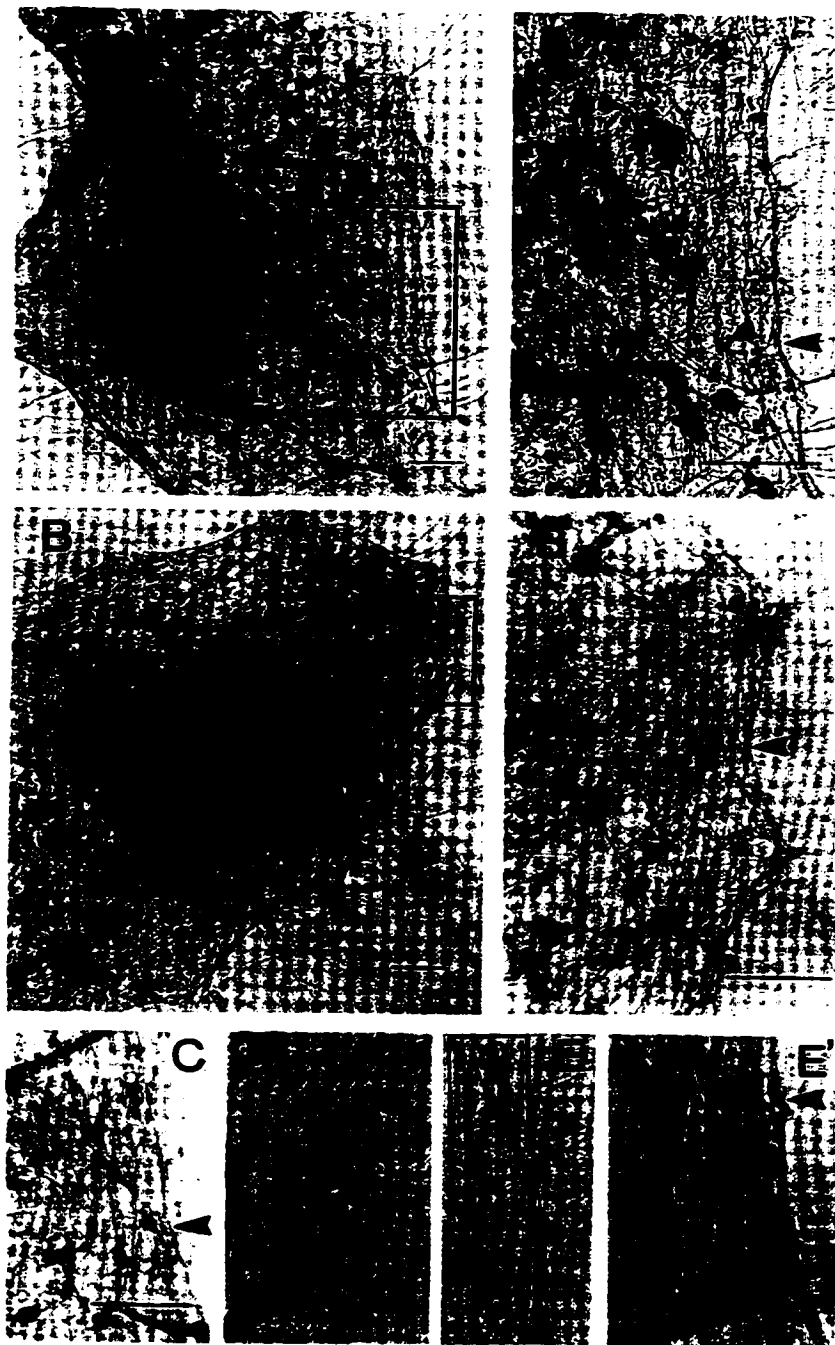


Figure 1.4: Electron micrographs of microfilament networks in resting chromaffin cells.

Chromaffin cells were cultured on Formvar-coated grids for 48 hr and then incubated with Locke's solution for 40 sec. After this period, the preparations were treated with 0.02% Na-azide in PBS, prefixed with a bifunctional protein cross linking reagent, and cytoskeletons were prepared by Triton X-100 extraction as described (Tchakarov et al. 1998). (A, B) Cytoskeletons from two resting cells are shown. (A', B') Higher magnifications of cortical subplasmalemmal areas indicated by square boxes (A,B) are shown. There is a compact network of filaments, especial in cortical subplasmalemmal areas (A', B'), with microfilaments frequently running parallel to the plane of the plasma membrane (A', C-E). A very high magnification of parallel filaments in the area of E marked by a square box is shown in E'. Here the filaments have diameters between 6 and 7 nm. Arrowheads indicate the position of the plasma membrane (From Tchakarov et al., 1998).

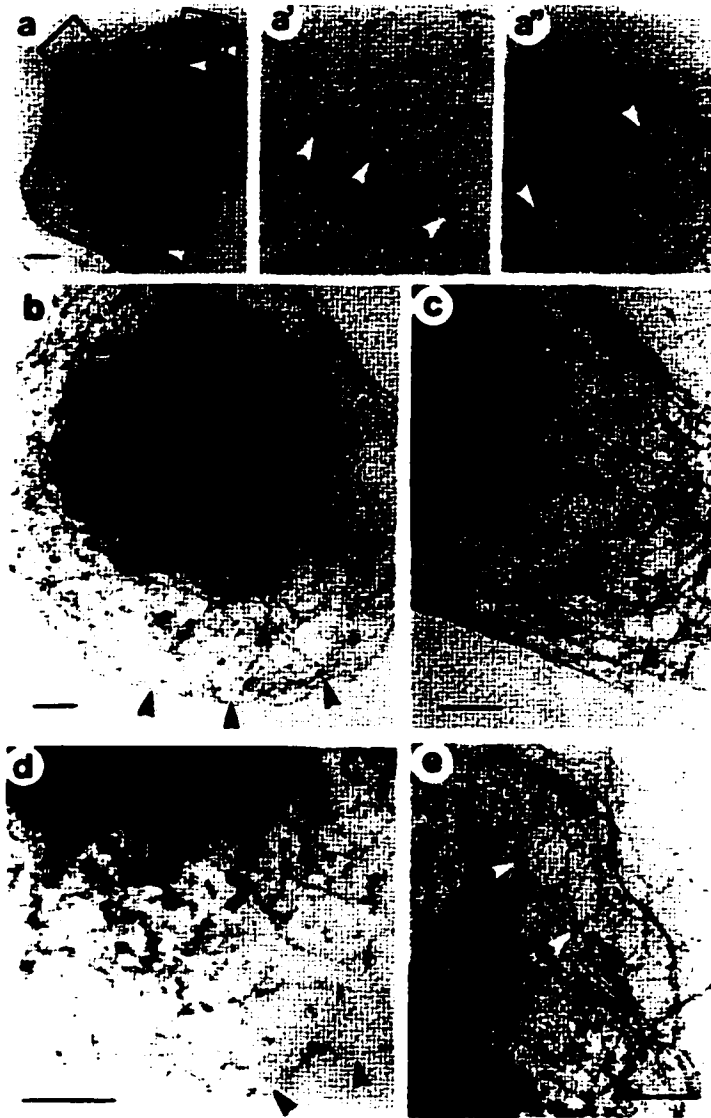


Figure 1.5: Electron micrographs of microfilament networks of chromaffin cells after nicotinic receptor stimulation.

Chromaffin cells were cultured on Formvar-coated grids for 48 hr and then incubated with Locke's solution in the presence of 10 μ M nicotine for 40 sec. After the stimulation period, cells were treated with 0.02% sodium azide in PBS, prefixed with a bifunctional protein cross linking reagent, and cytoskeletons were prepared by Triton X-100 extraction as described (Tchakarov et al. 1998). (a-e) Cytoskeletons from five different cells are shown. In all cases the fine and compact filament network observed in resting (control) cells (Tchakarov et al. 1998) is disrupted, with the appearance of polygonal area (arrowheads) in which microfilaments are either few or absent. In Fig. 1.4.a. the filament-free areas are localized at one pole of the cell.

These areas (boxes in fig. 1.4.a.) are seen at higher magnification in Figs. 1.4.a' and a''. In some cases the filament-free areas are more evenly distributed (b, c), occupying large areas of the cytoskeleton (b). High magnification of a cortical subplasmalemmal area almost devoid of filament (arrowheads) is shown in Figs. 1.4.d. and a.4.e. Bars represent 1 μ m (From Tchakarov et al., 1998).

Secretion can take two forms: constitutive (unregulated, following the rate of synthesis of secretory products) and regulated (the secretory products are stored in membrane-bound secretory vesicles or granules, whose contents are released in fixed amounts upon cell stimulation) (Tartakoff et al., 1978; Gumbiner and Kelly, 1985). The regulated form of secretion is characteristic of neurons and endocrine (with the exception of steroid-secreting cells) and exocrine cells. The membrane-bound vesicles allow the cell to store large amounts of material, which is protected from enzymatic degradation. They also permit the transport and release of quanta of secretory material (Trifaró, 1977; Trifaró and Poisner, 1982).

Secretory cells containing secretory vesicles, such as chromaffin cells, have been named “paraneurons”, because they are considered to be closely related to neurons in structure and function (Fujita, 1977). The release of secretory products by exocytosis is a mechanism whereby the membranes of vesicles fuse with the plasma membrane, and the contents of the secretory vesicles are released to the cell exterior. As described above, this regulated secretion is triggered by an increase in cellular Ca^{2+} . In chromaffin cells, catecholamines are released along with other secretory granule components such as ATP, chromogranin A, dopamine β -hydroxylase and other neuropeptides (Banks and Helle, 1965; Viveros et al., 1968; Lastowecka and Trifaró, 1974). It has been shown that in adrenal medulla the entire soluble content of the granule is released to the cell exterior while the granule’s membrane components are retained within the cell after exocytosis. Exocytosis has therefore been understood as an all-or-none release phenomenon (Viveros et al., 1968; Trifaró, 1977). Endocytosis of empty vesicles and regeneration of fresh vesicles follow exocytosis. The synaptic vesicle cycle is very fast and tightly regulated.

The cell's cytoskeleton plays a crucial role in this cascade of events, determining the positioning of secretory vesicles within the cell (Burgoyne, 1990; Trifaró, 1990). Moreover, it determines the actin filament interaction with the inner surface of the plasma membrane and also with the cytoplasmic surface of secretory vesicles through certain anchorage proteins such as α -actinin, (Jokush et al., 1977; Trifaró et al., 1985) synapsin I (expressed mainly in neurons; Greengard et al., 1993) and II (which is expressed in chromaffin cells; Haycock et al., 1988), and fodrin (Aunis and Perrin, 1984; Perrin and Aunis, 1985). Caldesmon (calmodulin dependent actin-binding protein) is another protein associated with chromaffin vesicles (Burgoyne et al., 1986). It binds and cross-links actin filaments in a Ca^{2+} -dependent manner. Synapsin I is a phosphoprotein associated with neuronal synaptic terminals (DeCamilli and Greengard, 1983); and it functions as a substrate for cAMP kinase (DeCamilli and Greengard, 1986) that can bind to spectrin (an actin binding protein) and actin (Baines and Bennet, 1985). Synapsin I serves as an anchor between synaptic vesicles and cytoskeleton (DeCamilli and Greengard, 1986). These cytoskeleton-associated proteins and many others could be involved in the control of cell viscosity and vesicle mobility; for instance, fodrin cross-links actin filaments resulting in a mesh (Perrin and Aunis, 1985). However, in certain conditions, (cell stimulation and Ca^{2+} increase) actin-severing proteins such as scinderin decrease local cell viscosity allowing the free movement of vesicles toward release sites on the plasma membrane (Rodriguez Del Castillo et al., 1990; Trifaró and Vitale, 1993). As will be shown in following chapters, it seems that scinderin plays a more significant role in neurotransmitter release than its close counterpart, gelsolin. During chromaffin cell stimulation, subplasmalemmal scinderin, but not gelsolin, is redistributed together with

F-actin disassembly; this Ca^{2+} -dependent redistribution precedes exocytosis and exocytosis sites are preferentially localized to areas of F-actin disassembly (Vitale et al., 1991).

It is obvious now that a large number of proteins are involved in exocytosis and membrane recycling; molecular cloning of these proteins is permitting functional studies designed to define their specific role.

1.4. Scinderin characteristics and role in chromaffin cell secretion

Scinderin is a calcium-dependent, filamentous, actin-severing-and-capping protein first discovered in chromaffin cells in our laboratory (Rodriguez del Castillo et al., 1990). This protein is present mainly in tissues with high secretory activity, such as adrenal medulla, hypophysis, testis, and platelets; and it is part of the exocytotic machinery (Zang et al., 1996; Trifaró et al. 1998). The scinderin gene has also been cloned in our laboratory (Marcu et al., 1994).

Scinderin requires Ca^{2+} to initiate its role in the secretory process (Rodriguez del Castillo et al., 1990). Equilibrium dialysis studies have demonstrated the presence of two scinderin Ca^{2+} - binding sites ($K_D=5.85 \times 10^{-7} \text{ M}$ and $K_d=2.85 \times 10^{-6} \text{ M}$) (Trifaró et al., 2000). Complete amino acid sequence analysis of scinderin (715 amino acids). Marcu et al., 1994) has revealed that it shares homology with gelsolin (63%) and villin (53%), two other F-actin-severing proteins (Marcu et al., 1994). Similar to gelsolin and villin, scinderin contains six domains (1-6) (Fig. 1.6). Strong similarities exist between domains 1 and 4, 2 and 5 and 3 and 6 in gelsolin, villin and scinderin.

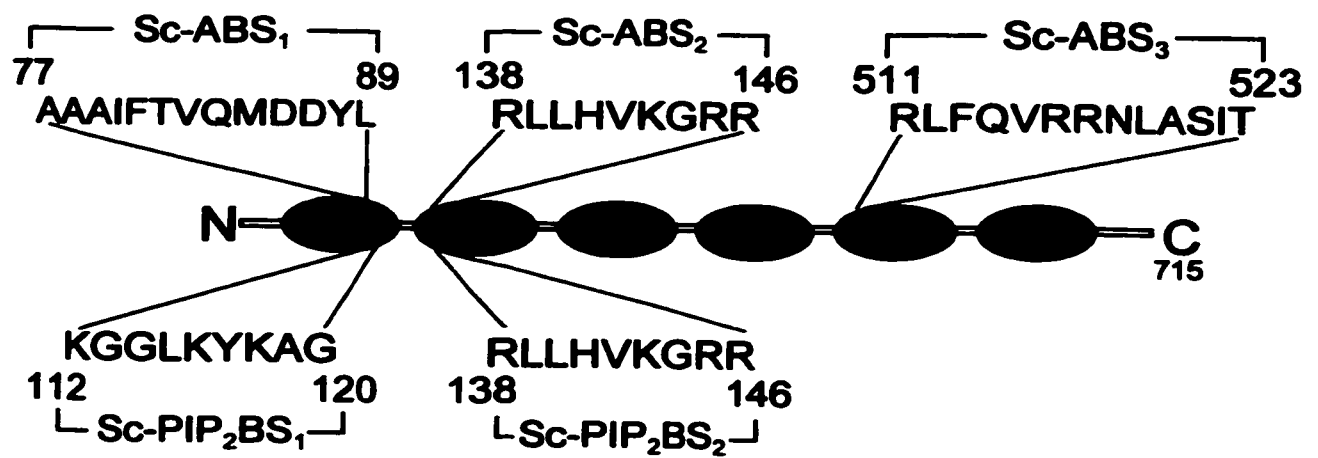


Figure 1.6: Schematic representation of scinderin domains. Sc 1-6 domains, the amino acid sequences and position of 3 actin binding sites (Sc-ABS1, Sc-ABS2, Sc-ABS3) and two PIP₂ binding sites are shown. (From: Trifaró et al., 1998).

It has also been suggested that this family of actin-filament-severing proteins may have evolved by tandem gene triplication with a predicted 14 kDa monomer unit of 129-139 amino acids residues. This is the size of domain 1 of gelsolin (Trifaró et al., 2000). Scinderin's actin-binding sites 1, 2, and 3 are present in domains 1, 2, and 5 respectively (fig. 1.6). The first two actin-binding sites are involved in the severing of actin filaments. There is high homology between these two actin-binding sites of scinderin and the corresponding ones of gelsolin.

Thus, the filament-severing activity of scinderin may reside in the domains, since it has been demonstrated for gelsolin that in addition to domain 1, a second binding site in domain 2 is necessary for full severing activity (Trifaró et al., 2000). The in vitro binding of domain 1 of gelsolin to actin seems to be Ca^{2+} independent (Bryan, 1988), whereas binding of its N-terminus of scinderin to actin requires the presence of Ca^{2+} (Trifaró et al., 1992). A third actin-binding site has been demonstrated in domain 5 of scinderin. Scinderin binds actin at this site in a Ca^{2+} independent manner, and thus nucleates actin assembly (Marcu et al., 1998). Therefore, in addition to binding actin on sites present in domains 1 and 2, scinderin must also bind actin on a third site in domain 5 in order to sever or nucleate actin effectively. Under resting conditions, scinderin is bound to plasma membrane phospholipids in a pH- and Ca^{2+} -dependent manner (Rodriguez del Castillo et al., 1992). Actin and phospholipids compete for binding to scinderin, indicating that a phospholipid binding site and at least one of the two actin-binding sites are localized in the same domain of scinderin (domain 2) (fig. 1.7). Moreover, phospholipids are more easily displaced from scinderin by actin under acidic rather than alkaline pH, providing 10^{-7} to 10^{-6} M Ca^{2+} is present (Rodriguez del Castillo et al., 1992).

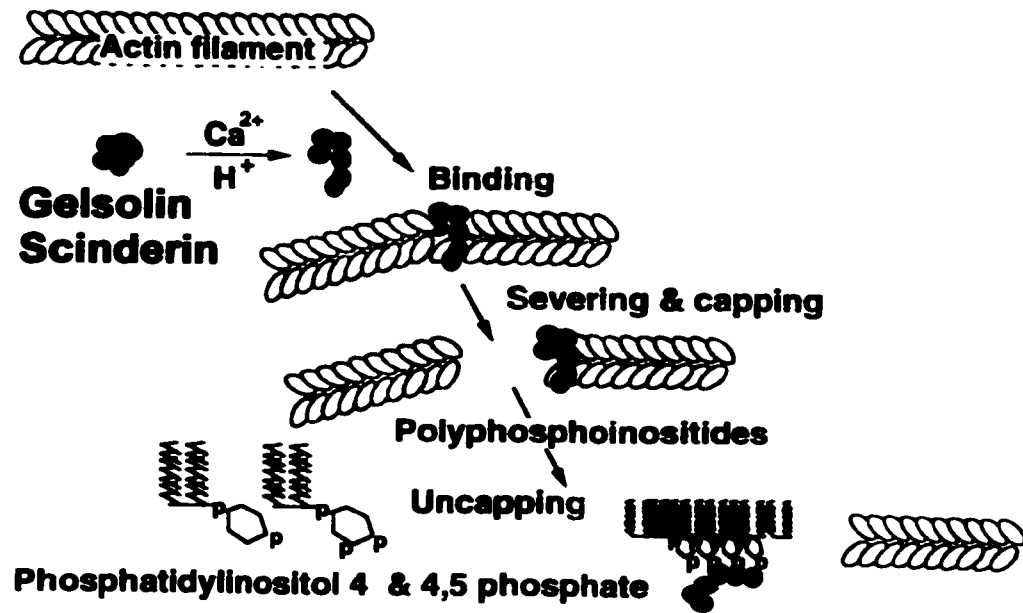


Figure 1.7: Regulation of gelsolin and/or scinderin activities by ions and polyphosphoinositides.
(From: Stossel T., review, 1993).

Therefore, under conditions that produce intracellular acidification and rises in Ca^{2+} , scinderin tends to leave its binding sites (phospholipids) on the plasma membrane to interact with and sever actin. Another indication of the competition between actin and phospholipids for scinderin is the fact that PIP2 (phosphatidylinositol-diphosphate) inhibits the actin-severing activity of scinderin (Rodriguez del Castillo et al., 1992). This suggests that cellular levels of PIP2 might regulate the activity of scinderin. Indeed, the synthesis of PIP2 and other phosphoinositides is regulated by small molecular G proteins such as Rac and Rho (Hartwig et al., 1995), suggesting that these proteins might indirectly regulate the activity of scinderin.

Two PIP2 binding sites on scinderin occur at amino acids 112-119 and 138-146, of domains 1 and 2 respectively (fig. 1.6). The PIP2 binding site in domain 2 of scinderin overlaps with the second actin-binding site (fig. 1.6), providing an explanation for the competition for scinderin between PIP2 and actin and for the inhibition by PIP2 of the actin-severing activity of scinderin (Trifaró et al., review, 2000).

The following model has been proposed for the regulation of scinderin activity (Rodriguez Del Castillo et al., 1992): Under resting conditions ($\text{pCa} = 8$; $\text{pH} = 6.98$), scinderin is divided into two pools, a soluble one and a pool bound to membrane phospholipids (fig. 1.8). Nicotinic stimulation causes a fast increase in intracellular Ca^{2+} concentration ($\text{pCa} = 6-5$) and slow rise in pH. High intracellular calcium concentration induces the release of scinderin from the membrane-associated pool, and the binding of Sc to F-actin with activation of scinderin severing activity.

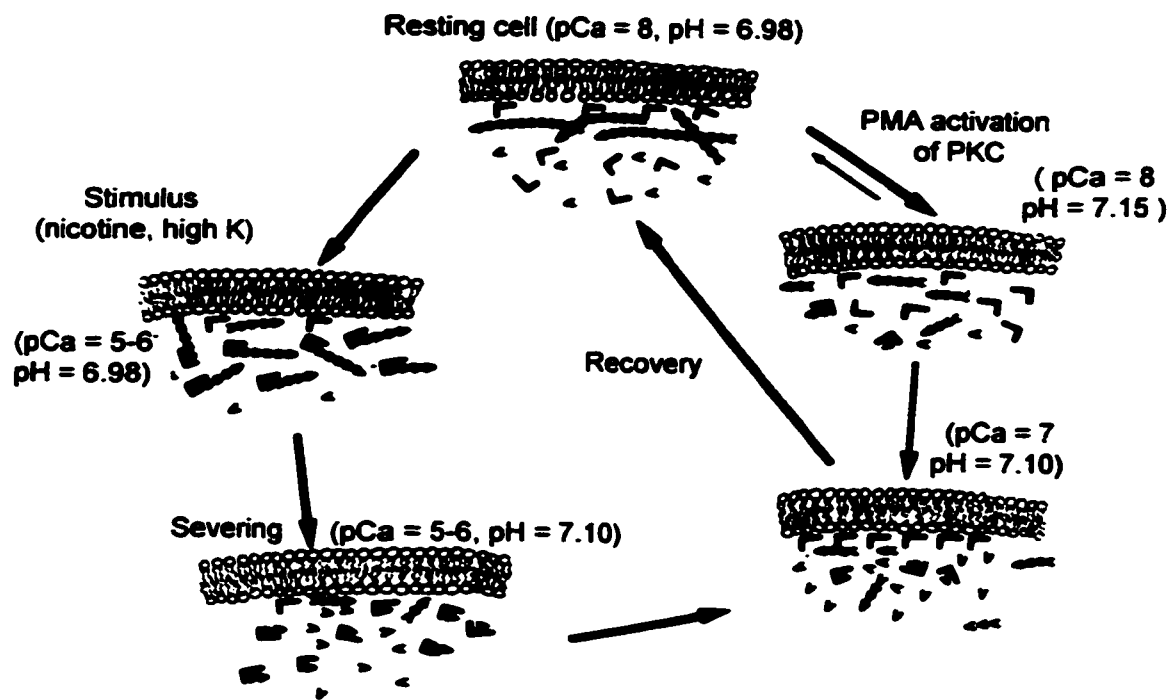


Figure 1.8: Integrated mechanism of actin assembly and disassembly by cell intracellular pH and free Ca²⁺.

→ = scinderin; <<< = F-actin; < = G-actin; \mathfrak{R} = membrane phospholipids (From: Dordiguez Del Castillo et al., 1992).

When Ca^{2+} concentration is $\sim 10^{-7}$ M and pH_i is still high (7.1), conditions in which scinderin expresses its maximal affinity for phospholipids, the remaining scinderin-actin complex is dissociated by competing phospholipids (PS and PIP₂). Finally, when Ca^{2+} concentrations return to basal values ($\text{pCa} = 8$), PKC activity decreases and chromaffin cell pH_i reaches resting values ($\text{pH} = 6.98$), scinderin is in equilibrium between its membrane-bound and cytoplasmic pools (fig. 1.8).

Adrenal medulla chromaffin cells possess a mesh of actin filaments (F-actin) underneath the plasma membrane. A decrease in F-actin concentration (Cheek and Burgoyne, 1986; Burgoyne et al., 1989) due to the disassembly of the cortical F-actin network (Cheek and Burgoyne, 1986; Trifaró et al., 1989) precedes exocytosis (Trifaró et al., 1982, 1984; Cheek and Burgoyne, 1986; Burgoyne and Cheek, 1987; Burgoyne, 1991). Ca^{2+} -dependent actin-binding proteins such as gelsolin and scinderin regulate the dynamics of actin filament length (Trifaró et al., 1985; Bader et al., 1986), playing an important role in the reorganization of cortical actin filaments brought about by cell stimulation. These two proteins are different in many ways, including tissue distribution: gelsolin (MW=87,000) is a widely distributed Ca^{2+} -dependent actin filament capping and severing protein (Yin and Stossel, 1979, Yin et al, 1981; Stossel et al., 1985). Scinderin, on the other hand, is also a Ca^{2+} -dependent actin-filament-severing protein, (first described by us in chromaffin cells (Bader et al., 1986; Rodriguez Del Castillo et al., 1990). It is only expressed in tissues with high secretory activity (Tchakarov et al., 1990). Immunocytochemical studies have shown that nicotinic receptor stimulation of chromaffin cells induces cortical F-actin disassembly and the simultaneous redistribution of subplasmalemmal scinderin (Vitale et al., 1991). During nicotinic receptor stimulation

there is a spatial relationship between scinderin and F-actin cortical redistribution: exocytotic sites are preferentially localized to cortical areas devoid of scinderin and F-actin (Vitale et al., 1991). The distribution of gelsolin, on the other hand, is not affected by either nicotinic receptor stimulation or K⁺-evoked depolarization (Vitale et al., 1991). Therefore, the effect of cell stimulation seems to be specific for scinderin (cell stimulation and Ca²⁺ entry bring about activation of scinderin with a consequent disassembly of cortical actin-filament networks). Previous studies in our laboratory have also demonstrated that PKC seems to be involved in the regulation of scinderin cellular distribution (Rodriguez Del Castillo et al., 1992). Other different characteristics of the two proteins (scinderin and gelsolin) include: different molecular weights, isoelectric points, amino acid composition and different peptide maps after limited proteolytic digestion (Rodriguez Del Castillo et al., 1990). Both proteins have an actin filament severing activity, which is Ca²⁺-dependent and inhibited by phosphatidylinositol 4,5 bisphosphate (Yin et al., 1988; Maekawa and Sakai, 1990). Immunocytochemical studies have shown that, in chromaffin cells, scinderin has a diffuse cytoplasmic and a more dense subplasmalemmal distribution, while gelsolin showed only a diffuse cytoplasmic distribution (Vitale et al., 1991; Rodriguez Del Castillo et al., 1990). Together, these experimental data suggest that gelsolin and scinderin are two distinct Ca²⁺-dependent F-actin severing proteins, differing in their chemical properties and fine regulation by intracellular messengers.

As described above, the cortical F-actin cytoskeleton represents a negative control for secretion, and must be locally disassembled to allow chromaffin vesicle exocytosis. It was concluded that cortical actin network dynamics could control the size of the release-

ready vesicle pool and, consequently, the initial rate of exocytosis (Vitale et al., 1995). It has also been suggested that cortical actin network dynamics are controlled by scinderin, a Ca²⁺-dependent F-actin severing protein (Rodriguez Del Castillo et al., 1990, 1992; Vitale et al., 1991).

1.5. Hypothesis

The purpose of this project was to further study scinderin, its molecular biology and the specific functions of its domains. As discussed above, adrenal chromaffin cells possess a network of actin filaments underneath their plasma membrane, and this physical barrier prevents the free movement of secretory vesicles and exocytosis. Release of the granule contents to the cell exterior through exocytosis is possible only when the actin filaments are severed at least locally. The existence of endogenous actin-binding and severing proteins (gelsolin, scinderin), which regulate actin network dynamics, suggests an important role for these proteins in the stimulus-evoked disassembly of F-actin and exocytosis.

Previous studies done in our laboratory showed that Scinderin, a Ca^{2+} -dependent actin severing protein contains two Ca^{2+} -dependent actin binding sites in domains 1 and 2 and one Ca^{2+} -independent actin binding site in domain 5. Moreover, in vitro studies showed that the first two actin-binding domains of Sc sever actin, and the last two domains nucleate and polymerize actin. Furthermore, studies done in our laboratory on permeabilized chromaffin cells showed that the first two domains stimulate secretion of neurotransmitters and the last two domains inhibit secretion. Therefore, our hypothesis was:

- If the first two actin-binding domains of Sc are responsible for the actin severing activity, then overexpression of these domains in chromaffin cells would potentiate the exocytosis due to an increased F-actin disassembly

- If the last two domains of Sc are responsible for the actin nucleating and polymerization activity, then overexpression of these domains in chromaffin cells would inhibit the exocytosis due to an increased actin polymerization

In order to address these questions, we first developed an efficient method of chromaffin cell transfection. However, because the transfection efficiency was of only 10 to 20 %, we decided to use a human growth hormone reporter system for regulated secretion. Furthermore, we tried to improve the hGH signal upon stimulation by improving the labeling of the ready to release pool of chromaffin vesicles

2 – MATERIALS AND METHODS

Materials

The polyclonal scinderin antiserum was generated in rabbits against purified bovine chromaffin cell scinderin as previously described (Rodriguez DelCastillo et al., 1990). Anti hGH polyclonal rabbit IgG and anti D β H monoclonal mouse IgG were purchased from Chemicon International, Inc. (MAB308, CA, USA). Monoclonal anti-Golgi 58K protein was purchased from Sigma (Mississauga, ON). BSA and mouse monoclonal α -tubulin antibody were obtained from Sigma Chemical Co. ESL (enhanced chemiluminescence) reagent was obtained from Amersham Pharmacia Biotech (Oakville, ON, Canada). Trizol reagent, Elongase amplification system, restriction endonuclease enzymes, DMEM and RPMI 1640 culture media, lipofectin and effectene transfection reagents were purchased from Life and Technologies (GIBCO, ON, Canada). The plasmid pEGFPC3, GFP – antibody and the sequencing primer were obtained from Clontech (Palo Alto, CA). First Strand cDNA Synthesis Kit was purchased from Fermentas (ON, Canada). DNA purification kits used for minipreps, medium and large-scale preparation of DNA as well as DNA–gel extraction kits were obtained from QIAGEN (Mississauga, Ontario). The PCR and sequencing primers were synthesized using a Beckman Oligo 1000 DNA synthesizer, at the faculty core facility (BRI). Sequencing of the Sc deletion mutants was done using an ABI PRISM BigDye Terminator Cycle Sequencing Kit (Applied Biosystems, Foster City, CA). CyQUANT Green cell proliferation assay kit used to determine the total DNA content was purchased from Molecular Probes, ON, Canada. The radioimmunoassay kit for hGH measuring was obtained from Nichols Institute, San Juan Capistrano, CA.

Methods

2.1 Chromaffin cell culture

2.1.a Isolation of cells

Bovine adrenal glands were obtained from a local slaughterhouse and chromaffin cells were isolated by collagenase digestion and further purified using percoll gradient followed by differential plating (Trifaró and Lee, 1980). Briefly, the glands were rinsed at the slaughterhouse with buffer I (Ca²⁺, Mg²⁺-free Locke's buffer, containing in millimolar: NaCl, 154; KCl, 2.6; K₂HPO₄, 1.25; KH₂PO₄, 0.5; glucose, 10; pH 7.0; antibiotics: penicillin, 200mg/l; streptomycin, 50 mg/l; gentamycin, 50 mg/l; 5mM HEPES and phenol red, 15 mg/l). On arrival at the laboratory, the glands were rinsed again and perfused with the same buffer via a polyethylene tube inserted in the main adrenal vein for 10 min. The glands were then dissected and their cortexes were removed. Each gland was perfused for 60 min, at 37°C, in a closed circuit perfusion chamber, with 30 ml buffer I containing an enzyme mixture (DNase I, 5.3 mg/l, collagenase, 548 U/gland and mycostatin, 25,000 U/l in 400 ml buffer I). The solution was previously sterilized through a millipore filter. The rate of perfusion was 10 ml/min. Once the glands were flaccid, the remaining cortexes were removed and the medullae minced. Then, preparations were transferred to a "trypsinizing flask" containing the same enzyme mixture pre-warmed at 37°C in a water bath. After stirring for 30 min, the undigested tissues were filtered and rinsed through a 44 µm sterile cloth mesh into a graduated cylinder containing buffer II (1.2 mM MgCl₂, 2.2 mM CaCl₂ added to buffer I, pH 7.2). An aliquot was removed and the cell number was determined by counting the cells in a

haemocytometer (Neubauer, Levy chamber Cat.500). The above preparation was centrifuged for 10 min (500 x g) at room temperature (RT), the sediment was washed again with 100 ml buffer II and centrifuged again at 500 x g for 15 min at RT. The cell sediment thus obtained was fractionated using Percoll gradients as described below. The number of Percoll gradients to be used was determined so that each gradient would contain 27×10^7 cells, according to Trifaró et al.. The sediment was resuspended in Eagle's Balance salt solution (EBSS) containing antibiotics (streptomycin 100 mg/l; penicillin, 100 mg/l; mycostatin, 25,000 U/l; gentamycin 50 mg/l). The cell suspension was then mixed with Percoll – colloidal silica coated with polyvinylpyrrolidone at pH 7.2 – and EBSS 10X in the ratio 8:9:1 (Trifaró and Lee, 1980). The mixture was centrifuged at 20°C, 45,000 x g, for 10 min. After discarding the top of the gradients, corresponding to cortical cells and debris, the bands corresponding to the chromaffin cell population were collected and pooled. This fraction was then diluted with five volumes of EBSS containing antibiotics and centrifuged at 500 x g, RT, for 15 min. The supernatant was discarded and the sediment containing the cells was washed with EBSS/ antibiotics. An aliquot was removed to determine the cell number and the cell yield was calculated prior to plating using a counting chamber. The cell sediment was resuspended in Dubecco's modified Eagle's medium (DMEM: 10% fetal calf serum, 0.1 mM ascorbic acid, 0.1% glucose and 15 mM HEPES, pH 7.2) with antibiotics (penicillin 100 µg/ml; gentamycin 50 µg/ml; streptomycin, 100 µg/ml; nystatin, 25,000 U/l; 10 mM 5-fluorodeoxyuridine) and 10 mM cytosar (complete feeding medium).

2.1.b. Differential plating of chromaffin cells.

The procedure described above resulted in a preparation containing 90-95% chromaffin

cells. The remaining cells were fibroblasts 4-9% and cortical cells 1% (Trifaró and Lee, 1980). A highly purified chromaffin cell culture was obtained by differential plating. This method is based on the differential affinity of chromaffin cells and fibroblasts for the plastic surface of the culture dish. Cells were plated at a cell density of $0.5 - 0.7 \times 10^7$ cells/cm² on plastic 100 mm Petri dishes and incubated for 5 hours at 37°C, in atmosphere of O₂ and 5% CO₂. Five hours after plating, cells were collected, the plastic culture dishes were washed two times with complete feeding medium (CFM) and cells were re-plated on collagen-coated Petri dishes or further processed for transfection. This procedure produces a 98- 99% chromaffin cell culture (Waymire et al., 1983).

2.2. Preparation of pEGFP vectors containing full-length Scinderin (Sc) or various Sc deletion constructs

2.2.a. Preparation of full-length Scinderin (Sc1-6)

Total RNA was isolated from 10⁷ chromaffin cells using the Trizol reagent (GIBCO, ON, Canada) according to manufacturer specifications. Trizol isolation of RNA is based on a single step extraction method, guanidine isothiocyanate/phenol/chloroform – mediated (Chomczynski and Sacchi, 1987). The total RNA thus obtained was used as a substrate for the first strand cDNA synthesis (First Strand cDNA Synthesis Kit - FERMENTAS, ON, Canada). This system uses the enzyme Moloney murine leukemia virus reverse transcriptase (M-MuLV) that exhibits low RNase H activity, allowing the synthesis of full-length cDNA from long templates (up to 9 Kb) (Sambrook et al., 1989). A primer specific to the 5' end of the scinderin gene was used to prime the first strand synthesis. The first strand cDNA thus obtained was then used as a template for full length Sc cDNA isolation and amplification by polymerase chain reaction (PCR). Full length Sc

cDNA was thus 'PCR-out' using an Elongase amplification system (GIBCO BRL, ON, Canada). This kit contains two enzymes: *Taq* and *Pyrococcus species* thermostable DNA polymerases and is able to amplify with high fidelity targets larger than 5 Kb (Westfall et al., 1994; Nathan et al., 1995). To facilitate subcloning in pEGFP-C3 vector (Clontech, Palo Alto, CA) (Fig. 2.1), the PCR primers were designed to include a Kpn I restriction site for the 5' end, in frame with the GFP sequence from the pEGFP-C3 vector, and a BamH I restriction site for the 3' end. Since many restriction enzymes cleave poorly when their recognition sites are located at the end of DNA fragments (Sambrook et al., 1989), additional bases were added to the 5' end of the PCR primers, next to the introduced recognition site to ensure efficient cleavage with the appropriate restriction endonuclease enzymes. The sequence of the forward primer (5' end of the Sc gene) was: 5' GCG GTA Ccc atg gCC CAG GGG CTG T 3' and the sequence of the reverse primer (3' end of Sc gene) was: 5' ATC gga tcc CAC CTG CTG GAA TCC CA 3' (restriction sites are represented in lower cases). The primers were synthesized using a Beckman Oligo 1000 DNA synthesizer. Hotstart PCR was performed with the following parameters: 94°C for 5 minutes, 30 cycles at (94°C for 45 sec., 58°C for 45 sec., 68 °C for 150 sec.) followed by a final extension at 75 °C for 5 min. Then, the amplification products were visualized by agarose gel electrophoresis and purified using a Qiaquick agarose gel extraction kit (Qiagen).

2.2.b. Cloning of full-length Scinderin Sc1-6 into pEGFPC3 vector

The full-length Sc obtained as described above was then cloned into pEGFPC3, a vector containing a red – shifted variant of wild type green fluorescent protein (Fig. 2.1). Sc1-6 was digested using Kpn I and BamH I restriction enzymes (GIBCO, ON, Canada) and

purified by the phenol/ chlorophorm/ isoamyl alcohol method. Once purified, the digested sequence was ligated into the pEGFPC3 vector, digested and purified in the same way as described above (T4 DNA Ligase - GIBCO BRL, ON, Canada). The ligation products were then transformed into the host *DH5 α* , using the CaCl₂ method (Sambrook et al., 1989). Positive transformants were selected by plating on kanamycin (100 μ g/ml) LB plates. To test the positive colonies for the presence of the insert, plasmid DNA minipreps were prepared using the alkaline lysis method (Sambrook et al., 1989) and then were double digested with Kpn I and BamH I. The digestion products were visualized by agarose gel electrophoresis. One positive clone was selected and sequenced as described in section 2.2.d.

2.2.c. Preparation of various deletion constructs of Sc and cloning into pEGFP-C3 vector

In order to test the role of the various Sc domains in chromaffin cell exocytosis, six deletion constructs of Sc were synthesized by PCR (PCR conditions were similar to those described in section 2.2.a.), using pEGFPSc1-6 as a template. A scheme with all the different Sc deletions is shown in Fig. 2.2. For Sc1-2 (first two Sc domains), Sc 5-6 (last two domains of Sc), ScL5 (domain 5 without the actin binding site) and Sc5 (domain 5), the PCR primers were designed in the manner described in section 2.2.a.

The PCR primers used to synthesize the Sc deletion constructs are as follows (restriction sites are represented in lower cases):

5' GCg gta ccc ATG GCC CAG GGG CTG T 3' forward for Sc1-2

5' ATC gga tcc CTA AGC TTT GGC TTT 3' reverse for Sc1-2

5' ACg gta ccG ATG GAA GGT CAG GCA CCA 3' forward for Sc5-6

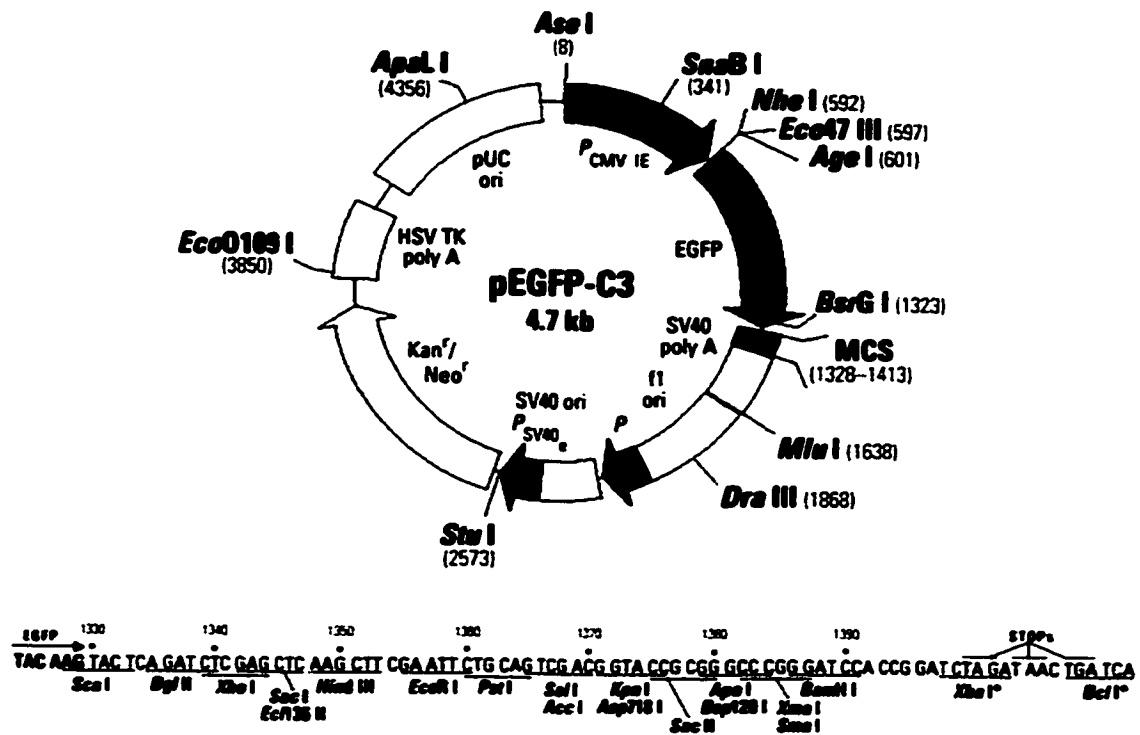


Figure 2.1: Schematic representation of the pEGFP-C3 vector. The gene encoding a red-shifted variant of the wild-type (EGFP) optimized for brighter fluorescence, is represented in green. The enhancer-promoter for high-level transcription (CMV), the polyadenylation signal and the kanamycin/neomycin resistance gene are also represented in the scheme. The multiple cloning site (MCS) is between the EGFP coding sequence and the SV40 polyA, and its sequence is shown at the bottom of the panel. Genes cloned into the MCS of the vector will be expressed as fusions to the C-terminus of the EGFP if they are in the same reading frame as EGFP and there are no intervening stop codons. Sc cDNA and Sc deletion constructs were cloned between restriction sites of Kpn I and Bam HI sites (Taken from Clontech vector information)

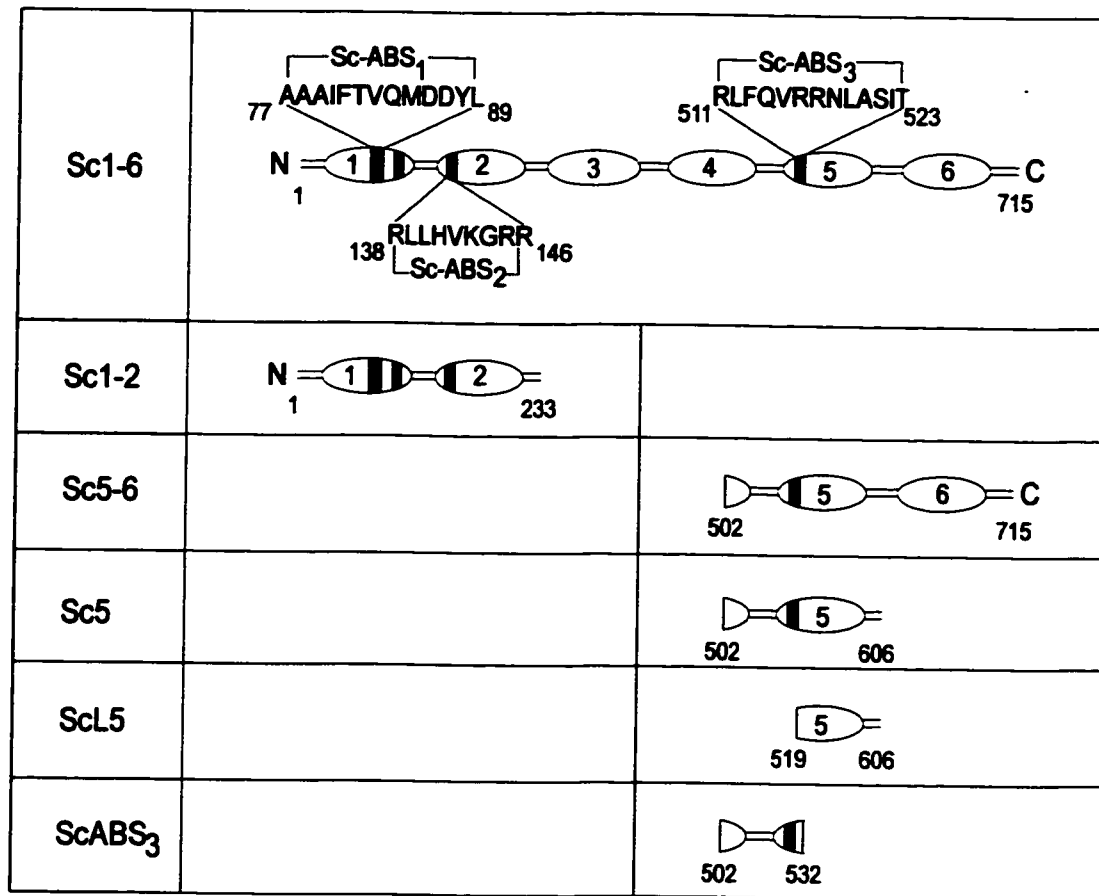


Figure 2.2: Schematic representation of Sc domains and various Sc deletion constructs obtained by PCR.

Full length Sc structure is represented at the top of the panel. Amino acid sequences and positions of the three scinderin actin-binding sites are also shown. The number of the first and last amino acid of every scinderin deletion construct is indicated.

5' ACT GCA ggt acc GAT GCT GGC TTC GAT CAC C 3' forward for ScL5

5' ATC gga tcc CAC CTG CTG GAA TCC CA 3' reverse for Sc 5-6, Sc6

5' GGT gga tcc CGT TAT TCT AGC AGA GGA GA 3' reverse for ScL5

For ScABS3 (composed of 90 bp spanning the Sc's third actin binding site) a different cloning strategy was used since the length of this fragment is very short. A PCR forward primer was designed specifically for the beginning of the GFP gene and included an Age I restriction site (Fig. 2.3). The reverse primer was designed to include a BamH I restriction site. The GFP-fused ScABS3 was amplified by PCR, using pEGFPSc5-6 as a DNA template, and using the same PCR conditions as described in section 2.2.a. The PCR fragment was subsequently digested with Age I and Bam HI restriction enzymes, and sub-cloned in the pEGFPC3 vector using the same restriction sites. The PCR primers were as follows:

5' GCT acc ggt CGC CAC CAT GGT GAG C 3' forward

5' AGG Tgg atc cCG TTA ATC AAC ATC TAC CTC C 3' reverse.

Recombinant plasmids were then transformed into the host *E. coli DH5 α* , and transformants were selected on kanamycin (100 μ g/ml) LB plates. For each Sc deletion construct several clones were tested for the presence of the proper insert, as described in section 2.2.a.

The sequences of the selected clones were confirmed by dideoxy sequencing as described in section 2.2.d.

2.2.d. DNA sequencing

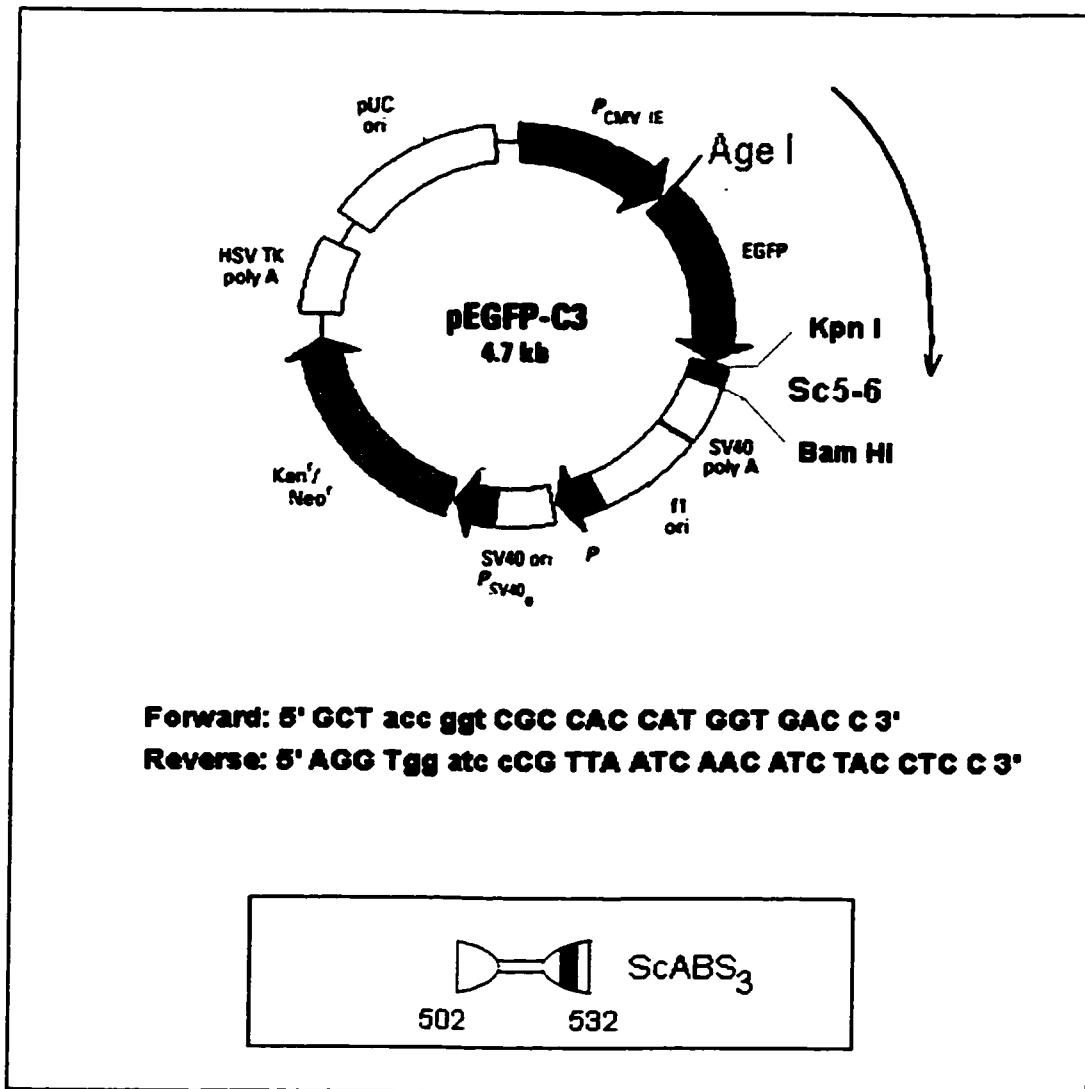


Figure 2.3: Schematic representation of the synthesis of the third Sc actin binding site construct (ScABS₃). pEGFPSc5-6 was used as a template to “PCR-out” the GFP-fused ScABS₃. The PCR forward and reverse primer sequences and the ABS₃ schematic representation are shown underneath the pEGFPSc5-6 scheme. The PCR forward primer was designed to bind at the beginning of the GFP gene and to include an Age I restriction site (represented in green). The reverse primer was designed to include a Bam HI restriction site. The arrow represents the direction of the PCR reaction. The PCR fragment was then digested with Age I and Bam HI restriction enzymes, and subcloned in the pEGFPc3 vector using the same sites (Age I and Bam HI).

All sequencing reactions were carried out following the dideoxy method (Sanger et al., 1977), using ABI PRISM BigDye Terminator Cycle Sequencing Kit (Applied Biosystems, Foster City, CA), at the faculty core facility (BRI).

Sequencing of the full-length Sc. The longest sequence that can be accurately determined by a single sequencing step is shorter than the Sc gene. Six different synthetic oligonucleotide primers (Beckman Oligo 1000 DNA synthesizer) were designed in order that their sequencing reactions would cover the whole Sc cDNA. These partial sequences were then analyzed for overlapping fragments. The scheme of the localization of the sequencing primers in the Sc molecule is shown in Fig. 2.4. Arrows indicate the length and direction of the sequencing reactions.

Sequencing of the Sc deletion constructs. Sc deletion constructs were sequenced using a primer complementary to the upstream sequence of the multiple cloning site in pEGFP vector (EGFP-C Sequencing Primer-Clontech).

2.3. Transient transfection of chromaffin cells

2.3.a. Chromaffin cell transient transfection using a liposome-mediated gene transfer system (Lipofectin)

Lipofectin was used as described in the manufacturer's specifications (Qiagen, Mississauga, ON). The preparation is a 1:1 mixture of the cationic lipid N-[1-(2, 3-dioleoyloxy) propyl]-N-N-N-trimethyl ammonia chloride (DOTMA) and dioleoyl phosphatidylethanolamine (DOPE) (Felgner et al., 1987).

Sequencing primer
pEGFP C3 sequencing primer (forward:1-422)
ATCGGATCCCTAAGCTTITGGCTTT (reverse: 699-154)
TGTGGCGTCTGGACTCAATCA (forward: 450-923)
TTAGGGAAAAGCCCAAAGCTT (forward: 762-1320)
ACGGTACCGATGGAAGGTCAGGCACCA (forward:1506-2000))
GGTGGATCCC GTTATTCTAGCAGAGGAGA (reverse:1818-1221)
ATCGGATCCCACCTGCTGGAATCCCA (reverse: 1245 - 1510)

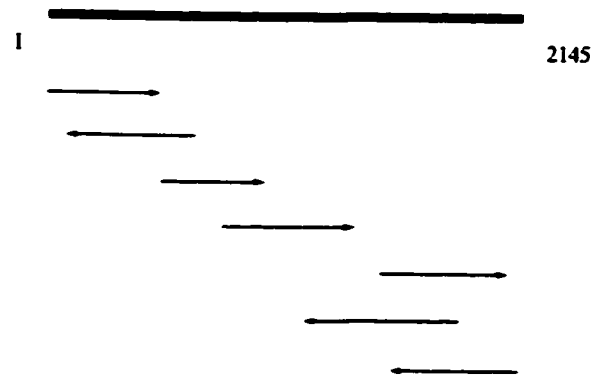


Figure 2.4: Sequence and localization on Sc gene of the primers used for segmental sequencing of Sc cDNA.

Primers sequences are represented on the left of the panel. Arrows (on the right of the panel) indicate the length and direction of the sequencing reaction.

Briefly, chromaffin cells were plated on 35 mm Petri dishes at a cell density of 106 cells/dish. Transfection was performed during the following day as follows: both DNA and lipofectin reagent were first diluted in 100 μ l each of serum free Opti-MEM® I. Then, they were mixed and incubated at RT for 30 min to allow the formation of the lipid-DNA complexes. After incubation, 800 μ l of DMEM was added to each complex solution and these were added to culture dishes containing cells previously rinsed twice with DMEM medium. Cells were incubated with the DNA-lipofectin complexes for 5 h at 37°C, in atmosphere of O₂ and 5% CO₂. Cells were then rinsed with complete feeding medium and incubated again for 24 h when cells were assayed for the efficiency of transfection. (Qiagen, Mississauga, ON). A summary of the whole procedure for the lipofectin transfection is shown in Fig. 2.5. To evaluate the transfection efficiency, cells were transfected with β -Gal and then stained with X-Gal as described in section 2.5. Two different DNA concentrations at two DNA:lipofectin ratios were used as shown in table 1.

2.3.b. Chromaffin cell transient transfection using a non-liposomal lipid-mediated gene transfer system (Effectene method)

Effectene transfection reagent (Qiagen, Mississauga, ON) is a non-liposomal lipid combined with a proprietary DNA-condensing enhancer. Transfection was conducted as suggested in the manufacturer specifications. In brief, chromaffin cells were plated on collagen-coated 35 mm Petri dishes at a cell density of 106 cells/dish. Transfection was performed the following day as follows: DNA was diluted with the DNA-condensation buffer (provided by the manufacturer) to a total volume of 100 μ l and incubated at room temperature for 5 minutes.

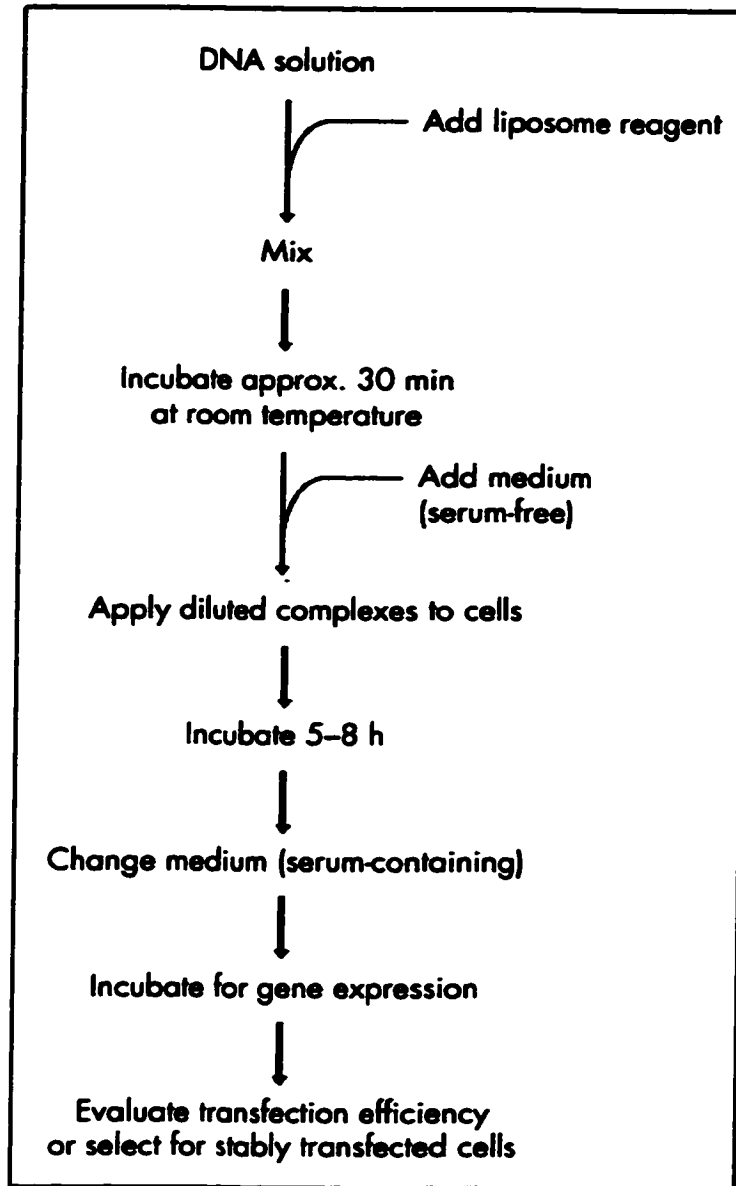


Figure 2.5: Flowchart of lipofectin-mediated transfection.

Briefly, chromaffin cells were plated on 35 mm Petri dishes at a cell density of 10^6 cells/dish. Transfection was performed 24 h later as follows: both DNA and lipofectin reagent were first diluted in $100\ \mu\text{l}$ each of serum free Opti-MEM® I. Then, they were mixed and incubated at room temperature for 30 min to allow the formation of the lipid-DNA complexes. After incubation, $800\ \mu\text{l}$ of DMEM was added to each complex solution and these were added to the cells in each dish previously rinsed two times with DMEM medium. Cultures were incubated with the DNA complexes for five h at 37°C , in an atmosphere of O_2 , and 5% CO_2 . Preparations were then rinsed with CFM and further incubated for 24 h when the cultures were assayed for the efficiency of transfection. (taken from the Instruction manual, Qiagen)

DNA	Lipofectin
4 μ g	4 μ g lipofectin 8 μ l DNA:lipofectin 1:2
8 μ g	8 μ g lipofectin 8 μ l DNA:lipofectin 1:1

Table 1. Optimization of transfection using lipofectin. Chromaffin cells were plated on 35 mm Petri dishes at a cell density of 10^6 cells/ dish. Twenty – four h later the cells were transfected using two different DNA concentrations and, for each DNA concentration, at two different DNA : lipofectin ratios.

Then, the Effectene transfection reagent was added to the DNA dilution and incubated again at RT for 10 minutes to allow the formation of DNA-lipid complex. After incubation, 1.6 ml of complete feeding medium was added to the mixture, mixed and added to the cells previously rinsed with fresh growth medium. After the addition of diluted DNA complexes to the cells, cultures were incubated at 37°C, in an atmosphere of O₂ and 5% CO₂. The assessment for the efficiency of transfection was done using X-Gal (as described in section 2.5), the day after transfection. Since the DNA:effectene ratio is an important parameter to optimize, two different DNA concentrations were used, and, for each DNA concentration, at two DNA:lipofectin ratios as shown in table 2. A summary of the effectene transfection procedure employed is presented in Fig. 2.6.

2.3.c. Chromaffin cell transient transfection using the calcium phosphate method

Calcium phosphate (CaPH) transfection was initially described in the early 1960s (Graham et al., 1973). The method involves mixing DNA in a phosphate buffer containing calcium chloride (Graham et al., 1973). The resulting calcium phosphate – DNA complexes adhere to the cell membrane and enter the cytoplasm by endocytosis. We used the improved CaPH method for bovine chromaffin cell transfection described by Wilson et al. (Wilson et al., 1995). In brief, 24 h prior to transfection, chromaffin cells were plated in collagen-coated 35 mm Petri dishes at a cell density of 10⁶ cells/ dish. Four different DNA amounts were used to determine the transfection efficiency. Samples of DNA, diluted in H₂O were mixed in sterile 15 ml polystyrene centrifuge tubes with aliquots containing 2 M CaCl₂ to give a solution of 20, 50, 100 or 140 µg DNA /ml and 250 mM CaCl₂. An equal volume of solution containing 280 mM NaCl, 1.5 mM sodium

DNA (μg)	Ratio DNA:Effectene	
	1:10	1:25
0.4	0.4 μg DNA 0.8 μl Enhancer 5 μl Effectene	0.4 μg DNA 0.8 μl Enhancer 12.5 μl Effectene
0.8	0.8 μg DNA 1.6 μl Enhancer 5 μl Effectene	0.8 μg DNA 1.6 μl Enhancer 12.5 μl Effectene

Table 2. Optimization of transfection efficiency using the effectene reagent. Chromaffin cells were plated on 35 mm Petri dishes at a cell density of 106 cells/ dish. Twenty-four h later, the cells were transfected using two different DNA concentrations and, for each DNA concentration, two different DNA : effectene ratios. The DNA : enhancer ratio of 1 : 8 was kept constant (according to the manufacturer specifications).

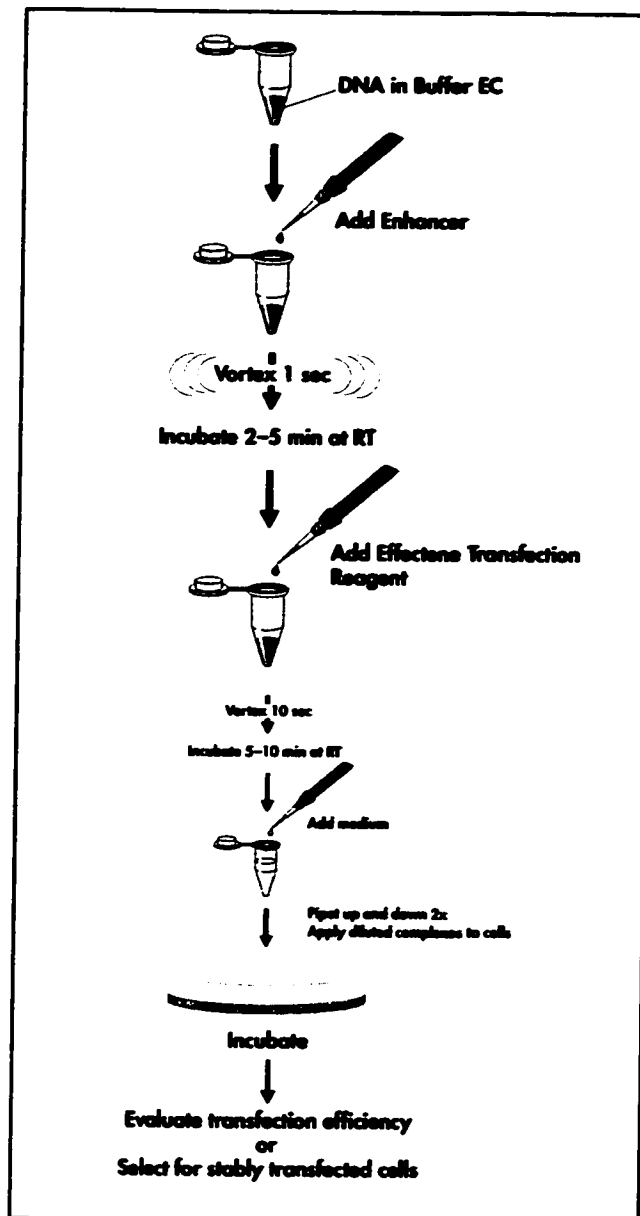


Figure 2.6: Flowchart of effectene-mediated transfection.

Chromaffin cells were plated on collagen-coated 35 mm Petri dishes at a cell density of 106 cells/ dish. Transfection was performed 24 h later as follows: DNA was diluted with the DNA-condensation buffer (Buffer EC-provided by the manufacturer) to a total volume of 100 μ l and incubated at room temperature for 5min. Then, the effectene transfection reagent was added to the DNA dilution and the mixture was incubated at RT for 10 min to allow DNA-lipid complex formation. After incubation, 1.6 ml of complete feeding medium was added to the mixture, mixed and added to the cells previously rinsed with growth medium. Cultures were incubated in an atmosphere of O₂ and 5% CO₂, at 37°C for 24 h. when cultures were assayed for the efficiency of transfection (Taken from the instruction manual, Qiagen).

phosphate and 40 mM PIPES pH: 6.95 was added and shaken briefly. This mixture was then allowed to stand for 30-40 min to allow the formation of the CaPH-DNA complexes. Aliquots of the mixture were then added to the cells. Then the cultures were incubated for 4 h at 37°C, in an atmosphere of O₂ and 5% CO₂. Next, the medium was removed, and the cultures were incubated for 3 min with 1 ml of 12.5% glycerol in serum free culture medium without antibiotics. The cultures were then rinsed with complete feeding medium and returned to the incubator. Twenty-four h after transfection, the efficiency of transfection was determined as described in section 2.5

2.3.d. Chromaffin cell transient transfection by electroporation

The use of high-voltage pulses to introduce DNA into cultured cells was first established by Wong and Neumann (1982), using fibroblasts. Cells placed in an electrocuvette are subjected to a short high-voltage pulse that causes the membrane potential of the cells to break down (Wong and Neumann, 1982). As a result, pores are formed through which macromolecules such as DNA can enter (Fig. 2.7). In short, chromaffin cells purified by differential plating (section 2.1) were scraped off the Petri dishes and pooled. Cell number was determined using a haemocytometer (Neubauer, Levy chamber) and then the cell suspension was centrifuged at 500g, RT, for 15 min. The supernatant was discarded and the cell pellet thus obtained was resuspended in ice cold, serum free RPMI 1640 medium (Armstrong et al., 1996).

Cell suspension was centrifuged again at 500g, RT, for 15 min, and the cell pellet was resuspended at a cell density of 10⁷ cells in 0.4 ml ice cold, serum free RPMI 1640 medium and placed in an electro-cuvette (Armstrong et al., 1996). Plasmid DNA (prepared using QIAGEN megaprep columns) was added to the electro-cuvette.

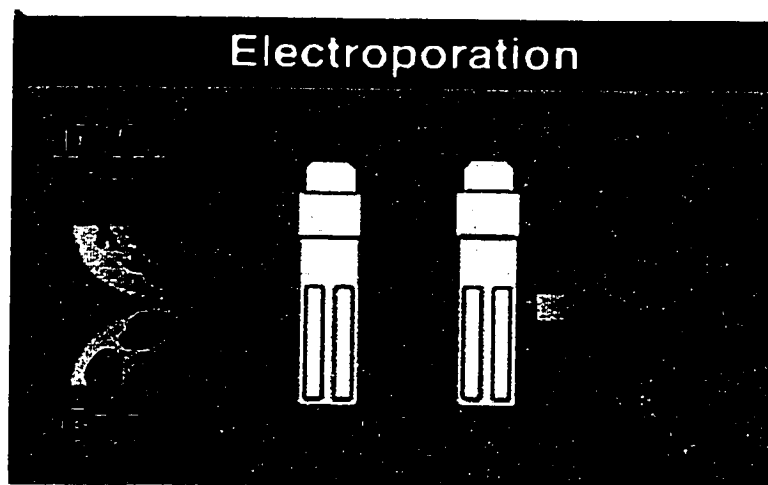


Figure 2.7: Electroporation principle. Electroporation uses high-voltage pulses to introduce DNA into cultured cells (Wong and Neumann, 1982). Cells placed in an electroporation cuvette were subjected to a high-voltage pulse. That caused the membrane potential to break down forming pores through which DNA could enter the cells (Wong and Neumann, 1982).

After incubation at 4 °C, for 10 min, the cells were electroporated using a Bio-Rad Gene Pulser (Bio-Rad, Hercules, CA) and placed on ice for 20 min. A summary of the electroporation procedure is presented in Fig. 2.8. To establish the best electroporation conditions (good transfection efficiency and minimal cell death), two different voltages (150 and 250 V) and three plasmid DNA concentrations (10µg, 25µg, and 50µg) were tested (Chu et al., 1987).

A typical transfection procedure was as follows: a cell suspension of 10⁷ cells in 0.4 ml serum free medium was placed in an electrocuvette with the gap width of 0.4 cm. One electric pulse (time constant of 34 to 39 msec) of 250 V, 1020 µF was passed through the preparation. Fifty µg plasmid DNA was used during a single transfection or, 25 µg (each) when cells were simultaneously transfected with two plasmids.

2.4. Determination of chromaffin cell viability following electroporation

Cell viability was investigated by measuring the relative cell number either directly by counting cells or indirectly by measuring total protein content or total DNA content using . For both methods, electroporated and non-electroporated cells (control) were plated at the same cell density of 1.5 x 10⁶ cells / 35 mm dish. Determination of cell viability was performed 24 hours after plating.

2.4.a. Determination of chromaffin cell number by counting cells.

Twenty four h after plating, cells were rinsed twice with Locke's solution in order to remove all dead cells. Cells were then counted under light microscopy. A minimum of three dishes and ten fields per dish were counted for both electroporated and non-electroporated (control) conditions. The results were plotted as mean ± S.E.M.

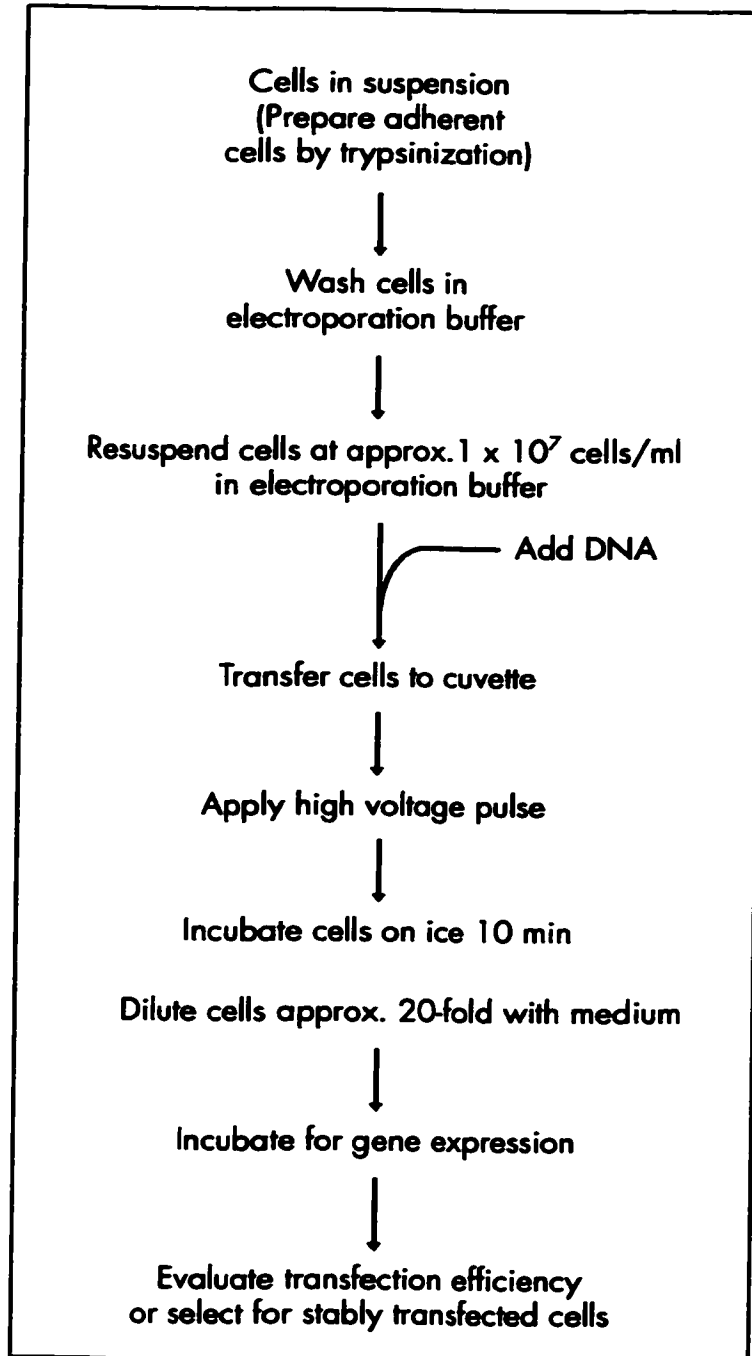


Figure 2.8: Flowchart of transfection by electroporation.

2.4.b. Determination of chromaffin cell number by measuring total DNA content

Total DNA content was determined using a CyQUANT cell proliferation assay kit (Molecular Probes, ON, Canada). The basis of the CyQUANT assay is the use of a proprietary green fluorescent protein dye, CyQUANT GR dye, which exhibits strong fluorescence enhancement when bound to cellular nucleic acid. A reference standard curve was created for converting sample fluorescence values into cell numbers. Non-electroporated chromaffin cells were used to obtain the standard curve. To generate the standard curve, a series of chromaffin cell dilutions were prepared, with cell number ranging from 50 to 20,000, according to the manufacturer specifications. Frozen cells were thawed and lysed by the addition of a lysing buffer (provided by the manufacturer-Molecular Probes) containing the CyQUANT GR dye. The fluorescence measurement was then performed using a fluorometer. Samples were placed in a quartz cuvette and fluorescence measurements were made using an excitation 485 nm and emission detection at 530 nm.

2.4.c. Determination of chromaffin cell number by measuring total protein content

Protein assays in the range of 1-20 µg were performed according to Bradford (1976), using a commercially available product (Bio-Rad protein assay, Richmond, CA). Bovine serum albumin (Sigma, Mississauga, ON) was used as a standard.

2.5. Measurement of chromaffin cell transient transfection efficiency

In experiments done to establish optimal transfection conditions, chromaffin cells were transfected with a plasmid containing the lacZ gene that encodes β- galactosidase (Fig.

2.9). LacZ is frequently used as a reporter gene system. Transfected cells were revealed cytochemically by staining for β -galactosidase with 5-bromo-4-chloro-3-indolyl- β -D-galactopyronside (X-Gal) (Sambrook et al., 1989; Sanes, 1986).

Chromaffin cells were plated at a cell density of 10^6 cells / 35 mm dish. Twenty-four h following transfection, cells were rinsed with Locke's solution (154 mM NaCl, 2.6 mM KCl, 1.25; KH₂PO₄, 2.3 mM MgCl₂, 2.2 mM CaCl₂, glucose, 10 mM, pH 7.2) and fixed in 3.7% formaldehyde in Locke's, for 20 minutes. Cells were then washed twice with 1 ml of phosphate buffered saline (PBS; 130 mM NaCl, 100 mM Na – phosphate, pH 7.0). The substrate-stain solution (1 mg/ml X-Gal, 5mM K- ferricyanide, 5 mM K-ferrocyanide, 2 mM MgCl₂ in PBS) was added, and cells were incubated between 2 and 24 h at RT (Sanes, 1986). Following staining, cells were rinsed with PBS and observed using light microscopy. Enzymatic hydrolysis of the X-Gal yields a dark blue colored precipitate. Therefore, the percentage of the blue, X-gal positive cells was determined for all transfection methods by direct counting of the cells from at least 3 dishes and 10 fields per dish were counted. When chromaffin cells were transiently transfected with two plasmids (pEGFP alone or including one of the Sc deletion mutants and pXGH5- plasmid including a hGH gene) cells were plated on collagen coated cover slips contained in 35 mm dishes at a cell density of 10^6 cells /cover slip. Cells were incubated at 37°C, under an atmosphere of O₂ and 5% CO₂. Thirty-six to 60 h after transfection, chromaffin cells were rinsed twice with Locke's solution, and fixed in 3.7% formaldehyde in Locke's for 20 minutes. Next, the cells were permeabilized with acetone as described by Trifaró et al. (Trifaró and Lee, 1980) and in section 2.7.b. Then, chromaffin cells were stained for hGH and visualized using fluorescence microscopy.

From the total number of cells, the percentage of cells expressing both hGH and GFP was determined. Moreover, in the population of cells expressing hGH, the percentage of cells that also expressed GFP was determined. In the GFP positive cells, the percentage of cells also expressing hGH was determined. Cells from at least 3 dishes and 10 fields per dish were counted for all conditions.

2.6. Improvement of hGH labeling of chromaffin cell vesicles using an extensive high K⁺ (56 mM) - induced depolarization

For a typical release experiment, transfected chromaffin cells were plated on 35 mm dishes, at a cell density of 3×10^6 cells / dish (calculated before electroporation). For immunocytochemical experiments, cells were usually plated at a cell density before electroporation of 10^6 cells/ collagen-coated cover slip. Twelve h after plating (when chromaffin cells were attached), cells were briefly rinsed with Locke's solution (154 mM NaCl, 2.6 mM KCl, 1.25; KH₂PO₄, 2.3 mM MgCl₂, 2.2 mM CaCl₂, glucose, 10 mM, pH 7.2). Cells were then stimulated for 8 min with depolarizing concentrations (56 mM) of K⁺ (Trifaró et al., 1984). This stimulation period was repeated three times at 8 min intervals. Between stimulations, cells were allowed to recover in Locke's solution. After the last depolarization, cells were rinsed with Locke's solution and incubated until required for further experiments in complete feeding medium (CFM) at 37°C, in an atmosphere of O₂ and 5% CO₂

2.7. Characterization of chromaffin cells expressing hGH and GFP-fused Sc deletion constructs

2.7.a. Determination of protein expression by electrophoresis.

immunoblotting and densitometric analysis

All proteins were analyzed by mono-dimensional 10% sodium dodecyl sulphate-polyacrylamide gel electrophoresis (SDS-PAGE) according to Doucet et al. (1988). Gels were usually run at 50 V until samples entered the separating gel, and then at 100 V for 2h or at 14 V overnight in a Bio-Rad Protein I apparatus (Bio-Rad Laboratories Inc., Richmond, CA). Following electrophoresis, proteins were electrotransferred onto polyvinylidene difluoride (PVDF) membranes (pore size: 0.2 μm , Bio-Rad, Mississauga, ON, Canada). Membranes were first blocked with 5% milk in 1% tween- PBS (130 mM NaCl, 100 mM Na – phosphate, pH 7.0), and then incubated for 60 min with antibodies raised against various antigens (hGH, Sc, tubulin, GFP). Membranes were next incubated with the corresponding HRP- conjugated secondary antibodies for another 60 min. Antibodies bound to the membrane were visualized by chemiluminescence after treatment with ECLTM (Amersham, Oakville, ON, Canada) followed by exposure to hyperfilmTM (Amersham, Oakville, ON, Canada). The intensity of the bands was analyzed using the NIH Image 1.61 software (NIH, Bethesda, MD). The areas under the peaks were integrated using the same program. In experiments done to see the expression of GFP-fused deletion mutants and hGH, tubulin was used as an endogenous control to normalize the results.

2.7.b. Analysis of hGH localization in chromaffin vesicles by immunocytochemistry and fluorescence microscopy

Chromaffin cells were transfected by electroporation at 250 V, 1020 μF using 50 μg pXGH5 plasmid DNA (as described in chapter 2.3). Cells were then plated on collagen coated cover slips in 35 mm dishes at a cell density of 10^6 cells /cover slip and incubated

at 37°C, in an atmosphere of O₂ and 5% CO₂.

To study the localization of hGH in chromaffin vesicles, 36 to 60 h post transfection, chromaffin cells were briefly rinsed with Locke's solution, fixed in 3.7% formaldehyde in Locke's solution for 20 min, and processed for fluorescence microscopy as previously described (Lee and Trifaró, 1981). Briefly, cells were permeabilized using three successive incubations of five min each of 50, 100, and 50% acetone. Then, cover slips were washed 6 times with PBS, and blocked for 1 h in 1% BSA in PBS. Chromaffin cells were then successively incubated at RT with a polyclonal rabbit antibody against hGH (diluted 1:100 in 0.1% BSA in PBS) for 60 min and then with a rhodamine-conjugated goat anti-rabbit IgG for another 60 min. For D β H staining, cells were further incubated successively with a monoclonal mouse D β H antibody (diluted 1:2000, 0.1% BSA in PBS) for 60 min and then with a fluorescein isothiocyanate (FITC) labeled donkey antimouse IgG (diluted 1:300 in 0.1% BSA in PBS). Finally, cover slips were washed with PBS and mounted in glycerol:PBS (1:1). Slides were observed with a Bio-Rad 1024 confocal system (Bio-Rad, Richmond, CA) attached to an Olimpus AX-70 microscope, using a 1.4 numerical aperture oil 60X objective (for fluorescence and differential interference contrast or DIC). When indicated, images were acquired at 50 nm interval following the Z-axis of the cell. Images of 512 X 12 pixels using an aperture (pinhole) of 2 maximum were collected, processed with Confocal Assistance 4.12 software (Bio-Rad) and exported into Adobe Photoshop 4.0 for final enhancements and presentation.

2.8. Analysis of cortical F-actin distribution in resting and stimulated chromaffin cells

2.8.a. Fluorescence microscopy

To study the cortical F-actin distribution, cells expressing GFP alone (control) or one of the GFP-fusion Sc deletion constructs were briefly washed with Locke's solution and incubated for 1 minute either with Locke's solution or with depolarizing concentration (56 mM) of K⁺ in Locke's (Vitale et al., 1991). In other experiments, cells were incubated for 40 sec with either Locke's solution or Locke's solution containing 10 μ M Nicotine. At the end of the incubation period, cells were fixed for 20 minutes with 3.7% of formaldehyde in Locke's solution. Preparations were then rinsed several times with PBS and then permeabilized by three successive exposures of five minutes each to 50, 100, and 50% acetone. Permeabilized cells were then washed several times with PBS and incubated at RT for 40 min with 0.3 μ M rhodamine-labeled phalloidin (Molecular Probes, Inc, Eugene, OR) a probe for filamentous actin (Faulstich et al., 1988). At the end of incubation, cover slips were washed six times with PBS and mounted in glycerol:PBS (1:1). Between 50 and 100 cells per cover slip, expressing either the vector alone or one of the GFP-Sc fusion constructs were classified as having either "continuous" staining or a "discontinuous" patched staining pattern (Vitale et al., 1991). This was done without knowing what insert was expressed in the cells or whether cells were from control or stimulated preparations (single blind design) (Vitale et al., 1991).

2.8.b. Video-enhanced image processing

Color pictures were taken using a Sony digital camera and digital pictures were acquired using a Northern Eclipse Software (Empix Inc.). Digital images were then imported into

Adobe Photoshop 4.0 software for further processing. Quantitative analysis of cortical rhodamine fluorescence (F-actin) was performed using a Hamamatsu Photonic KK Argus 50/CL Image Processor (Hamamatsu Photonic Systems; Bridgewater, NJ) coupled to a TV3M Zeiss video camera, as previously described (Vitale et al. 1995). Video camera parameters (i.e. gain, offset and sensitivity) were kept constant and fluorescence intensity was expressed in arbitrary units (Vitale et al., 1995).

2.9. Analysis of the effects of Sc1-6 or Sc deletion constructs overexpression on high K⁺- or nicotine- evoked chromaffin cell exocytosis

To study the effects of different Sc deletion overexpressions on regulated secretion, plasmid GFP –Sc- fusion vectors and the reporter plasmid pXGH5 (fig. 2.10, a) encoding the hGH protein, were transiently co-transfected by electroporation as previously described (section 2.3.d). Human GH was expressed using pXGH5 (Fig. 2.10, a.) in which hGH expression was driven by a mouse metallothionein-I promoter (Selden et al., 1986; Searle et al., 1985). This plasmid is available as part of the radioimmuno assay kit (Nichols Institute, San Juan Capistrano, CA).

The Nichols Institute Diagnostics Immunoassay incorporates two monoclonal antibodies with high affinity and specificity for the hormone. These two antibodies (obtained from mouse) are specific for different and distinct epitopes on the hGH molecule, so that they bind without competition or steric interference from each other, and form a soluble sandwich complex (Fig. 2.10, b): Ab(1) - hGH – Ab(2). One of these monoclonal antibodies is radio labeled (Fig. 2.10, b.), while the other is coupled to biotin.

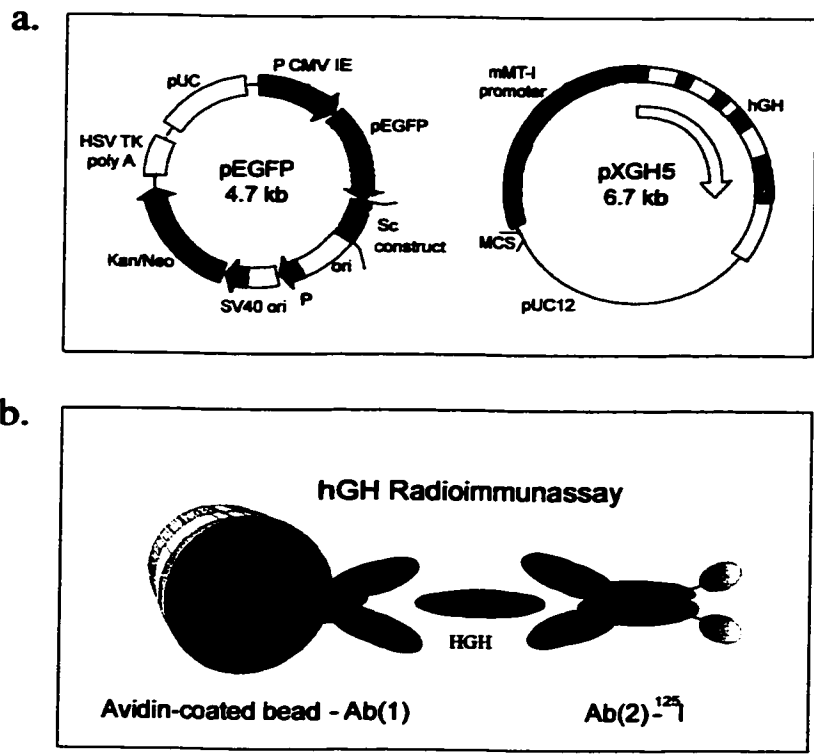


Figure 2.10: Scheme of the hGH reporter system used to study regulated secretion

- a. Schematic representation of the pEGFP carrying a Sc deletion construct and the pXGH5 vector carrying the hGH gene. Plasmids pEGFPC3 (alone or containing a Sc construct) pXGH5 encoding the hGH protein, were transiently transfected in chromaffin cells by electroporation. hGH expression is driven by a mouse metallothionein-I promoter (Selden et al., 1986; Searle et al., 1985)
- b. The hGH transient assay is based on a simple immunological detection of hGH secreted by the transfected cells [(Selden et al., 1986). The Nichols Institute Diagnostics Immunoassay incorporates two monoclonal mouse-derived antibodies. These antibodies are specific for different and distinct epitopes on the hGH molecule. One of these monoclonal antibodies is radio labeled, while the other is coupled to biotin. The incubation of the two samples and the two antibodies with an avidin-coated plastic bead allows the formation of a sandwich: Avidin coated bead – biotin Ab(1) – hGH – Ab(2)* . At the end of incubation, the bead is washed to remove unbound components and the radioactivity bound to the solid phase is measured in a gamma counter. A concentration-response curve of radioactivity vs. concentration is generated using results obtained with standards provided by the manufacturer.

The addition to the reaction mixture of an avidin-coated plastic bead provides a specific and efficient means of binding the sandwich to a solid phase via high affinity interaction between biotin and avidin: Avidin-coated bead – biotin Ab(1) – hGH – Ab(2)*. In the assay system, standards, controls or samples are incubated with a solution containing the radiolabeled antibody, the biotin-coupled antibody and an avidin coated plastic bead. At the end of incubation, the bead is washed to remove the unbound components and the radioactivity bound to the solid phase is measured in a gamma counter. Since the formation of a sandwich complex occurs only in the presence of an hGH molecule, the radioactivity of the avidin bound sandwich complex is directly proportional to the amount of hGH in the sample. A concentration-response curve of radioactivity vs. concentration is generated using results obtained from the standards provided by the manufacturer.

Typical release experiments were conducted as follows: chromaffin cells highly purified by differential plating as described in section 2.1 (Waymire et al., 1983) were transiently transfected by electroporation using 25 μ g DNA of pEGFP (alone or with Sc insert) and 25 μ g of pXGH5. Cells electroporated in the absence of any plasmid (mock) were used as a control. Cells were plated at a cell density of 3×10^6 and incubated at 37°C, in an atmosphere of O₂ and 5% CO₂. Twelve hours post transfection, cells were extensively depleted of the intra-cellular stores by three pulses of depolarizing concentration (56 mM) K⁺, as described in section 2.6 (Trifaró et al., 1984). Release experiments were usually carried out 24 or 48 h following depolarization. All solutions were equilibrated at room temperature prior to the experiment. Briefly, chromaffin cells were rinsed several times with 1 ml of Locke's solution and then incubated for 2 min with 0.5ml regular Locke's solution, followed by 0.5 ml of depolarizing concentration (56 mM) of K⁺ (high

potassium Locke's solution) for 2 min. In other experiments, cells were incubated for 40 sec with 0.5 ml regular Locke's and then with 0.5 ml of 10 μ M nicotine in Locke's solution for 40 sec. Incubation solutions were saved on ice for further processing. Cells were lysed in 0.3 ml (3 times 0.1 ml) of 10 mM HEPES (pH 7.4) and 0.2 mM EDTA. Detergent was not used in these experiments because it interferes with hGH assay (Holz et al., 1995). In order to release hGH from the chromaffin vesicles, cell lysates were prepared by sonication (Holz et al., 1995). Aliquots from the incubation medium and cell lysates were then processed for the determination of hGH content, by adding 100 μ l of ¹²⁵I-labeled antibody solution and an avidin-coated bead. The samples were incubated at 4 °C for 24 h. Solutions were then aspirated and the beads were washed with 1 ml wash solution 4 times, for 10 min each time. The radioactivity of the beads was then measured using a γ - counter. The hGH output was then calculated as a percentage of total cell hGH content after subtracting the values obtained from the mock cells.

2.10. Statistical analysis

Mean and standard error (mean \pm SEM) values for the data obtained from experiments were calculated and plotted using the Sigma Plot software (version 5). Significant differences among the means were determined with the Student-t test (paired or unpaired), using the Slide Write Software (Advanced Graphic Software Inc.). When more than two groups were compared and /or multiple comparisons were performed, the Anova test was used (Corel Quatro Pro, Corel Corp.). The word "significant" refers to a statistical difference with "p" values less than 0.05 ($p < 0.05$), 0.01 ($p < 0.01$), or 0.001 ($p < 0.001$).

3 – RESULTS

Characterization of the co-transfection gene system

To study the role of different scinderin domains in regulated secretion, we needed to express the constructs in chromaffin cells. Since chromaffin cells are primary cultures difficult to transfect, and only a small population of cells are transfected, we decided to use a reporter system for regulated secretion (hGH reporter system). A key part of this approach is to co-transfect into chromaffin cells an effector plasmid (pEGFP alone or with different Sc fragments) together with a reporter plasmid encoding human growth hormone (hGH) – pXGH5. Figure 3.1 shows a schematic representation of vector pXGH5 and the localization of hGH in chromaffin cells. Consequently, the first approach was to compare different techniques of transfection in order to obtain the best possible system to study the secretory process. Secretion from transfected cells, and, therefore, the effects of Sc fragments on secretion, was determined by measuring hGH release, using a radioimmunoassay as described in Chapter 2 (Materials and Method)

3.1. Transient transfection of chromaffin cells

Chromaffin cells are non-dividing, primary cells that are quite difficult to transfect. Therefore, the choice of the transfection method might strongly influence transfection results. Four different transfection methods were used and compared for their ability to transiently transfect chromaffin cells. To investigate the transfection efficiency, a plasmid for β -galactosidase was also transfected into chromaffin cells. This was followed by X-GAL staining as described in Chapter 2 (Materials and Methods). The percentage of X-GAL positive cells was then determined for all transfection methods.

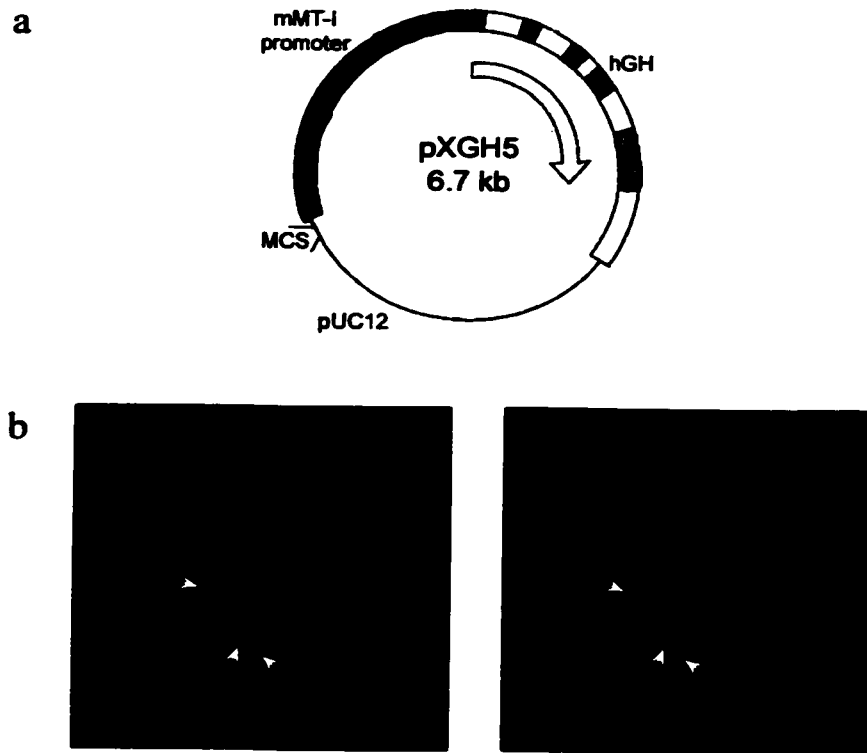


Figure 3.1: pXGH5 vector map.

Human growth hormone (hGH) gene is represented in red. Chromaffin cells were transiently transfected by electroporation with plasmid pXGH5 as described in Materials and methods. Cells were then plated on collagen coated cover slips contained within 35 mm dishes, at a cell density of 106 cells / cover slip and they were incubated at 37°C, under an atmosphere of O₂ and 5% CO₂. Thirty six h following transfection, cells were fixed, permeabilized and processed for immunofluorescence using anti-hGH and anti-dopamine β-hydroxylase (DBH), a chromaffin vesicle marker.

Slides were observed with a Bio-Rad 1024 confocal system (Bio-Rad, Richmond, CA) attached to an Olympus AX-70 microscope, using a 1.4 numerical aperture oil immersion 60X objective (for fluorescence and differential interference contrast or DIC) (b). Two chromaffin cells are shown in panel b (left) after staining for DBH. Staining for hGH (right) shows that only one cell is transfected. Arrows indicate secretion vesicles positive for both DBH and hGH.

3.1.a. Chromaffin cell transient transfection using lipofectin

Lipofectin is a positively charged liposome that interacts with negatively charged DNA to form a stable complex (Felgner et al., 1987). The DNA concentration and the lipid:DNA ratio and overall lipid concentrations used in forming these complexes are important parameters for efficient gene transfer (Chang et al., 1988). Two different DNA concentrations were used as described in Chapter 2. Using 4 μg DNA and a lipid: DNA ratio of 1:2, approximately 0.1% of the cells were transfected. Increasing the DNA concentration to 8 μg , while keeping the amount of lipofectin constant (ratio 1:1), resulted in doubling the transfection efficiency (Fig. 3.2) ($0.2 \pm 0.025\%$, $n=3$).

3.1.b. Chromaffin cell transient transfection using effectene

Effectene is a non-liposomal lipid-mediated gene transfer technique. DNA was strongly condensed by interaction of negatively charged phosphate groups of the nucleic acid with a specific positively charged enhancer (Ausubel et al., 1991). The condensed DNA was then coated with a cationic non-liposomal lipid (Ausubel et al., 1991). The DNA concentration and the DNA:effectene ratio used to form these complexes are important for the efficiency of gene transfer (Ausubel et al., 1991). Two different DNA concentrations at two different DNA:effectene ratios were used. The best transfection ($0.5\% \pm 0.05\%$, $n=3$) was obtained at a DNA concentration of 0.8 μg and a DNA:effectene ratio of 1:25 (Fig. 3.3).

3.1.c. Chromaffin cell transient transfection using calcium phosphate

The calcium phosphate (CaPH) method involves mixing DNA in a phosphate buffer containing calcium chloride (see Materials and Methods).

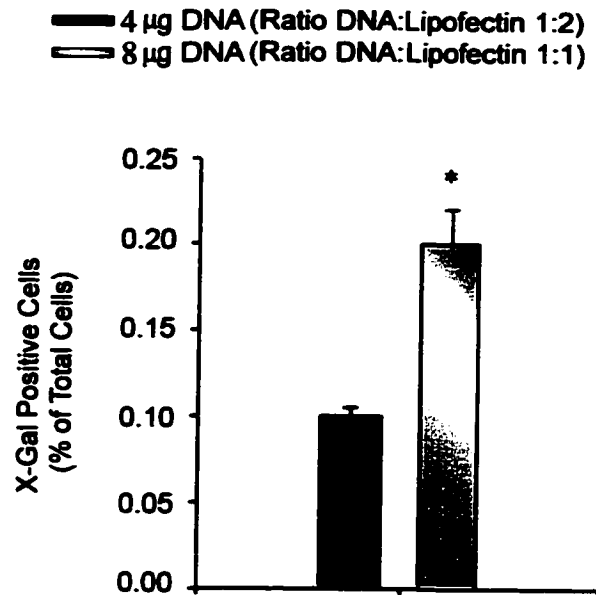


Figure 3.2: Lipofectin mediated transfection.

Chromaffin cells were plated on 35 mm dishes at a cell density of 106 cells/dish. After 24 h in culture, cells were transfected with β -Gal, using two different DNA concentrations and for each DNA concentrations two different DNA:lipofectin ratios were used. Transfected cells were revealed cytochemically by staining for β -galactosidase (as described in Materials and Methods). The percentage of X-Gal positive cells was determined by directly counting the blue-stained cells. Doubling the DNA concentration, resulted in doubling the percentage of transfected cells. Bars represent the mean \pm S.E.M of $n = 3$ experiments. In each experiment, each condition was assayed in quadruplicate. * $p < 0.05$.

■ 0.4 μ g DNA (Ratio DNA:effectene 1:10)
 ■ 0.4 μ g DNA (Ratio DNA:effectene 1:25)
 ■ 0.8 μ g DNA (Ratio DNA:effectene 1:25)
 ■ 0.8 μ g DNA (Ratio DNA:effectene 1:10)

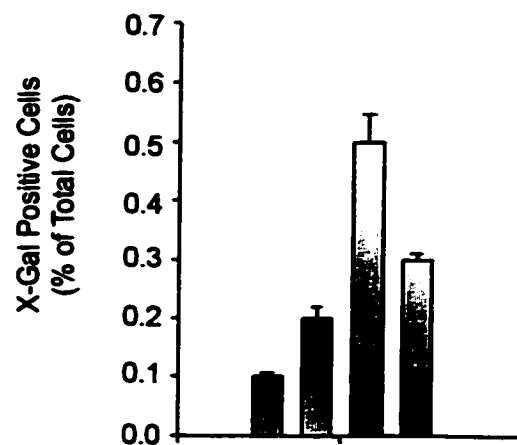


Figure 3.3: Effectene mediated transfection.
 Chromaffin cells were plated on 35 mm dishes at a cell density of 106 cells/dish. After 24 h in culture, cells were transfected with β -Gal, using two different DNA concentrations and for each DNA Concentration two different DNA:Effectene ratios were used. Increasing the DNA concentration led to an increase in transfection efficiency. Increasing the DNA:Effectene ratio resulted in an increase of the efficiency of transfection. The best transfection efficiency was obtained with 8 μ g DNA and a DNA:Effectene ratio of 1:25. Bars represent mean \pm S.E.M. of n = 3 to 5 experiments. In each experiment, each condition was assayed in quadruplicate. The results yielded by all of the conditions imposed were significantly different from each other ($p < 0.05$).

The resulting calcium-phosphate-DNA complexes adhere to the cell membrane and enter the cytoplasm by endocytosis (Graham and Van der Eb, 1973). The amount of DNA used the time of the incubation of cells with the precipitate and the glycerol shock following incubation are important factors for the efficiency of the transfer (Wigler et al., 1978). Increases in DNA amount did not result in a linear increase in transfection efficiency (Fig. 3.4). The optimal transfection ($2.2 \pm 0.4\%$, $n=3$) was observed with a plasmid DNA concentration of $50\mu\text{g/ml}$ in the final mixture. Higher DNA concentrations resulted in lower β -galactosidase expression ($0.2 \pm 0.03\%$, $n=3$) as showed in Fig. 3.4.

3.1.d. Chromaffin cell transient transfection by electroporation

Electroporation involves the exposure of cells to an electric field during a fixed period of time. This induces the formation of pores in the plasma membrane (Potter, 1992). The amount of DNA, current intensity, voltage and the time of incubation on ice before and after the application of the electric pulse are important parameters for the efficiency of transfection and for cell viability (Chu et al., 1987). Several studies have been performed to investigate the optimal conditions for electroporation in mammalian cells (Potter H, 1999). The best transfection efficiency with minimal cell death has been obtained using low voltage and high capacitance settings (Chu et al., 1987). In the present studies, cell viability was determined by plating the cells exposed or not exposed (control) to an electric field, on parallel plates, allowing them to attach, and then measuring the relative cell number either directly by counting or indirectly, by measuring either total protein content or total DNA content as described in Chapter 2 (Materials and Methods). Two different voltages were tested (150 V and 250 V) at a given capacitance of $1020\ \mu\text{F}$. Cells were assayed for survival and efficiency of transfection.

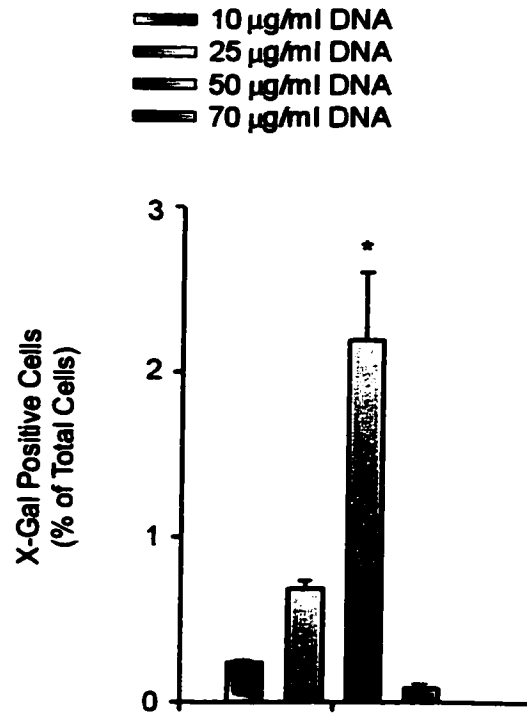


Figure 3.4: Calcium phosphate – mediated transfection.

This method involves mixing DNA in a phosphate buffer containing calcium chloride (Graham et al., 1973). The resulting calcium phosphate – DNA complexes adhere to the cell membrane and enter the cytoplasm by endocytosis. Twenty-four h prior to transfection, chromaffin cells were plated on collagen-coated 35 mm Petri dishes at a cell density of 106 cells/dish. Four different DNA amounts were used to determine the best transfection efficiency. Increases in DNA amount did not result in a linear increase in transfection efficiency. The optimal transfection was observed with a plasmid DNA concentration of 50 µg/ml in the final mixture. Higher DNA concentrations resulted in lower β-galactosidase expression. Each bar represents the mean ± SEM of the percentage of blue cells of 4 to 6 dishes from three different chromaffin cell cultures.

*p < 0.05.

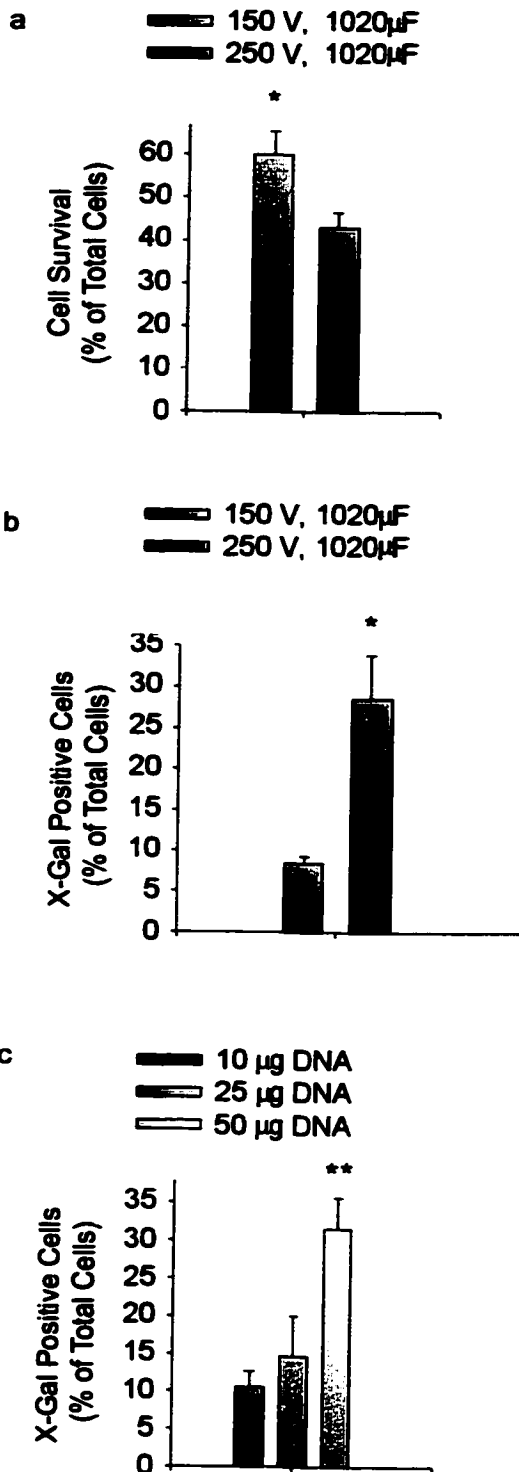


Figure 3.5: Transfection using electroporation.

Chromaffin cells purified by differential plating (section 2.1) were collected from Petri dishes by several washings with culture medium. Then the cell suspension was centrifuged at 500 g, at RT, for 15 min. The supernatant was discarded and the cell sediment thus obtained was resuspended in ice cold, serum free RPMI 1640 medium (Armstrong et al., 1996). Cell suspension was centrifuged again at 500 g, RT, for 15 min, and the cell pellet was resuspended at a cell density of 107 cells in 0.4 ml ice cold, serum free RPMI 1640 medium and placed in an electro-cuvette (Armstrong et al., 1996). The plasmid DNA was added to the electro-cuvette and cells were incubated at 4°C, for 10 min. Cells were then electroporated using a Bio-Rad Gene Pulser (Bio-Rad, Hercules, CA) and placed on ice for an additional 20 min. Two different voltages (150 V and 250 V), at a capacitance of 1020 μ F were tested for cell survival (a) and for transfection efficiency (b). Efficiency of transfection was tested for one pulse of 1020 μ F and 250 V, in the presence of increasing DNA concentrations (c). Bars represent mean \pm S.E.M. of 3 to 4 experiments. For each experiment, each condition was assayed in quadruplicate.

* $p < 0.05$.

** $p < 0.005$ This is the significance vs. each of the other two conditions.

Voltage increase from 150 to 250 V resulted in a 27% decrease in cell viability (Fig. 3.5. a). However, a voltage of 250 V resulted in a 3.4 times increase in transfection efficiency when compared with the efficiency at 150 V (Fig. 3.5, b). Furthermore, transfection efficiency increased with increases in plasmid DNA concentration in the medium (Fig.3.5, c). The following transfection conditions were found optimal with respect to cell viability and transfection efficiency: one pulse of 250 V, 1020 μ F and 50 μ g DNA/ 10⁷ cells (in a volume of 400 μ l), for a time of 34 to 39 msec, in a 0.4 cm diameter cuvette. These parameters were used in all subsequent experiments.

3.2. Localization of hGH in chromaffin vesicles

Human growth hormone (hGH) is normally expressed and secreted from somatotrophs of the anterior pituitary (Herlant, 1964). These cells store growth hormone in dense core granules, which are released by exocytosis upon cell stimulation. The following experiments were undertaken to determine the localization within chromaffin cells of transiently expressed hGH.

3.2.a. hGH localization in chromaffin cells by immunocytochemistry

Immunofluorescence studies were used to determine the localization of hGH within secretory vesicles. Chromaffin cells were transiently transfected with plasmid pXGH5 as described in Chapter 2 (Materials and Methods). Thirty-six hours following transfection, cells were fixed, permeabilized and processed for immunofluorescence using anti-hGH and anti -dopamine β - hydroxylase (DBH), a chromaffin vesicle marker (Trifaró et al. 1976). DBH, an enzyme involved in the conversion of dopamine to noradrenaline, is present in chromaffin vesicles in two forms: a soluble (50%) and a membrane bound (50%) form (Trifaró et al. 1976).

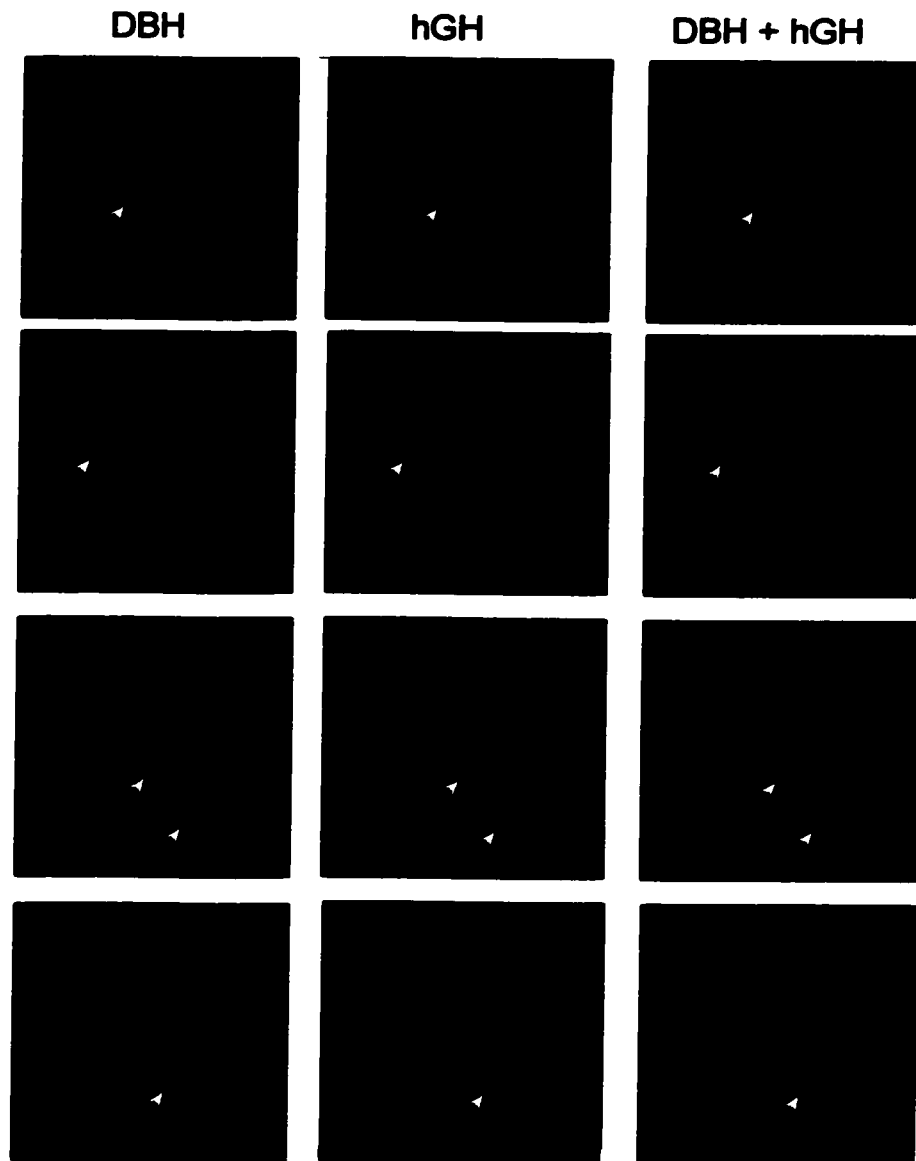


Figure 3.6: Immunohistochemical localization of DBH and hGH. Chromaffin cells were transiently transfected by electroporation with plasmid pXGH5 and plated on collagen-coated cover slips, as described in Chapter 2 (Materials and Methods). Thirty-six hours following transfection, cells were fixed, permeabilized and labeled using anti-hGH and anti -dopamine β - hydroxylase (D β H), a chromaffin vesicle marker. Slides were observed under a Bio-Rad 1024 confocal system (Bio-Rad, Richmond, CA) attached to a Olimpus AX-70 microscope, using a 60X /1.4 oil immersion objective (for fluorescence and differential interference contrast or DIC). Over each cell, we performed a Z-series of optical sections (Z step 50 nm). Each panel shows four of the sections of a single cell. Images were acquired in the fluorescein (left) and rhodamine (middle) channels and were superimposed for double exposures (right). All vesicles stained for hGH were also positive for D β H. Conversely, not all the D β H positive vesicles were positive for hGH. The perinuclear red staining (middle panels) is probably due to the accumulation of hGH in the Golgi apparatus. Arrows show vesicles that were positive for both D β H and hGH.

Small amounts of the enzyme are also found in the Golgi apparatus of chromaffin cells. Images shown in Fig. 3.6 were acquired by confocal microscopy. The images were subsequently integrated using a BioRad software, assigning a different pseudocolour to each channel, as described in Chapter 2 (Materials and Methods). Figure 3.6 shows localizations of hGH and DBH. Integrated confocal images indicate that there was extensive overlap in the staining; with both markers showing similar dot-like staining. This staining corresponds to secretory vesicles; all vesicles stained for hGH were also positive for DBH. On the other hand, not all the DBH positive vesicles were positive for hGH. This can be explained by the fact that hGH is synthesized, packed and distributed only in newly synthesized chromaffin vesicles, whereas DBH and catecholamines are present in both newly synthesized vesicles and vesicles present prior to transfection. The perinuclear red staining is probably due to the accumulation of hGH in the Golgi apparatus. The absence of the red staining in the non-transfected cells demonstrates the specificity of the staining for hGH (data not shown).

3.2.b. Transiently expressed hGH undergoes secretion from chromaffin cells in response to cell depolarization

To further demonstrate that transiently expressed hGH was packed and selectively stored in functional secretory vesicles, cells were stimulated to secrete 60 h following transfection (Materials and Methods). Chromaffin cells were incubated in Regular Locke's solution or in 56 mM K⁺ Locke's (high K⁺) solution for 2 minutes. At the end of the incubation period, cells were lysed and total hGH was measured. Results shown in Fig. 3.7 were expressed as a percentage of total hGH cell content. Chromaffin cells stimulated with 56 mM K⁺ released up to $6.3 \pm 0.53\%$ (n=4) of the total hGH content.

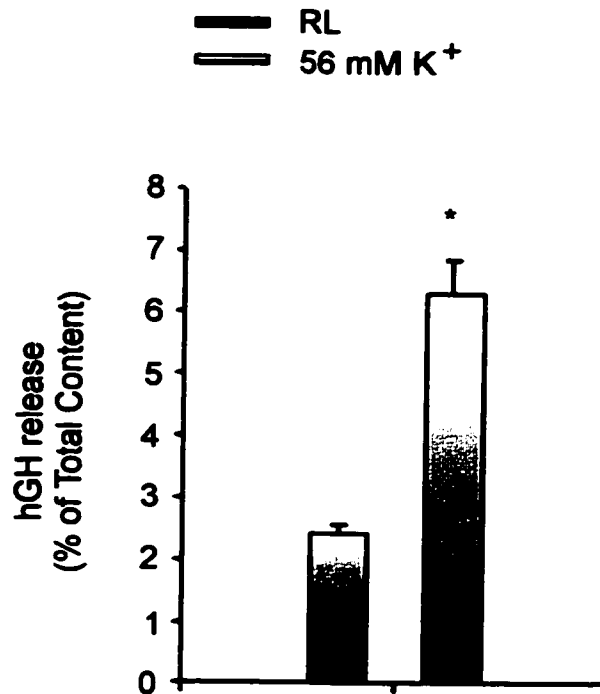


Figure 3.7: Transiently expressed hGH undergoes secretion from chromaffin cells in response to cell depolarization.

Chromaffin cells highly purified by differential plating (Waymire et al., 1983) were transiently transfected by electroporation using 25 μ g DNA of pEGFP and 25 μ g of pXGH α . Cells were plated at a cell density of 3×10^6 and incubated at 37°C, under an atmosphere of O₂ and 5% CO₂. Chromaffin cells were incubated in Regular Locke's or in 56 mM K⁺ Locke's solution for 2 min. At the end of the incubation, cells were lysed and total hGH was measured as described in Materials and Methods. hGH output was expressed as a percentage of total hGH content. Bars represent mean \pm S.E.M. of n = 4 experiments. For each experiment, each condition was assayed in quadruplicate.

*p < 0.05.

The data obtained indicated that transiently expressed hGH was targeted to secretory organelles, which are similar if not identical to chromaffin granules and have the ability to undergo regulated exocytosis.

3.3. Improvement of hGH expression in chromaffin cells

A critical part of the approach is a sensitive and precise method for measuring GH released into the medium and retained by the transfected cells. The following adaptation of the assay for chromaffin cells, allows detection of 100-200 pg of hGH in samples as large as 0.5 ml. This sensitivity allows accurate determination of secretion of 0.9 % of hGH in 40,000-60, 000 transfected cells.

3.3.a. Improvement of chromaffin vesicle labeling with hGH

Three pulses of 56 mM K⁺ Locke's solution, of 8 minutes each applied at 9 minutes intervals, 36 h following transfection, resulted in a significant depletion in the number of chromaffin vesicles (Trifaró et al., 1984). Following the last stimulation period with high K⁺, cells were fixed in 56 mM of K⁺ Locke's solution containing 3.7% formaldehyde whereas the control preparations were fixed in regular Locke's solution also containing 3.7% formaldehyde. Immunofluorescence studies show that the pattern DBH and hGH staining in depolarized cells changed when compared to that of non-depolarized cells (Fig. 3.8, a). Both DBH and hGH staining disappeared from the perinuclear areas and was mainly concentrated in the cell periphery. Cells double labeled for DBH and hGH and examined 48 hours after stimulation showed a higher degree of hGH positive vesicles when compared to resting cells (Fig. 3.8, b). Percentages of DBH positive vesicles labeled for hGH, were determined for both control (non-depolarized cells) and depolarized cells.

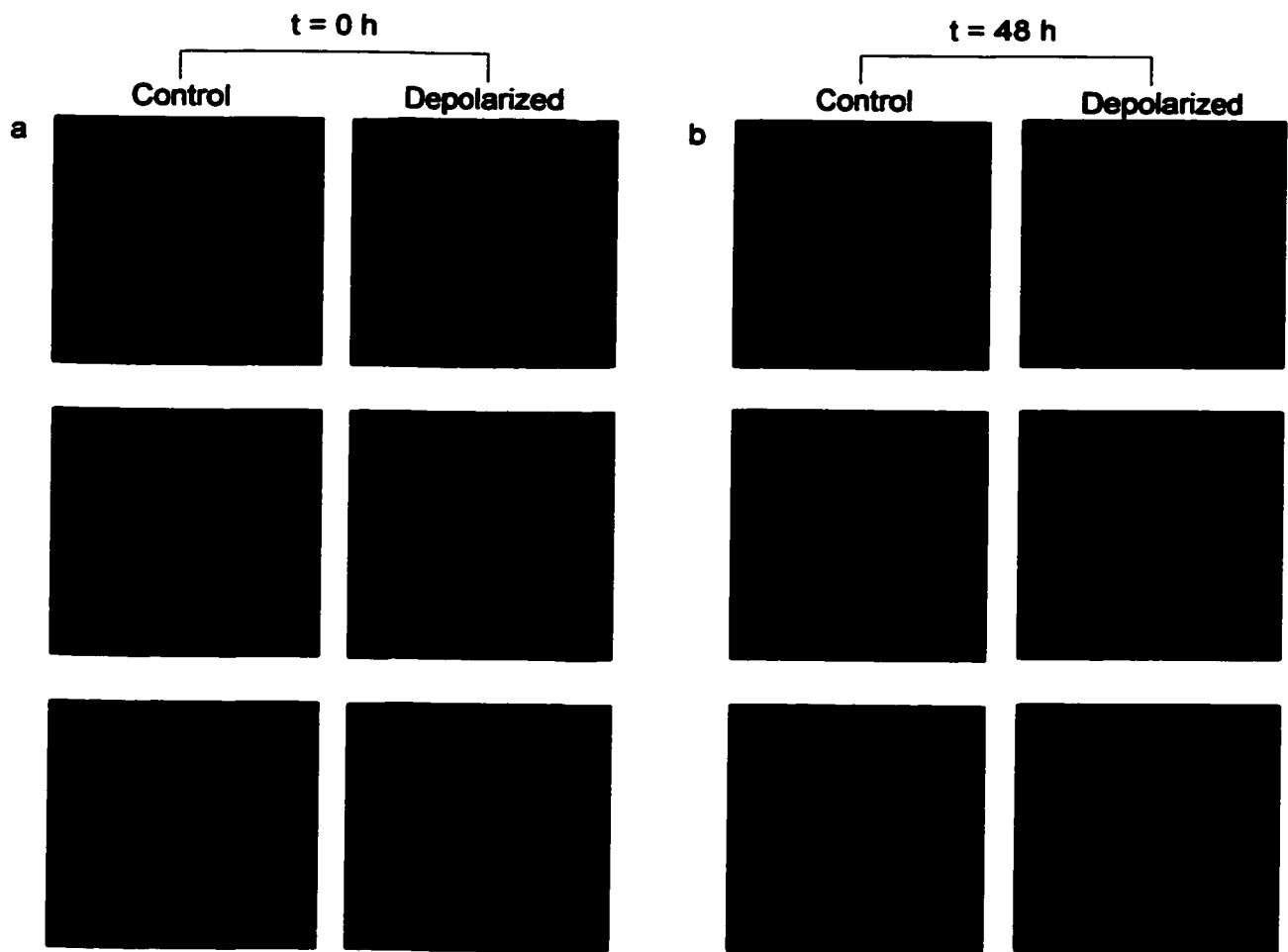


Figure 3.8: Effects of extensive depolarization of transfected chromaffin cells on the distribution pattern of hGH and DBH staining. Transfected chromaffin cells were plated on 35 mm dishes, at a cell density of 3×10^6 cells / dish. Four dishes were used as control. Twelve h after plating (when chromaffin cells had attached) half of the dishes were treated as follows: cells were rinsed two times with Locke's solution. Then, cells were stimulated for 8 minutes with a depolarizing concentration (56 mM) of K^+ . The stimulation period was repeated three times at 8 min intervals. Between stimulations, cells were allowed to recover in regular Locke's solution. After the last depolarization, half of the cover slips of both control (non-depolarized cells) and depolarized cells were fixed and stained for hGH and DBH. Four of the dishes were allowed to recover for 48 h following depolarization, and then, they were fixed and stained for hGH and $D\beta H$. Slides were observed under a Bio-Rad 1024 confocal microscope (Bio-Rad, Richmond, CA) attached to a Olimpus AX-70 microscope, using a 60X /1.4 oil immersion objective (for fluorescence and differential interference contrast or DIC). Images were acquired in the fluoresceine (upper panels) and rhodamine (middle panels) channels and were superimposed in one double exposure (lower panels). Images show the pattern of hGH and DBH distribution and co localization in control (left) and depolarized (right) cells fixed and stained immediately after depolarization (a) or 48 h following depolarization (b).

Figure 3.9 shows a significant increase in hGH labeling of DBH positive vesicles.

Fifty percent of DBH positive vesicles were labeled with hGH in resting chromaffin cells and 70% of DBH positive vesicles showed hGH staining in chromaffin cells previously depolarized by high K⁺.

3.3.b. hGH release from resting and stimulated chromaffin cells.

Twelve hours following electroporation, chromaffin cells were exposed to three pulses of 8 min each of 56 mM K⁺ Locke's solution, repeated at 9 min intervals, to induce an extensive depletion of intracellular amine stores (Trifaró et al., 1984). hGH release experiments were performed 48 hours after the depletion of intracellular stores, as described in Chapter 2 (Materials and Methods). As expected, stimulation of chromaffin cells by three pulses of a depolarizing concentration of K⁺ performed 36 hours following transfection, resulted in an increase in hGH labeling as shown in Fig. 3.9. The better labeling resulted in a 37% increase in depolarization induced hGH release in cells previously challenged with high K⁺ (Fig. 3.10). Furthermore, there was a doubling in the spontaneous release from the cells.

3.4. Co-transfection of Sc fragments and hGH gene into chromaffin cells and characterization of the double – labeled system

Vectors containing Sc constructs fused in frame with the gene encoding green fluorescent protein (GFP) were transiently transfected into chromaffin cells together with the vector encoding hGH which was used as a reporter for regulated secretion. To obtain transient expression of hGH and Sc constructs, transfection was performed by electroporation, under conditions previously selected, using a total plasmid DNA amount of 50µg/10⁷ cells (25µg of each plasmid DNA).

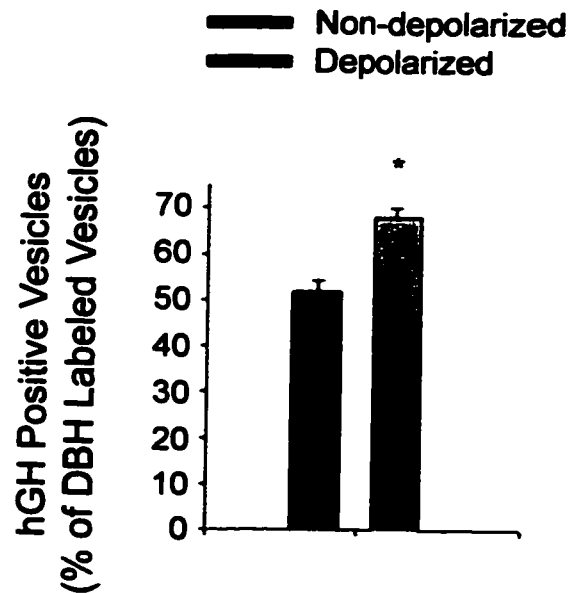


Figure 3.9: Efficiency of hGH labeling of chromaffin vesicles.

Chromaffin cells transfected with plasmid pXGH5 were plated on 35 mm dishes, at a cell density of 3×10^6 cells / dish. Twelve hours after plating (when chromaffin cells had attached) four dishes were treated as follows: cells were rinsed two times with Locke's solution. Cells were then stimulated for 8 min with a depolarizing concentration (56 mM) of K^+ . The stimulation period was repeated three times at 8 min intervals. Between stimulations, cells were allowed to recover in regular Locke's solution. Four dishes were used as control. Cells were allowed to recover for 48 h following depolarization, and then they were fixed and stained for hGH and D β H, as described in legend for figure 3.8. The percentage of DBH positive chromaffin vesicles labeled for hGH, was determined for both control (non-depolarized cells) and depolarized cells, 48 h following depolarization. Each bar represents the mean \pm SEM of the percentage of hGH stained from the total vesicles, D β H – positive. 100-150 vesicles were counted for each cell (n=10) from two different cultures.

*p < 0.05.

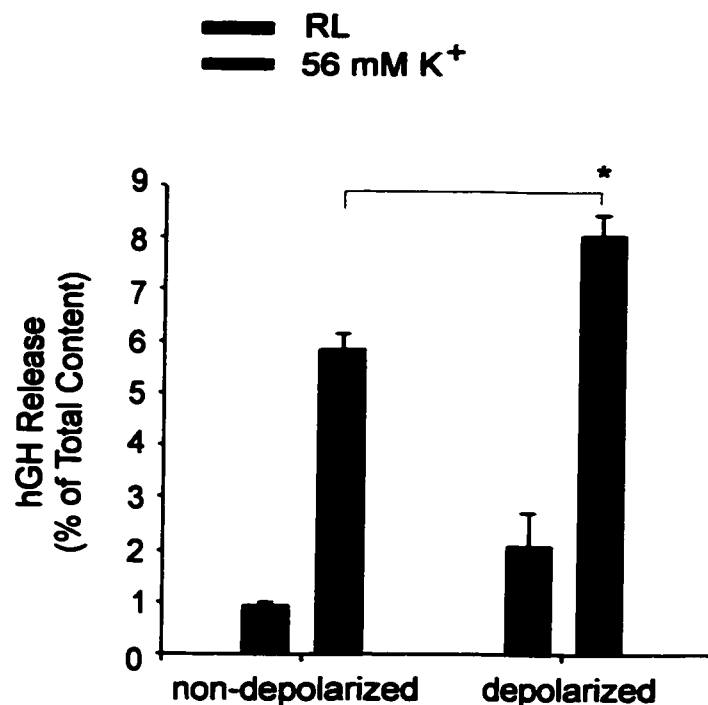


Figure 3.10: High K⁺-stimulated hGH release from control (non-depolarized) and previously depolarized chromaffin cells.

Chromaffin cells highly purified by differential plating as described in section 2.1, were transiently transfected with plasmid pXGH5 by electroporation as described in Materials and Methods. Twelve h following electroporation, chromaffin cells were exposed to an extensive depletion of intracellular stores by applying 3 pulses of 8 min each of 56 mM K⁺ Locke's solution, repeated at nine min intervals. hGH release experiments were performed 48 h after the depletion of intracellular stores. Chromaffin cells were rinsed several times with 1 ml of Locke's solution and then subsequently incubated for 2 min each with 0.5 ml regular Locke's solution, followed by 0.5 ml of depolarizing concentrations (56 mM) of K⁺ (high potassium Locke's solution). Cells were then lysed in 0.3 ml (3 times 0.1 ml) of 10 mM HEPES (pH 7.4) containing 0.2 mM EDTA. hGH content was determined using a radioimmunoassay kit, as described in Materials and Methods. Bars represent the mean \pm SEM of 4 experiments. In each experiment, each condition was assayed in quadruplicate.

* $p < 0.05$.

Different truncations of Sc cDNA, obtained by PCR, were subcloned into expression vector pEGFPC3 (Clontech), using the restriction sites *KpnI* and *BamHI* as described in Chapter 2 (Materials and Methods). Vector pEGFP provides a red-shifted GFP variant, which is 350 times brighter than the wild type GFP (clontech specifications).

3.4.a. Chromaffin cell survival following co – transfection by electroporation

In order to determine whether transfection efficiency was the same for all Sc deletion constructs, a survival assay was performed. Chromaffin cells were co-transfected with hGH and either GFP (alone) or one of the GFP-fused Sc constructs. Cell viability was investigated by measuring the relative number of cells either directly by counting them or indirectly by measuring total protein content or total DNA content as described in Chapter 2 (Materials and Methods). As shown in Fig. 3.11, there was a difference in terms of cell viability between cultures transfected with different GFP-fused Sc constructs. Cell survival ranged from 50.5 to 75.5%. Cells transfected with Sc1-2 showed the lowest survival rates. Fifty percent of the cells survived and this figure was 25% lower than the rate for control cells.

3.4.b. Co-expression of Sc fragments and hGH in chromaffin cells

Chromaffin cells co-transfected with hGH and GFP-fused Sc constructs, were cultured at 37°C, in an atmosphere of O₂ and 5% CO₂. Eighty-four hours following transfection, cells were scraped off the plates and lysed by sonication as described in Chapter 2. Aliquots of chromaffin cell lysate (10 µg protein / well) were subjected to SDS-PAGE, followed by electro transfer onto nitrocellulose membranes.

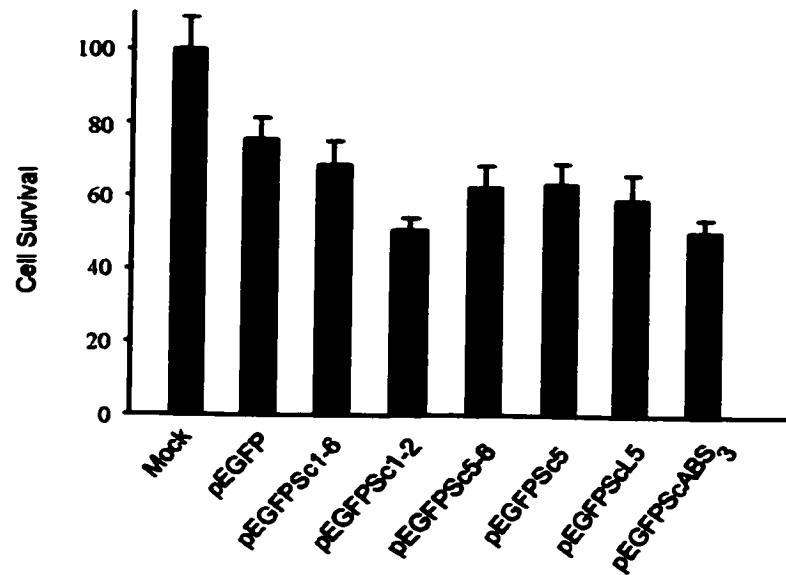


Figure 3.11: Comparison of cell survival in cultures transfected with various Sc deletion constructs.

Cell viability was investigated by measuring the relative cell number either by direct counting or indirectly by measuring total protein content. In both cases, electroporated and non-electroporated cells were plated at the same relative cell density (1.5×10^6 cells / 35 mm dish) and the cell number 24 h after transfection was compared. The bars represent mean \pm SEM of 4 culture dishes for each condition from three different chromaffin cultures.

Immunoblotting (Fig. 3.12) was performed with antibodies raised against hGH, Sc, tubulin and GFP, followed by incubation with corresponding HRP-conjugated secondary antibodies. Detection of protein bands was performed by enhanced chemiluminescence, as described in Chapter 2 (Materials and Methods). The Sc antibody raised against recombinant Sc recognized different Sc truncations (Sc 1-6, Sc1-2, Sc5-6, Sc5, ScL5) but did not recognize ScABS3. As shown in Fig. 3.12, there was a high level of expression of Sc constructs. Considering that only a small fraction of the cells were transfected with Sc constructs, it appears that there was a high overexpression of the proteins within these cells.

3.4.c. Co-transfection efficiency in chromaffin cells

Cells transfected with both hGH and GFP-Sc constructs were cultured at 37°C, in an atmosphere of O₂ and 5% CO₂, for 36 h. Cells were then fixed using 3.7% formaldehyde in regular Locke's solution, permeabilized with acetone and stained for hGH as described in Chapter 2. Cells co-transfected with both pXGH5 and either pEGFP alone (control cells) or with one pEGFP-fused Sc construct were fixed, permeabilized and stained for hGH (Fig. 3.13). Cells showing positive fluorescence were then counted under fluorescence microscopy. Figure 3.14, shows the co-transfection efficiency for control cells, as well as for cells transfected with different Sc constructs. Differences in the GFP – tagged Sc constructs transfection efficiencies were detected. Co-transfection efficiency varied from $6.4 \pm 0.51\%$ (n = 4) for cells co-transfected with hGH and GFP-Sc5-6 to $20.47 \pm 1.25\%$ (n = 4) for control cells (Fig. 3.14, a).

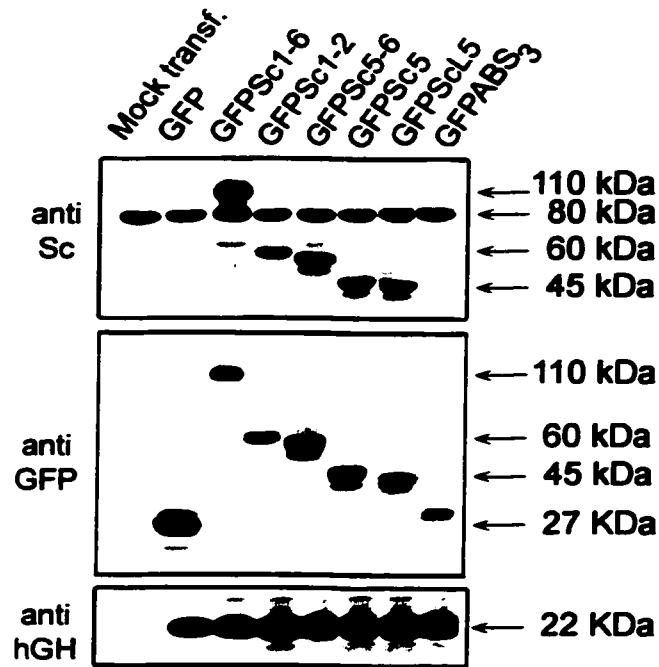


Figure 3.12: Expression of Scinderin deletion constructs and hGH in chromaffin cells. Chromaffin cells co-transfected with hGH and GFP-fused Sc constructs, were cultured at 37°C, in an atmosphere of O₂ and 5% CO₂. Eighty-four hours following transfection, cells were scraped off the plates and lysed by sonication. Aliquots of chromaffin cell lysate (10 µg protein / well) were subjected to SDS-PAGE, followed by electro transfer onto nitrocellulose membranes. Immunoblotting was performed with antibodies raised against hGH, Sc, tubulin and GFP, followed by incubation with corresponding HRP-conjugated secondary antibodies, and detection was performed by an enhanced chemiluminescence technique, as described in Chapter 2.

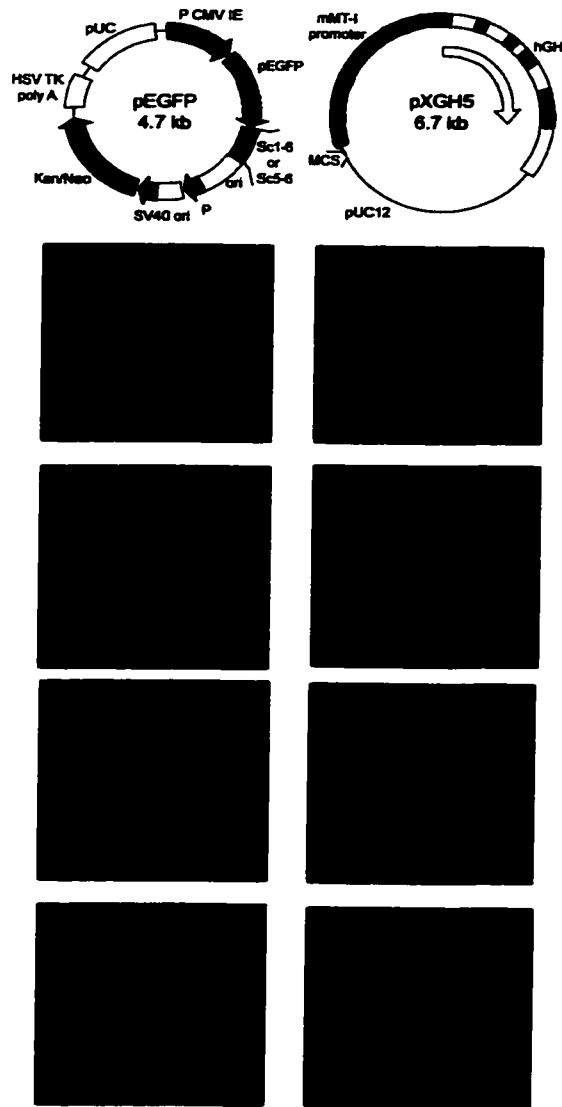


Figure 3.13: Intracellular localization of hGH and Scinderin deletion constructs in chromaffin cells.

Cells co-transfected by electroporation with both pXGH5 and pEGFP alone (control cells) or with one pEGFP-fused Sc construct insert were plated on collagen-coated cover slips at a cell density of 106 cells/ cover slip and cultured at 37°C, under an atmosphere of O₂ and 5% CO₂, for 36 h. Cells were then fixed, permeabilized and stained for hGH using a polyclonal rabbit antibody against hGH (dilution 1:100 in 0.1% BSA in PBS) and a rhodamine conjugated donkey anti-rabbit IgG (dilution 1 in 300 in 0.1% BSA in PBS). Cover slips were then mounted in glycerol:PBS (1:1) and images were taken with a Sony digital camera and saved using a Northern Eclipse software (Empix, Mississauga, ON, Ca). Images were then digitally imported into Adobe Photoshop software for further processing. Four cells expressing hGH and 4 different Scinderin constructs are shown.

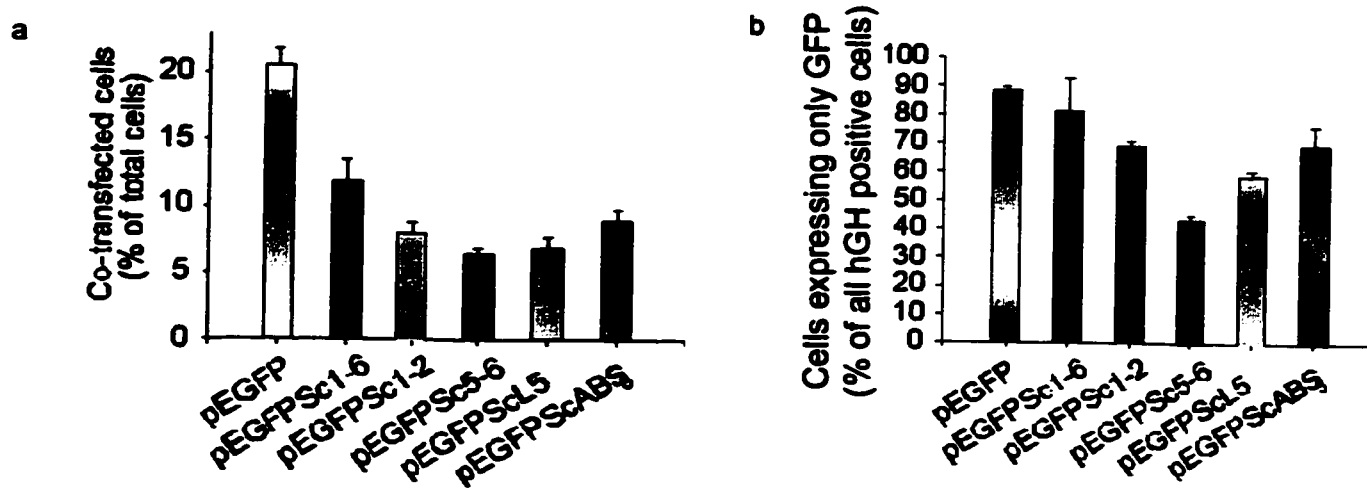


Figure 3.14: Co-transfection efficiency for cells transfected with pXGH5 and pEGFP-C3, alone or containing a Sc construct.

Cells co-transfected by electroporation with vector pXGH5 and pEGFP, this latter either alone (control cells) or carrying one pEGFP-fused Sc construct insert were plated on collagen-coated cover slips at a cell density of 106 cells/ cover slip and cultured at 37°C, under atmosphere of O₂ and 5% CO₂, for 36 h. Cells were then fixed, permeabilized and stained for hGH using a polyclonal rabbit antibody against hGH (dilution 1:100 in 0.1% BSA in PBS) and a rhodamine conjugated donkey anti-rabbit IgG (dilution 1 in 300 in 0.1% BSA in PBS). Panel a shows the percentage of the cells expressing both hGH and DβH. Panel b shows the percentage of the cells expressing GFP-fusion construct as a percentage of total cells expressing hGH. Bars represent mean ± SEM of n = 3 different experiments. In each experiment, each condition was assayed in quadruplicate.

In the co-transfected chromaffin cell culture, the sub population of cells expressing both hGH and GFP is the only one relevant for the determination of the role of Sc fragments in regulated secretion. However, the presence of a sub population of cells expressing only the hGH can account for distortions in the observed effects on secretion. In the growth hormone-expressing cell population, the percentage of the cells also expressing the GFP or GFP-fusion construct was determined (Fig. 3.14, b). Cells transfected with full scinderin displayed an efficiency of transfection that was 8% lower than that of control cells (transfected with the vector alone). Cells transfected with Sc1-2 displayed an efficiency of transfection 22% lower than control cells. Cells transfected with the Sc5-6 construct displayed an efficiency of transfection 48% lower than control cells. Cells transfected with Sc5 had an efficiency of transfection 30% less than control cells. Cells transfected with ScL5 displayed an efficiency of transfection 35% lower than control cells. Cells transfected with ScABS3, a construct containing only the third actin binding site of scinderin, displayed an efficiency of transfection 22% lower than that of control cells. In each case, the transfection efficiency was carefully recorded since it represents an important parameter for the normalization of the secretion results obtained in the release experiments.

3.4.d. Cortical F-actin network and intracellular localization of GFP-fused Sc constructs using immunofluorescence microscopy

Cell cultures co-transfected with pXGH5 and pEGFP either alone (control) or carrying one of the Sc constructs, were cultured at 37°C, in an atmosphere of O₂ and 5% CO₂ for 36h following transfection.

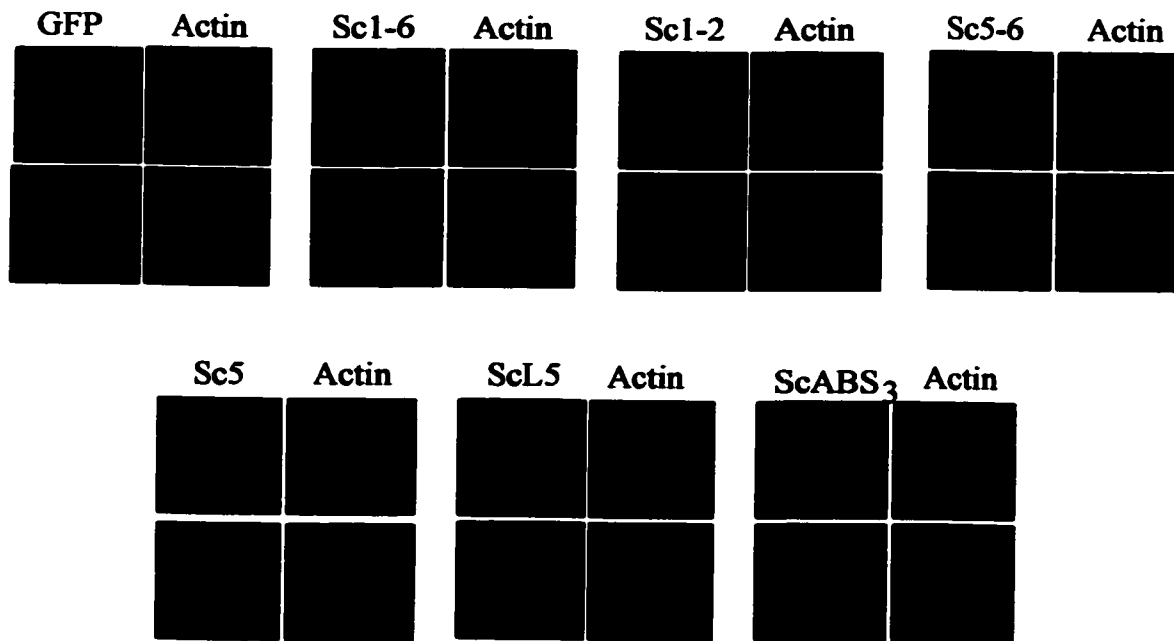


Figure 3.15: Cortical F-actin network and intracellular localization of GFP-fused Sc constructs.

Cells co-transfected by electroporation with vector pXGH5 and pEGFP either alone (control cells) or with vector carrying pEGFP-fused Sc construct inserts were plated on collagen-coated cover slips at a cell density of 106 cells/ cover slip and cultured at 37°C, under an atmosphere of O₂ and 5% CO₂, for 36 h. Cells were then fixed, permeabilized and stained for F-actin with 0.3 μM rhodamine-labeled phalloidin (Molecular Probes, Inc, Eugene, OR). Images were taken with a Sony digital camera, saved using a Northern Eclipse software (Empix, Mississauga, ON, Ca), and they were then digitally imported into Adobe Photoshop software for further analysis. Each panel shows two cells expressing the GFP-fused Sc insert and it's cortical F-actin distribution.

Cells were then fixed with 3.7% formaldehyde in regular Locke's solution, permeabilized and stained for F-actin with rhodamine phalloidine (a probe for filamentous actin). The double staining was visualized under a laser scanning confocal microscope as described in Chapter 2 (Materials and Methods). Previous data from our laboratory obtained from studies on cultured chromaffin cells has demonstrated a cortical cellular localization of Sc (Vitale et al., 1991; Rodriguez del Castillo et al., 1992). Fluorescence microscopy showed (Fig. 3.15) that in control cells and in cells transfected with ScL5, GFP had a cytoplasmic distribution. On the other hand, in cells transfected with GFP-Sc1-6, Sc1-2, Sc5-6, Sc5 and Sc ABS3, GFP staining was localized in the sub cortical regions of cells and in the cytoplasm. Furthermore, co-transfection of vector carrying hGH with any of the GFP-fused Sc constructs, did not affect the packing and storage of hGH in secretory vesicles (Fig. 3.12)

Effects of Sc or Sc deletion mutant overexpression on stimulation-induced cortical F-actin disassembly and chromaffin cell exocytosis

3.5. Stimulation induced changes in the organization of cortical F-actin cytoskeleton in chromaffin cells overexpressing Sc deletion mutants

3.5.a. High potassium-evoked F-actin disassembly

Previous work from our laboratory at the fluorescence microscopy level has demonstrated that when resting chromaffin cells are stained with rhodamine-labeled phalloidin (a probe for filamentous actin), a cortical and continuous fluorescent ring of rhodamine fluorescence is observed (Vitale et al., 1991). Three-dimensional image analysis of the ring of rhodamine fluorescence (Vitale et al., 1991) showed a uniform

cortical fluorescent intensity pattern (Vitale et al., 1991). Stimulation of the chromaffin cells with depolarizing concentrations of K⁺ or nicotinic receptor stimulation induces disruption of the uniform fluorescent ring (Vitale et al., 1991). The distribution of the fluorescent ring is the result of cortical F-actin disassembly (depolarization). Moreover, cortical F-actin disassembly is the result of scinderin activation. To study the effect of high K⁺-evoked depolarization on cortical F-actin dynamics in chromaffin cells overexpressing Sc or Sc deletion mutants, cells were transfected with pEGFP (control) or pEGFP carrying Sc 1-6 or Sc deletion mutants, as described in Materials and Methods. Twenty-four h post transfection, chromaffin cells were incubated for 1 min, with either regular Locke's solution (resting) or high K⁺ Locke's solution (stimulated). Then, the cells were fixed, permeabilized and stained for F-actin with rhodamine-phalloidin (Materials and methods). Transfected chromaffin cells, stained for F-actin were observed with a fluorescence microscope (Materials and Methods) and quantitative analysis of cortical rhodamine fluorescence (F-actin) was performed as described in Materials and methods. Figures 3.16 (a), 3.17 (a), 3.18 (a), 3.19 (a), 3.20 (a), 3.21 (a), 3.22 (a) show resting (non-depolarized) chromaffin cells, transfected with vector alone (control), Sc1-6, Sc1-2, Sc5-6, Sc5, ScL5 and ScABS3 respectively. Both control and cells overexpressing either Sc1-6 or Sc deletion mutants, showed a compact network of F-actin filaments. Three-dimensional image analysis of these rings also showed a uniform fluorescent pattern [Figures 3.16 (b), 3.17 (b), 3.18 (b), 3.19 (b), 3.20 (b), 3.21 (b), and 3.22 (b)].

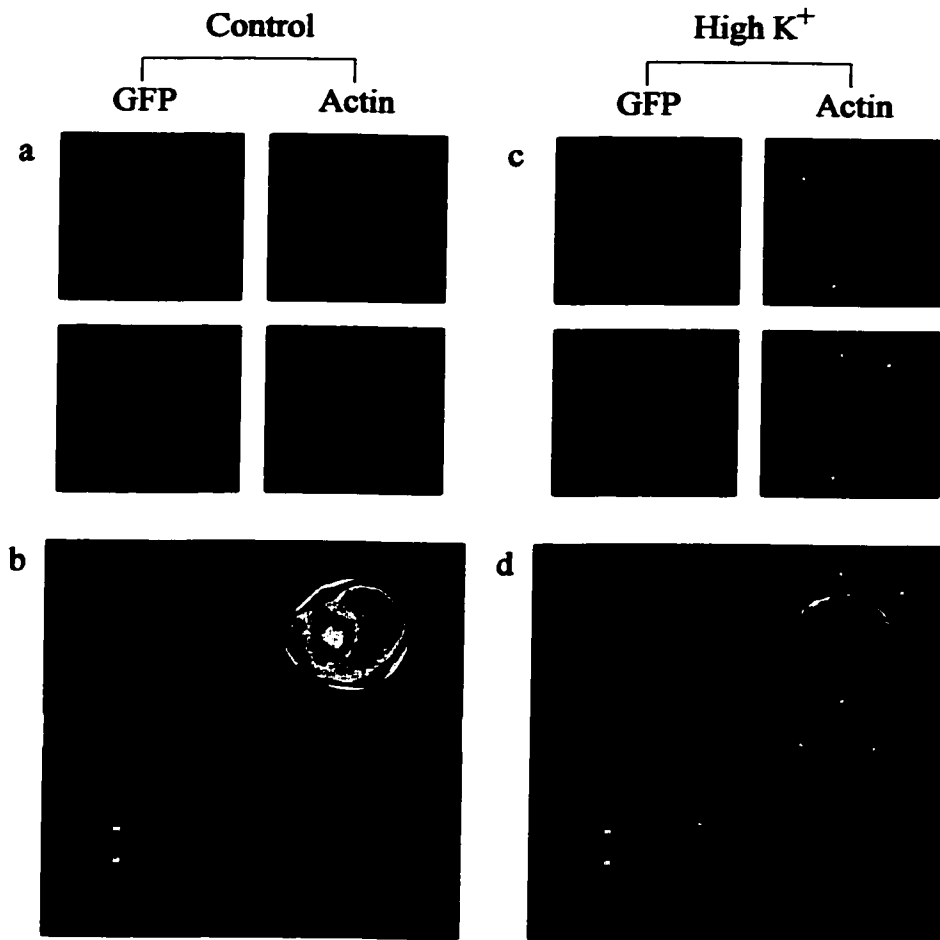


Figure 3.16: Cortical F-actin distribution in resting and High K⁺ stimulated chromaffin cells transfected with pEGFP vector.

Chromaffin cells were transiently transfected with plasmid pEGFP by electroporation as described in Materials and Methods. Forty eight h following electroporation, chromaffin cells were briefly washed with Locke's solution and incubated for 40 sec with either regular Locke's solution or Locke's solution containing a depolarizing concentration (56 mM) of K⁺ (Vitale et al., 1991). At the end of the incubation time, cells were fixed, permeabilized and incubated with rhodamine-labeled phalloidin as described in Materials and Methods. Cover slips were then mounted in glycerol:PBS (1:1). Pictures were taken with a Sony digital camera, using Northern Eclipse Software (Empix Inc.). Quantitative analysis of cortical rhodamine fluorescence (F-actin) was performed using a Hamamatsu Photonic KK Argus 50/CL Image Processor (Hamamatsu Photonic Systems; Bridgewater, NJ) coupled to a TV3M Zeiss video camera, as previously described (Vitale et al. 1995). Panels a and c show 3 chromaffin cells expressing GFP (green) stained for F-actin (red) in resting (a) and depolarized (c) state. Arrows show patches of fluorescence in the disrupted F-actin rings of stimulated chromaffin cells. Panels b and d show three-dimensional image analysis of F-actin cortical rings of the cells situated at the bottom of panels a and c, respectively.

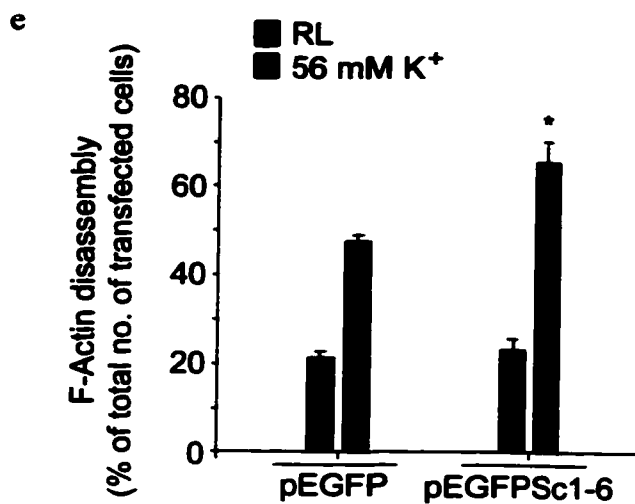
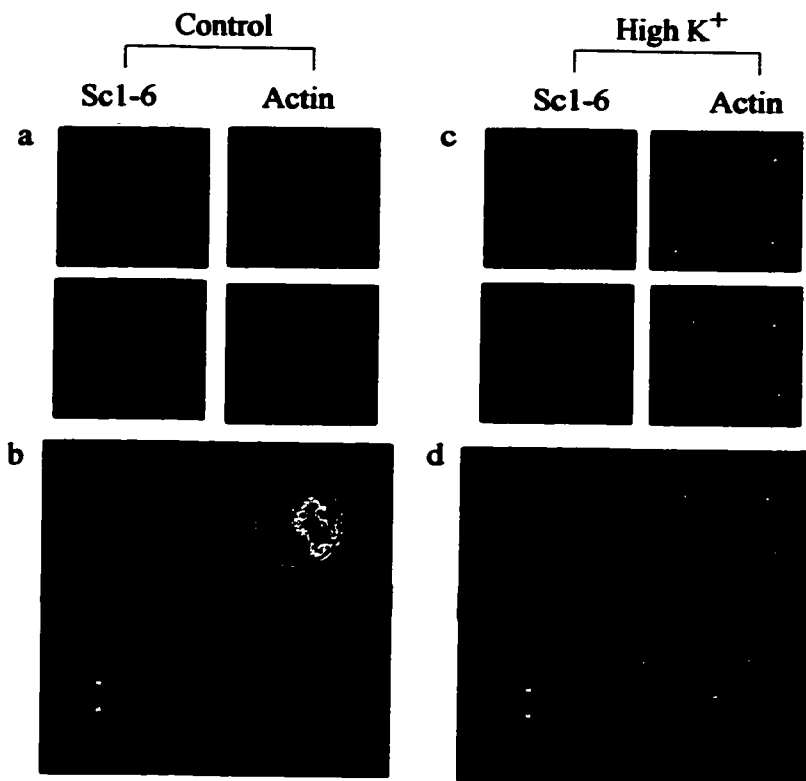


Figure 3.17: Cortical F-actin distribution in resting and High K⁺ stimulated chromaffin cells transfected with pEGFPSc1-6. Chromaffin cells were transiently transfected with plasmid pEGFPSc1-6 by electroporation as described in materials and methods. Forty-eight h following electroporation, chromaffin cells were washed with regular Locke's solution and incubated for 40 sec with either regular Locke's solution or with Locke's solution containing a depolarizing concentration (56 mM) of K⁺ (Vitale et al, 1991). At the end of the incubation, cells were fixed, permeabilized and incubated with rhodamine-labeled phalloidin as described in Materials and methods. Cover slips were then mounted in glycerol:PBS (1:1). Pictures were taken with a Sony digital camera. Quantitative analysis of cortical rhodamine fluorescence (F-actin) was performed as described in the legend accompanying Fig. 3.16. Panels a and c show 2 chromaffin cells expressing GFP (green) stained for F-actin (red) in resting (a) and depolarized (c) state.

Arrows show patches of fluorescence in the disrupted F-actin rings of stimulated chromaffin cells. Panels b and d show three-dimensional image analysis of F-actin rings of the cells situated at the bottom of panels a and c, respectively. Panel e shows the percentage of chromaffin cells showing F-actin disassembly for both control (vector alone) and cells expressing pEGFPSc1-6. Between 50 and 100 cells per cover slip, expressing either the vector alone or GFP-fused Sc1-6 were classified as having a 'continuous' or 'discontinuous' staining pattern. This was done without knowing what insert was expressed in the cells or whether cells were from control or stimulated preparations (single blind design) (Vitale et al., 1991). Bars represent mean \pm SEM of n = 3 different experiments. In each experiment, 3 or 4 cover slips were assayed for each condition. *p < 0.05.

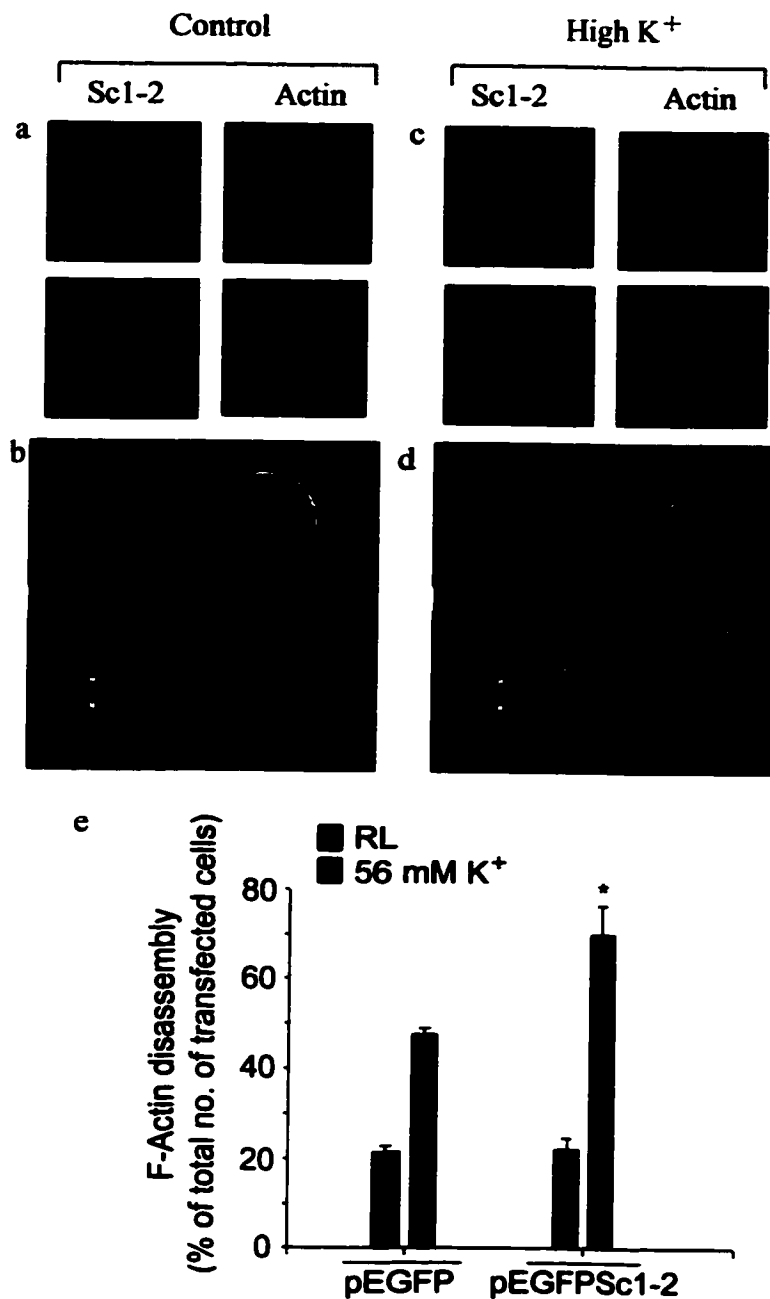


Figure 3.18: Cortical F-actin distribution in resting and High K⁺ stimulated chromaffin cells transfected with pEGFPSc1-2. Chromaffin cells were transiently transfected with plasmid pEGFPSc1-2 by electroporation as described in Materials and Methods. Forty-eight h following electroporation, chromaffin cells were briefly washed with Locke's solution and incubated for 40 sec with either regular Locke's solution or Locke's solution containing a depolarizing concentration (56 mM) of K⁺ (Vitale et al., 1991). At the end of the incubation time, cells were fixed, permeabilized and incubated with rhodamine - labeled phalloidin as described in Materials and Methods. Cover slips were then mounted in glycerol:PBS (1:1). Pictures were taken with a Sony digital camera, using Northern Eclipse Software (Empix Inc.). Quantitative analysis of cortical rhodamine fluorescence (F-actin) was performed as described in the legend accompanying Fig. 3.16. Panels a and c show 2 chromaffin cells expressing GFP (green) stained for F-actin (red) in resting (a) and depolarized (c) state.

Arrows show patches of fluorescence in the disrupted F-actin rings of stimulated chromaffin cells. Panels b and d show three-dimensional image analysis of F-actin rings of the cells situated at the bottom of panels a and c, respectively. Panel e shows the percentage of chromaffin cells showing F-actin disassembly for control (vector alone) and cells expressing pEGFPSc1-2, determined as described in the legend accompanying Fig. 3.17. Bars represent mean \pm SEM of n = 3 different experiments. In each experiment, 3 or 4 cover slips were assayed for each condition. *p < 0.05.

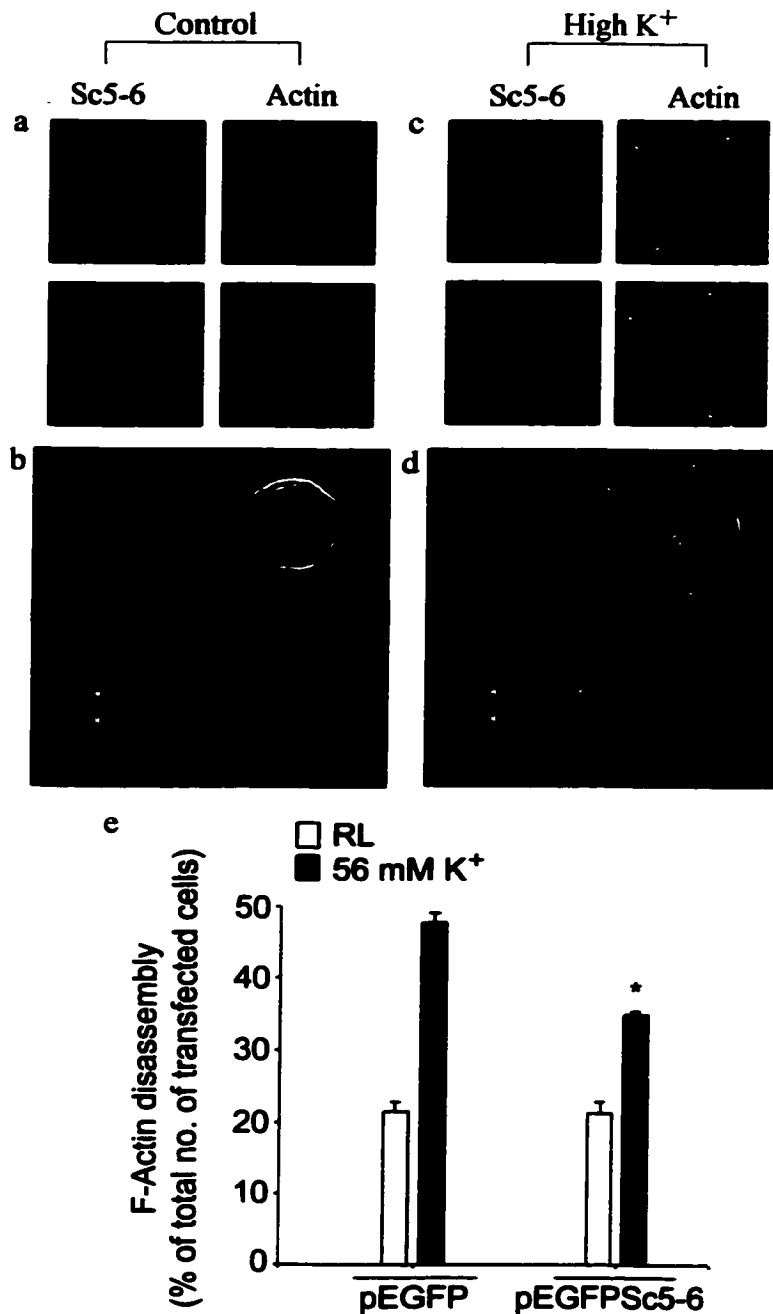


Figure 3.19: Cortical F-actin distribution in resting and High K⁺ stimulated chromaffin cells transfected with pEGFPSc5-6. Chromaffin cells were transiently transfected with plasmid pEGFPSc5-6 by electroporation as described in Materials and Methods. Forty-eight h following electroporation, chromaffin cells were briefly washed with Locke's solution and incubated for 40 sec with either regular Locke's solution or Locke's solution containing a depolarizing concentration (56 mM) of K⁺ (Vitale et al., 1991). At the end of the incubation time, cells were fixed, permeabilized and incubated with rhodamine-labeled phalloidin as described in Materials and Methods. Cover slips were then mounted in glycerol:PBS (1:1). Pictures were taken with a Sony digital camera. Quantitative analysis of cortical rhodamine fluorescence (F-actin) was performed as described in the legend accompanying Fig. 3.16. Panels a and c show 3 chromaffin cells expressing Sc5-6 (green) stained for F-actin (red) in resting (a) and depolarized (c) state.

Arrows show patches of fluorescence in the disrupted F-actin rings of stimulated chromaffin cells. Panels b and d show three-dimensional image analysis of F-actin rings of the cells situated at the bottom of panels a and c, respectively. Panel e shows the percentage of chromaffin cells showing F-actin disassembly for control (vector alone) and cells expressing pEGFPSc5-6, determined as described in the legend accompanying Fig. 3.17. Bars represent mean \pm SEM of n = 3 different experiments. In each experiment, 3 or 4 cover slips were assayed for each condition. *p < 0.05.

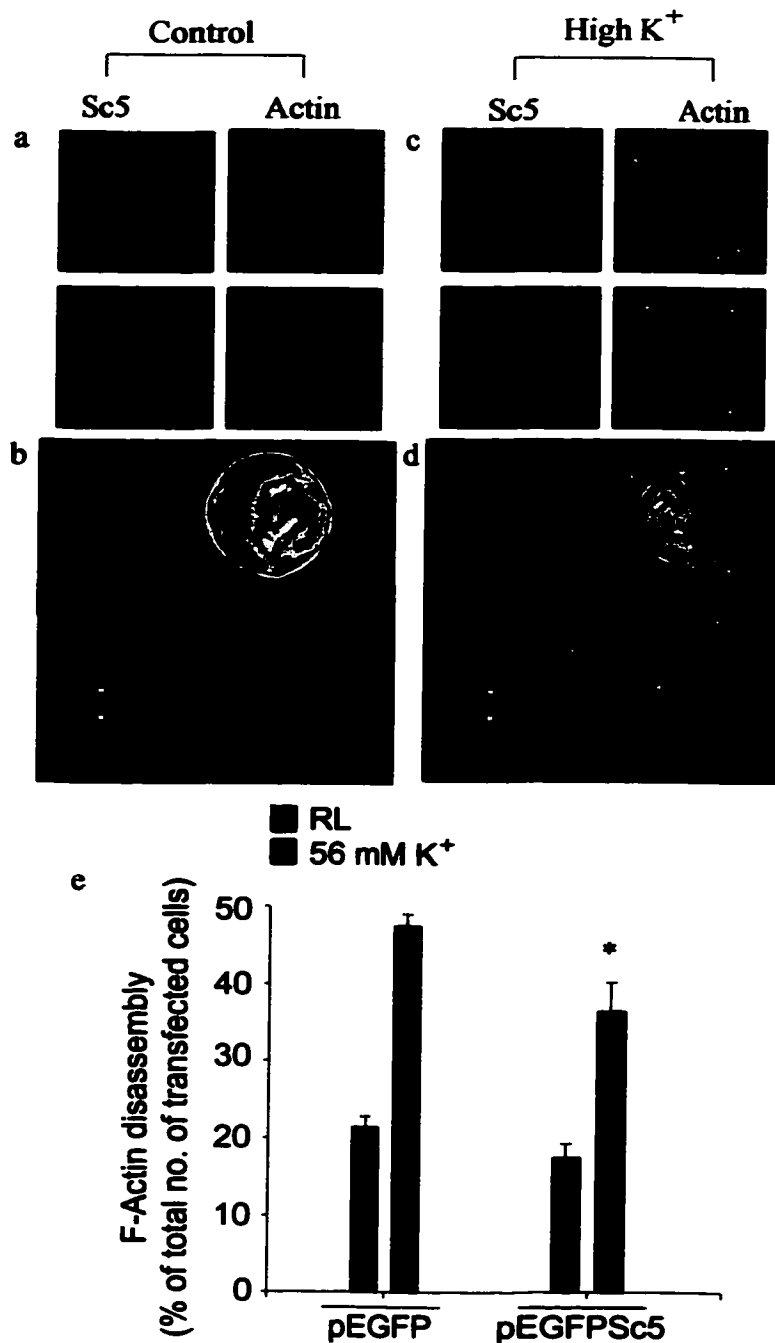


Figure 3.20: Cortical F-actin distribution in resting and High K⁺ stimulated chromaffin cells transfected with pEGFPSc5. Chromaffin cells were transiently transfected with plasmid pEGFPSc5 by electroporation as described in Materials and Methods. Forty eight h following electroporation, chromaffin cells were briefly washed with Locke's solution and incubated for 40 sec with either regular Locke's solution or Locke's solution containing a depolarizing concentration (56 mM) of K⁺ (Vitale et al., 1991). At the end of the incubation time, cells were fixed, permeabilized and incubated with rhodamine-labeled phalloidin as described in Materials and Methods. Cover slips were then mounted in glycerol:PBS (1:1). Pictures were taken with a Sony digital camera. Quantitative analysis of cortical rhodamine fluorescence (F-actin) was performed as described in the legend accompanying Fig. 3.16. Panels a and c show 2 chromaffin cells expressing Sc5 (green) stained for F-actin (red) in resting (a) and depolarized (c) state.

Arrows show patches of fluorescence in the disrupted F-actin rings of stimulated chromaffin cells. Panels b and d show three-dimensional image analysis of F-actin rings of the cells situated at the bottom of panels a and c, respectively. Panel e shows the percentage of chromaffin cells showing F-actin disassembly for control (vector alone) and cells expressing pEGFPSc5, determined as described in the legend from Fig. 3.17. Bars represent mean \pm SEM of n = 3 different experiments. In each experiment, 3 or 4 cover slips were assayed for each condition. *p < 0.05.

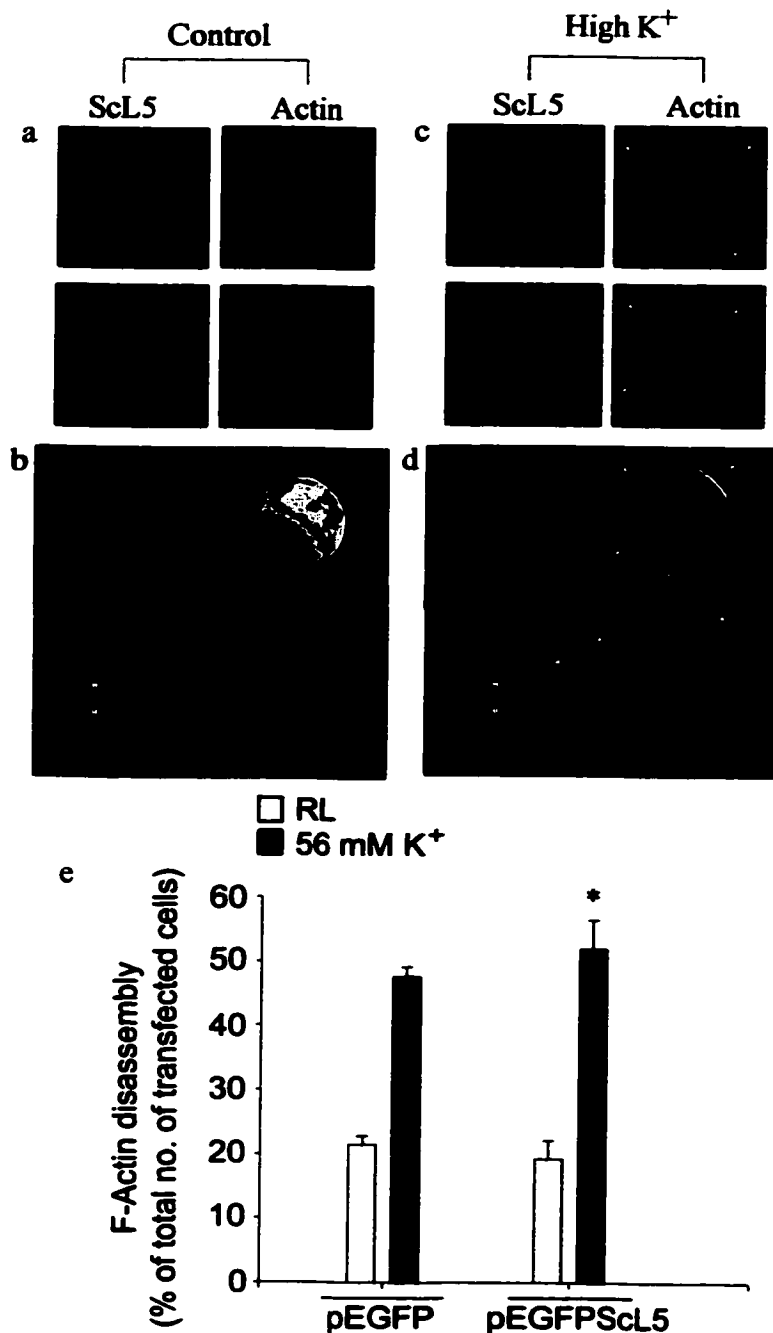


Figure 3.21: Cortical F-actin distribution in resting and High K⁺ stimulated chromaffin cells transfected with pEGFPScL5. Chromaffin cells were transiently transfected with plasmid pEGFPScL5 by electroporation as described in Materials and Methods. Forty-eight h following electroporation, chromaffin cells were briefly washed with Locke's solution and incubated for 40 sec with either regular Locke's solution or Locke's solution containing a depolarizing concentration (56 mM) of K⁺ (Vitale et al., 1991). At the end of the incubation time, cells were fixed, permeabilized and incubated with rhodamine-labeled phalloidin as described in Materials and Methods. Cover slips were then mounted in glycerol:PBS (1:1). Pictures were taken with a Sony digital camera. Quantitative analysis of cortical rhodamine fluorescence (F-actin) was performed as described in the legend accompanying Fig. 3.16. Panels a and c show 2 chromaffin cells expressing ScL5 (green) stained for F-actin (red) in resting (a) and depolarized (c) state.

Arrows show patches of fluorescence in the disrupted F-actin rings of stimulated chromaffin cells. Panels b and d show three-dimensional image analysis of F-actin rings of the cells situated at the bottom of panels a and c, respectively. Panel e shows the percentage of chromaffin cells showing F-actin disassembly for control (vector alone) and cells expressing pEGFPScL5, determined as described in the legend accompanying Fig. 3.17. Bars represent mean \pm SEM of n = 3 different experiments. In each experiment, 3 or 4 cover slips were assayed for each condition. *p < 0.05.

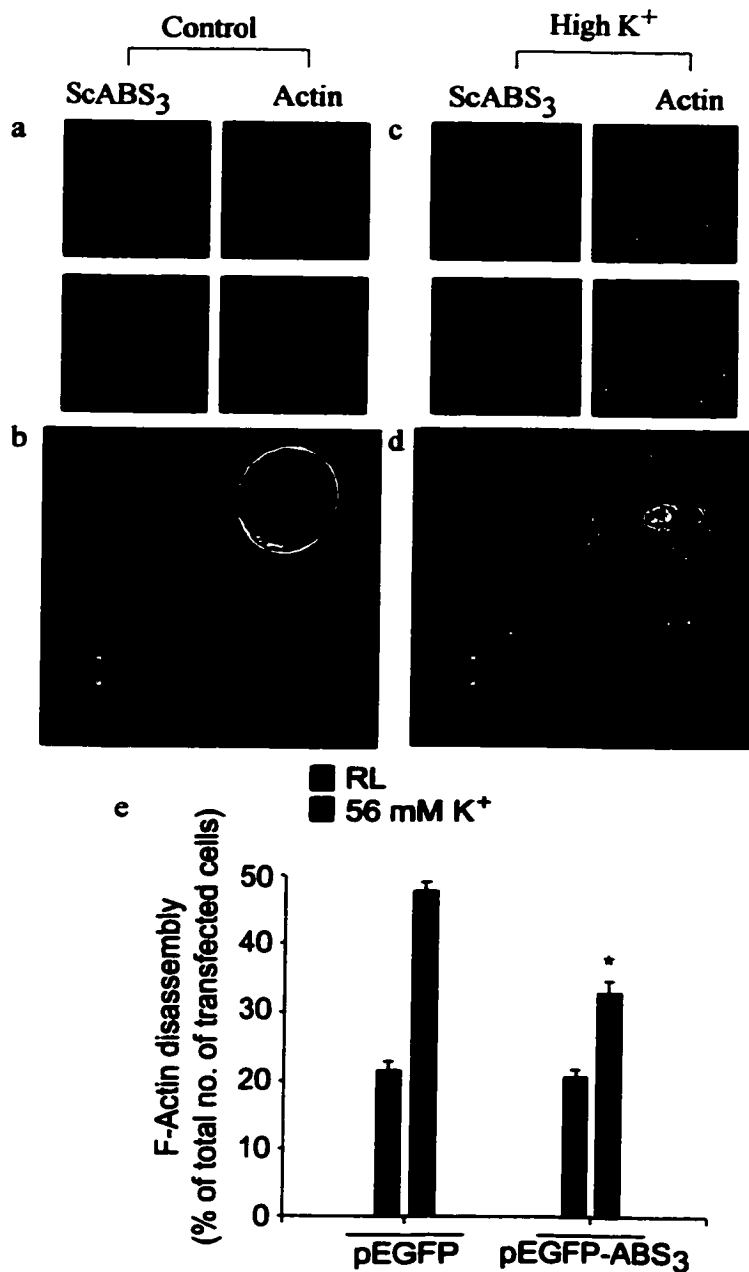


Figure 3.22: Cortical F-actin distribution in resting and High K⁺ stimulated chromaffin cells transfected with pEGFPScABS3. Chromaffin cells were transiently transfected with plasmid pEGFPScABS3 by electroporation as described in Materials and Methods. Forty eight h following electroporation, chromaffin cells were briefly washed with Locke's solution and incubated for 40 sec with either regular Locke's solution or Locke's solution containing a depolarizing concentration (56 mM) of K⁺ (Vitale et al., 1991). At the end of the incubation time, cells were fixed, permeabilized and incubated with rhodamine-labeled phalloidin as described in Materials and Methods. Cover slips were then mounted in glycerol:PBS (1:1). Pictures were taken with a Sony digital camera. Quantitative analysis of cortical rhodamine fluorescence (F-actin) was performed as described in the legend accompanying Fig. 3.16. Panels a and c show 2 chromaffin cells expressing ScABS3 (green) stained for F-actin (red) in resting (a) and depolarized (c) state.

Arrows show patches of fluorescence in the disrupted F-actin rings of stimulated chromaffin cells. Panels b and d show three-dimensional image analysis of F-actin rings of the cells situated at the bottom of panels a and c, respectively. Panel e shows the percentage of chromaffin cells showing F-actin disassembly for control (vector alone) and cells expressing pEGFPScABS3, determined as described in the legend accompanying Fig. 3.17. Bars represent mean \pm SEM of n = 3 different experiments. In each experiment, 3 or 4 cover slips were assayed for each condition. *p < 0.05.

On the other hand, Figures 3.16 (c), 3.17 (c), 3.18 (c), 3.19 (c), 3.20 (c), 3.21 (c), and 3.22 (c) show depolarized chromaffin cells, transfected with vector control, Sc1-6, Sc1-2, Sc5-6, Sc5, scL5 or ScABS3 respectively. High K⁺-evoked stimulation of transfected chromaffin cells produced a disruption in the compact actin filament network in both control (vector transfected cells) and cells overexpressing Sc1-6 or some Sc deletion mutants. The cortical surface of stimulated cells showed disrupted fluorescent rings characterized by patches of fluorescence that appeared to be separated by valleys in the three dimensional image analysis [Figures 3.16 (d), 3.17 (d), 3.18 (d), 3.19 (d), 3.20 (d), 3.21 (d), and 3.22 (d)]. As previously demonstrated (Vitale et al., 1991), the valleys corresponded to areas of F-actin disassembly, whereas the peaks represented areas in which the F-actin network remains intact.

To determine the magnitude of high K⁺ stimulation, the percentage of transfected chromaffin cells showing F-actin disassembly was calculated. To accomplish this, 50 to 100 transfected, single-round chromaffin cells per cover slip were examined. Each cell was classified as having either a 'continuous' or 'discontinuous' cortical rhodamine fluorescent ring (Vitale et al., 1991). The percentage of chromaffin cells showing F-actin disassembly was calculated for each experimental condition. Under these conditions, chromaffin cells overexpressing Sc1-6 (Fig. 3.17, e) or Sc1-2 (Fig. 3.18, e) showed a 38.3 or 47.2% increase respectively in the number of cells showing F-actin disassembly upon K⁺-evoked depolarization, when compared to control cells. Moreover, chromaffin cells overexpressing Sc5-6 (Fig. 3.19, e), Sc5 (Fig. 3.20, e) or ScABS3 (Fig. 3.22, e) showed a 27.2, 23.4 or 30.9% decrease respectively in the number of cells showing F-actin disassembly upon depolarization, when compared to control cells.

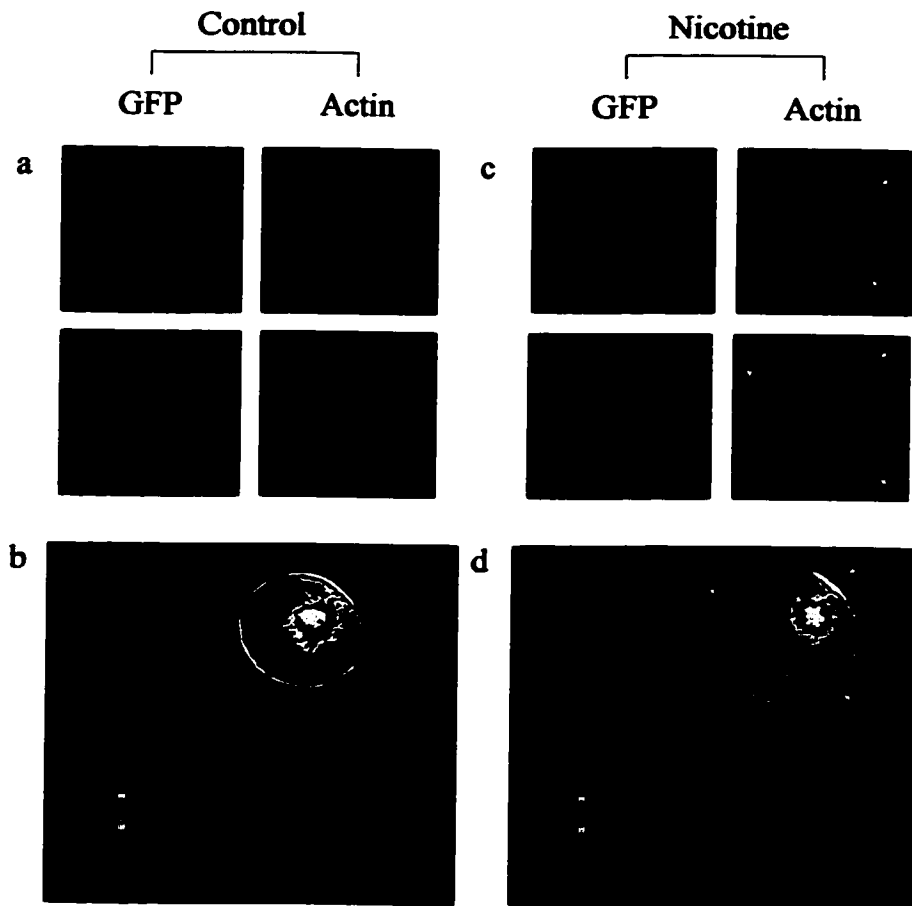


Figure 3.23: Cortical F-actin distribution in resting and nicotine stimulated chromaffin cells transfected with pEGFP vector. Chromaffin cells were transiently transfected with plasmid pEGFP by electroporation as described in Materials and Methods. Forty eight h following electroporation, chromaffin cells were briefly washed with regular Locke's solution and incubated for 40 sec with either regular Locke's solution or Locke's solution containing 10 μ M nicotine (Vitale et al., 1991). At the end of the incubation time, cells were fixed, permeabilized and incubated with rhodamine-labeled phalloidin as described in Materials and Methods. Cover slips were then mounted in glycerol:PBS (1:1). Pictures were acquired with a Sony digital camera. Quantitative analysis of cortical rhodamine fluorescence (F-actin) was performed as described in the legend accompanying Fig. 3.16. Panels a and c show 3 chromaffin cells expressing GFP (green) stained for F-actin (red) in resting (a) and depolarized (c) state. Arrows show patches of fluorescence in the disrupted F-actin rings of stimulated chromaffin cells. Panels b and d show three-dimensional image analysis of F-actin rings of the cells situated at the bottom of panels a and c, respectively.

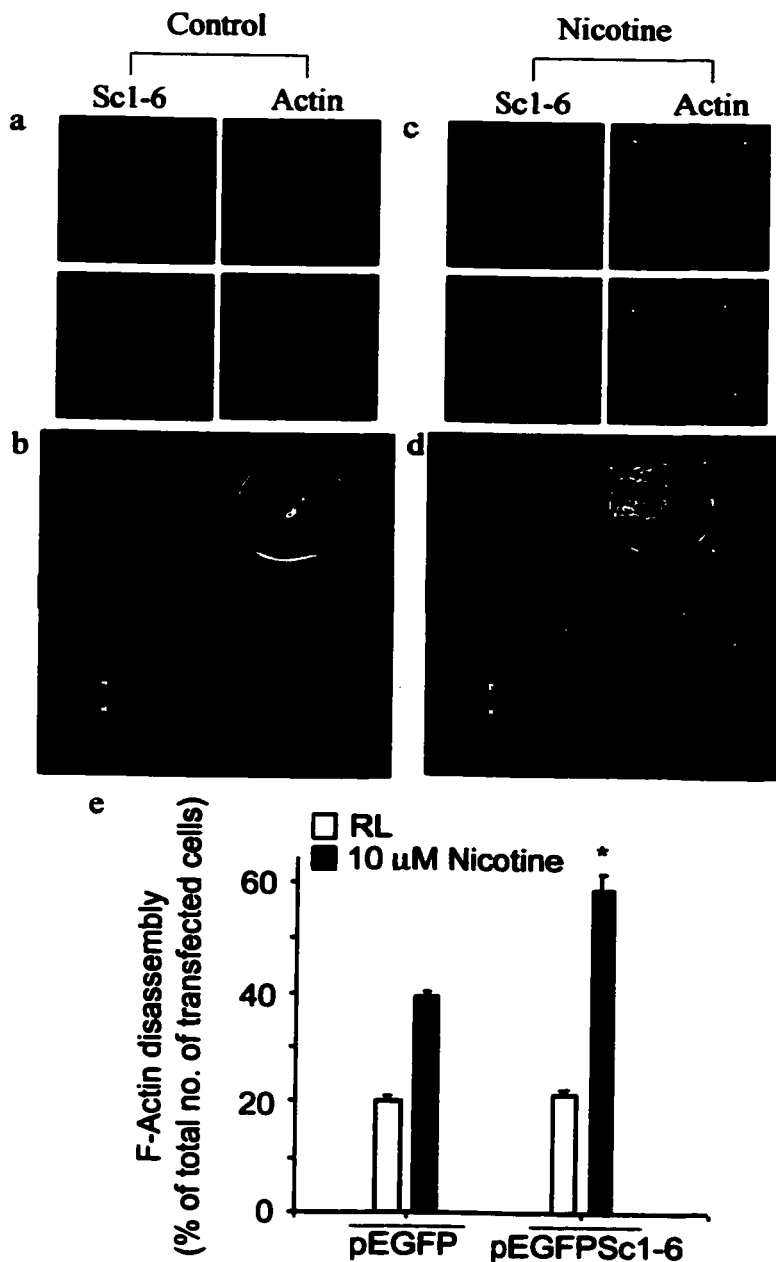


Figure 3.24: Cortical F-actin distribution in resting and nicotine stimulated chromaffin cells transfected with pEGFPSc1-6. Chromaffin cells were transiently transfected with plasmid pEGFPSc1-6 by electroporation as described in Materials and Methods. Forty-eight h following electroporation, chromaffin cells were washed with regular Locke's solution and incubated for 40 sec with either regular Locke's solution or Locke's solution containing 10 μ M nicotine (Vitale et al., 1991). At the end of the incubation, cells were fixed, permeabilized and incubated with rhodamine-labeled phalloidin as described in materials and methods. Cover slips were then mounted in glycerol:PBS (1:1). Pictures were acquired with a Sony digital camera. Quantitative analysis of cortical rhodamine fluorescence (F-actin) was performed as described in the legend accompanying Fig.3.16. Panels a and c show 2 chromaffin cells expressing Sc1-6 (green) stained for F-actin (red) in resting (a) and depolarized (c) state.

Arrows show patches of fluorescence in the disrupted F-actin rings of stimulated chromaffin cells. Panels b and d show three-dimensional image analysis of F-actin rings of the cells situated at the bottom of panels a and c, respectively. Panel e shows the percentage of chromaffin cells showing F-actin disassembly in control (vector alone) and cells expressing pEGFPSc1-6, determined as described in the legend accompanying Fig. 3.17. Bars represent mean \pm SEM of n = 3 different experiments. In each experiment, 3 or 4 cover slips were assayed for each condition. *p < 0.05.

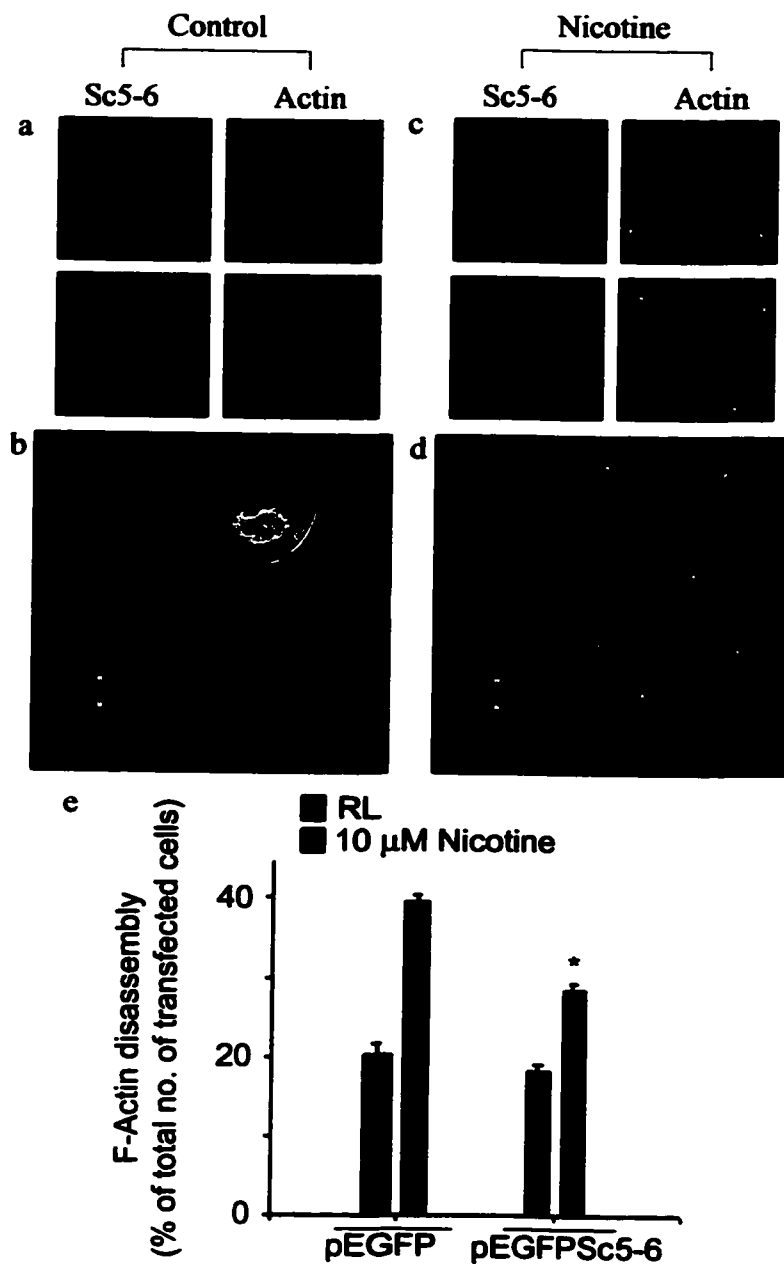


Figure 3.25: Cortical F-actin distribution in resting and nicotine stimulated chromaffin cells transfected with pEGFPSc5-6.

Chromaffin cells were transiently transfected with plasmid pEGFPSc5-6 by electroporation as described in Materials and Methods. Forty-eight h following electroporation, chromaffin cells were washed with regular Locke's solution and incubated for 40 sec with either regular Locke's solution or Locke's solution containing 10 μM nicotine (Vitale et al., 1991). At the end of the incubation, cells were fixed, permeabilized and incubated with rhodamine-labeled phalloidin as described in materials and methods. Cover slips were then mounted in glycerol:PBS (1:1). Pictures were acquired with a Sony digital camera. Quantitative analysis of cortical rhodamine fluorescence (F-actin) was performed as described in the legend accompanying Fig.3.16. Panels a and c show 3 chromaffin cells expressing Sc5-6 (green) stained for F-actin (red) in resting (a) and depolarized (c) state.

Arrows show patches of fluorescence in the disrupted F-actin rings of stimulated chromaffin cells. Panels b and d show three-dimensional image analysis of F-actin rings of the cells situated at the bottom of panels a and c, respectively. Panel e shows the percentage of chromaffin cells showing F-actin disassembly in control (vector alone) and cells expressing pEGFPSc5-6, determined as described in the legend accompanying Fig. 3.17. Bars represent mean ± SEM of n = 3 different experiments. In each experiment, 3 or 4 cover slips were assayed for each condition. *p < 0.05.

Furthermore, chromaffin cells overexpressing ScL5 did not show a significant increase or decrease in the number of cells showing F-actin disassembly upon depolarization (Fig. 3.21, e).

3.5.b. Nicotine-induced F-actin disassembly

In order to test the effects of nicotinic receptor stimulation on the cortical F-actin of chromaffin cells overexpressing Sc or a Sc deletion mutant, cells were transfected with pEGFP (control) or pEGFP carrying Sc 1-6 or Sc5-6. Twenty-four hours following transfection, cells were incubated for 40 sec with either regular Locke's solution or the same solution containing 10 μ M nicotine, as described in Materials and methods. Cells were then fixed, permeabilized and incubated with rhodamine-palloidin. As with transfected chromaffin cells stimulated with high K⁺, nicotine stimulation resulted in a disruption in the compact actin filament network in cells transfected with vector alone (control), and cells overexpressing Sc1-6 or Sc5-6. Moreover, chromaffin cells overexpressing Sc1-6 (Fig. 3.24, e), showed a 48.7% increase in the number of cells showing F-actin disassembly upon nicotine stimulation, when compared to control cells. On the other hand, chromaffin cells overexpressing Sc5-6 (Fig. 3.25, e), showed a 28.1% decrease in the number of cells showing F-actin disassembly upon depolarization, when compared to control cells.

3.6. Stimulation-induced exocytosis in chromaffin cells overexpressing Sc deletion constructs

3.6.a. High-potassium evoked chromaffin cell exocytosis

Chromaffin cells were co-transfected with pXGH5 (vector carrying the hGH gene) and pEGFP (control) or pEGFP carrying the Sc gene or Sc deletion mutants. Transfection was done by electroporation, as described in Materials and Methods (Chapter 2). To obtain a better hGH labeling of chromaffin vesicles, twelve hours following electroporation, transfected cells were exposed to three pulses of 8 min each of 56 mM K⁺ Locke's solution. This was done to induce an extensive depletion of intracellular amine stores (Trifaró et al., 1984). Forty eight h following stimulation, transfected chromaffin cells were incubated, for 2 minutes, with either regular Locke's solution (control) or Locke's solution containing a depolarizing concentration of K⁺ (56 mM), as described in Materials and Methods. At the end of the incubation period, cells were lysed and both total and hGH output was measured in both control and stimulated cells (Radioimmunoassay kit, Nichols Institute). Under these conditions, chromaffin cells overexpressing the full sequence of Sc (Fig. 3.26) or Sc1-2 (Fig. 3.27) showed a 50% or 62% increase respectively in hGH secretion upon depolarization, when compared with stimulated cells previously transfected with vector alone. In contrast, chromaffin cells overexpressing Sc5-6 (Fig. 3.28), Sc5 (Fig. 3.29) or ScABS3 (Fig. 3.31), showed a decreased secretory response.

Inhibitions in this case were 27.8%, 28.3% or 29.6% in the high K⁺-evoked hGH responses, when compared to control cells. Furthermore, chromaffin cells overexpressing ScL5 did not show a significant difference in hGH secretion upon depolarization, when compared with control cells (fig. 3.30).

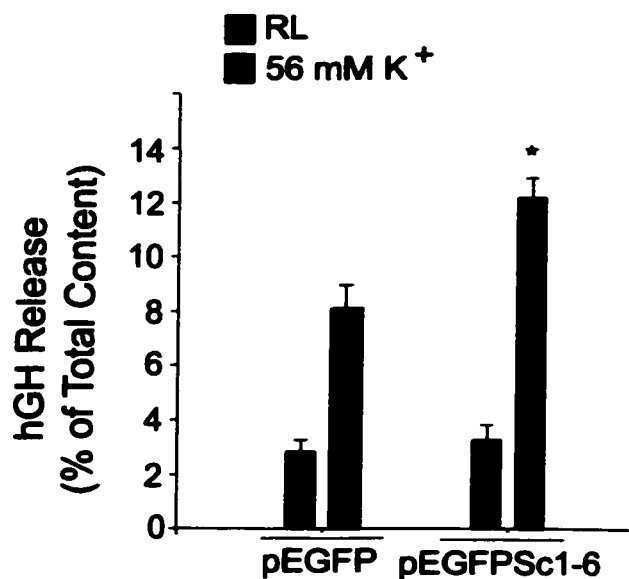


Figure 3.26: The effect of Sc1-6 overexpression on high K⁺- evoked chromaffin cell exocytosis.

Chromaffin cells highly purified by differential plating (Waymire et al., 1983) were transiently transfected by electroporation using 25 μ g DNA of pEGFP or pEGFPSc1-6 and 25 μ g of pXGH5. Cells were plated at a cell density of 3×10^6 and incubated at 37°C, under an atmosphere of O₂ and 5% CO₂. Twelve hours following electroporation, chromaffin cells were exposed to an extensive depletion of intracellular stores by applying 3 pulses of 8 min each of 56 mM K⁺ Locke's solution, repeated at 9 min intervals. hGH release experiments were performed 48 hours after the depletion of intracellular stores (Materials and Methods). Chromaffin cells were rinsed several times with 1 ml of regular Locke's solution and then subsequently incubated for 2 min each with 0.5ml regular Locke's solution, followed by 0.5 ml of Locke's solution containing a depolarizing concentration (56 mM) of K⁺. Cells were then lysed in 0.3 ml (3 times 0.1 ml) of 10 mM HEPES (pH 7.4) and 0.2 mM EDTA. hGH content was determined using a radioimmunoassay kit (Nichols Institute, San Juan Capistrano, CA), as described in Materials and Methods. Bars represent the mean \pm SEM of n = 4 experiments. In each experiment, each condition was assayed in quadruplicate. *p < 0.05.

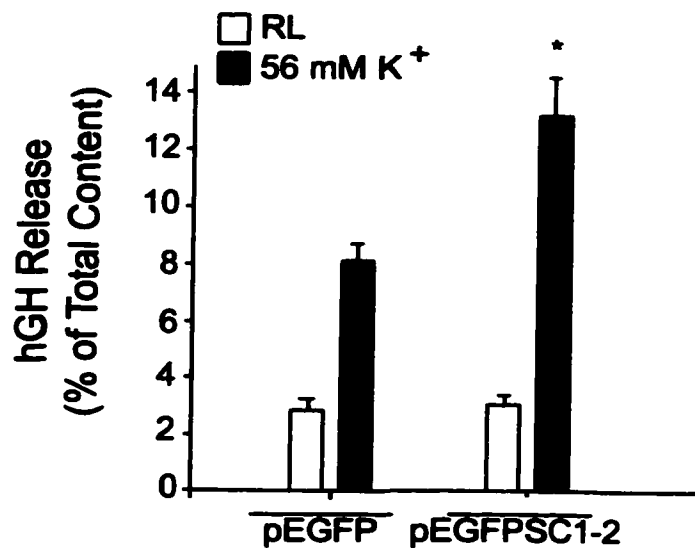


Figure 3.27: The effect of Sc1-2 overexpression on high K⁺- evoked chromaffin cell exocytosis.

Chromaffin cells highly purified by differential plating (Waymire et al., 1983) were transiently transfected by electroporation using 25 μ g DNA of pEGFP or pEGFPSc1-2 and 25 μ g of pXGH5. Cells were plated at a cell density of 3×10^6 and incubated at 37°C, under an atmosphere of O₂ and 5% CO₂. Twelve hours following electroporation, chromaffin cells were exposed to an extensive depletion of intracellular stores by applying 3 pulses of 8 min each of 56 mM K⁺ Locke's solution, repeated at 9 min intervals. hGH release experiments were performed 48 hours after the depletion of intracellular stores (Materials and Methods). Chromaffin cells were rinsed several times with 1 ml of regular Locke's solution and then subsequently incubated for 2 min each with 0.5ml regular Locke's solution, followed by 0.5 ml of Locke's solution containing a depolarizing concentration (56 mM) of K⁺. Cells were then lysed in 0.3 ml (3 times 0.1 ml) of 10 mM HEPES (pH 7.4) and 0.2 mM EDTA. hGH content was determined using a radioimmunoassay kit (Nichols Institute, San Juan Capistrano, CA), as described in Materials and Methods. Bars represent the mean \pm SEM of n = 4 experiments. In each experiment, each condition was assayed in quadruplicate. *p < 0.05.

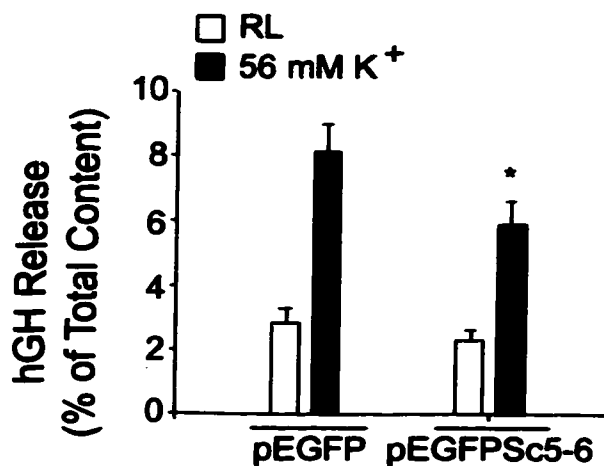


Figure 3.28: The effect of Sc5-6 overexpression on high K⁺- evoked chromaffin cell exocytosis.

Chromaffin cells highly purified by differential plating (Waymire et al., 1983) were transiently transfected by electroporation using 25 μ g DNA of pEGFP or pEGFPSc5-6 and 25 μ g of pXGH5. Cells were plated at a cell density of 3×10^6 and incubated at 37°C, under an atmosphere of O₂ and 5% CO₂. Twelve hours following electroporation, chromaffin cells were exposed to an extensive depletion of intracellular stores by applying 3 pulses of 8 min each of 56 mM K⁺ Locke's solution, repeated at 9 min intervals. hGH release experiments were performed 48 hours after the depletion of intracellular stores (Materials and Methods). Chromaffin cells were rinsed several times with 1 ml of regular Locke's solution and then subsequently incubated for 2 min each with 0.5ml regular Locke's solution, followed by 0.5 ml of Locke's solution containing a depolarizing concentration (56 mM) of K⁺. Cells were then lysed in 0.3 ml (3 times 0.1 ml) of 10 mM HEPES (pH 7.4) and 0.2 mM EDTA. hGH content was determined using a radioimmunoassay kit (Nichols Institute, San Juan Capistrano, CA), as described in Materials and Methods. Bars represent the mean \pm SEM of n = 4 experiments. In each experiment, each condition was assayed in quadruplicate. *p < 0.05.

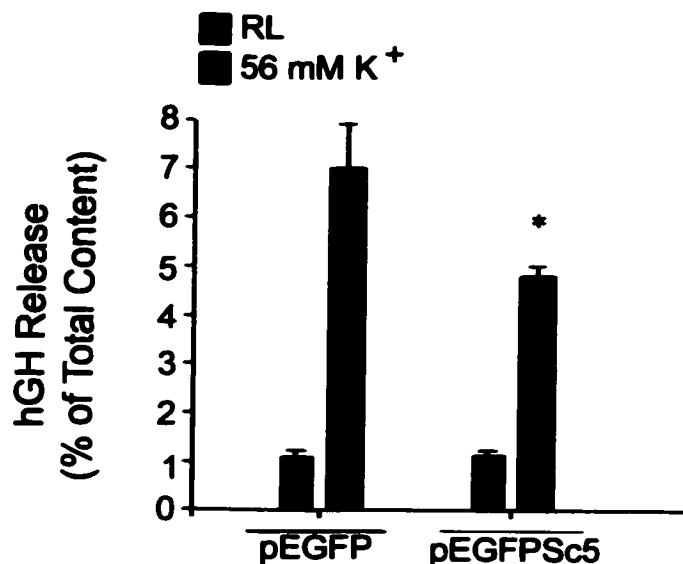


Figure 3.29: The effect of Sc5 overexpression on high K⁺- evoked chromaffin cell exocytosis.

Chromaffin cells highly purified by differential plating (Waymire et al., 1983) were transiently transfected by electroporation using 25 μ g DNA of pEGFP or pEGFPSc5 and 25 μ g of pXGH5. Cells were plated at a cell density of 3×10^6 and incubated at 37°C, under an atmosphere of O₂ and 5% CO₂. Twelve hours following electroporation, chromaffin cells were exposed to an extensive depletion of intracellular stores by applying 3 pulses of 8 min each of 56 mM K⁺ Locke's solution, repeated at 9 min intervals. hGH release experiments were performed 48 hours after the depletion of intracellular stores (Materials and Methods). Chromaffin cells were rinsed several times with 1 ml of regular Locke's solution and then subsequently incubated for 2 min each with 0.5ml regular Locke's solution, followed by 0.5 ml of Locke's solution containing a depolarizing concentration (56 mM) of K⁺. Cells were then lysed in 0.3 ml (3 times 0.1 ml) of 10 mM HEPES (pH 7.4) and 0.2 mM EDTA. hGH content was determined using a radioimmunoassay kit (Nichols Institute, San Juan Capistrano, CA), as described in Materials and Methods. Bars represent the mean \pm SEM of n = 4 experiments. In each experiment, each condition was assayed in quadruplicate.*p < 0.05.

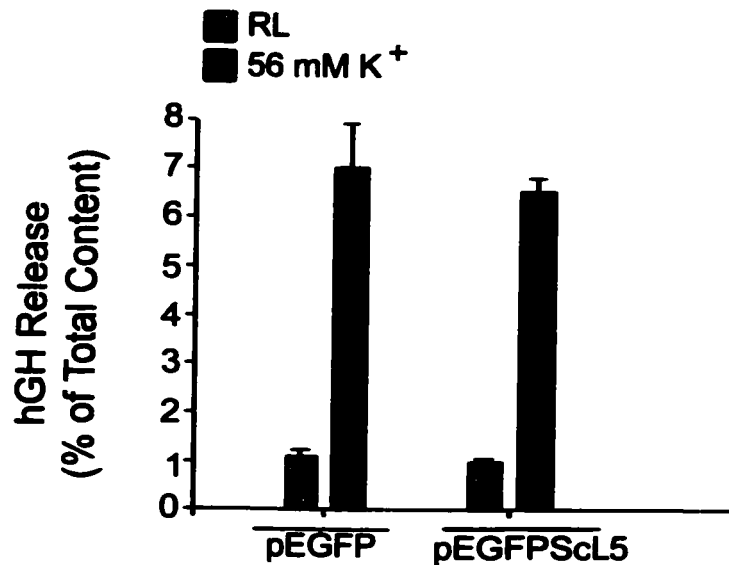


Figure 3.30: The effect of ScL5 overexpression on high K⁺- evoked chromaffin cell exocytosis.

Chromaffin cells highly purified by differential plating (Waymire et al., 1983) were transiently transfected by electroporation using 25 μ g DNA of pEGFP or pEGFPScL5 and 25 μ g of pXGH5. Cells were plated at a cell density of 3×10^6 and incubated at 37°C, under an atmosphere of O₂ and 5% CO₂. Twelve hours following electroporation, chromaffin cells were exposed to an extensive depletion of intracellular stores by applying 3 pulses of 8 min each of 56 mM K⁺ Locke's solution, repeated at 9 min intervals. hGH release experiments were performed 48 hours after the depletion of intracellular stores (Materials and Methods). Chromaffin cells were rinsed several times with 1 ml of regular Locke's solution and then subsequently incubated for 2 min each with 0.5ml regular Locke's solution, followed by 0.5 ml of Locke's solution containing a depolarizing concentration (56 mM) of K⁺. Cells were then lysed in 0.3 ml (3 times 0.1 ml) of 10 mM HEPES (pH 7.4) and 0.2 mM EDTA. hGH content was determined using a radioimmunoassay kit (Nichols Institute, San Juan Capistrano, CA), as described in Materials and Methods. Bars represent the mean \pm SEM of n = 4 experiments. In each experiment, each condition was assayed in quadruplicate. *p < 0.05.

3.6.b. Nicotine-induced chromaffin cell exocytosis

Chromaffin cells were co-transfected with pXGH5 and pEGFP vector (control) or carrying full Sc sequence or Sc5-6. Transfected chromaffin cells were further depleted of their catecholamine content, as described above. Forty eight hours post transfection, chromaffin cells were treated for 40 seconds each, with either regular Locke's solution or Locke's solution containing 10 μ M of nicotine, as described in Materials and Methods. At the end of the incubation period, cells were lysed and hGH output was measured in both the incubation medium and in the cells (Radioimmunoassay kit, Nichols Institute). Similar to the high K⁺-evoked hGH release in transfected cells, chromaffin cells overexpressing Sc1-6 showed a 58% increase in nicotine-induced hGH release, when compared to control (Fig. 3.32). Furthermore, chromaffin cells overexpressing Sc5-6 presented a 32.8% decrease in Nicotine-evoked hGH release when compared to control cells (Fig. 3.33).

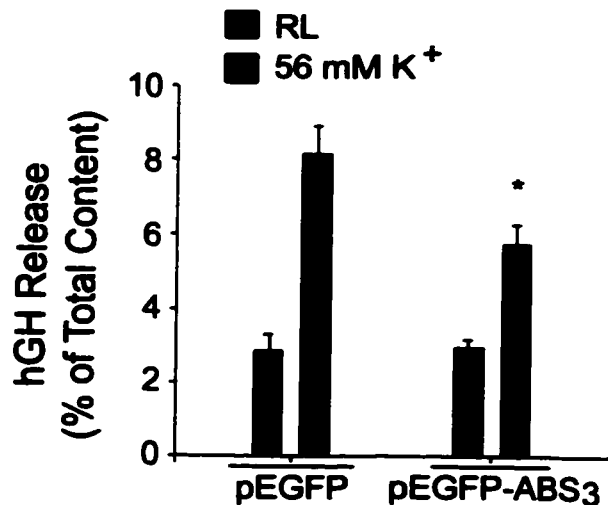


Figure 3.31: The effect of ScABS3 overexpression on high K⁺- evoked chromaffin cell exocytosis. Chromaffin cells highly purified by differential plating (Waymire et al., 1983) were transiently transfected by electroporation using 25 μ g DNA of pEGFP or pEGFPScABS3 and 25 μ g of pXGH5. Cells were plated at a cell density of 3×10^6 and incubated at 37°C, under an atmosphere of O₂ and 5% CO₂. Twelve hours following electroporation, chromaffin cells were exposed to an extensive depletion of intracellular stores by applying 3 pulses of 8 min each of 56 mM K⁺ Locke's solution, repeated at 9 min intervals. hGH release experiments were performed 48 hours after the depletion of intracellular stores (Materials and Methods). Chromaffin cells were rinsed several times with 1 ml of regular Locke's solution and then subsequently incubated for 2 min each with 0.5ml regular Locke's solution, followed by 0.5 ml of Locke's solution containing a depolarizing concentration (56 mM) of K⁺. Cells were then lysed in 0.3 ml (3 times 0.1 ml) of 10 mM HEPES (pH 7.4) and 0.2 mM EDTA. hGH content was determined using a radioimmunoassay kit (Nichols Institute, San Juan Capistrano, CA), as described in Materials and Methods. Bars represent the mean \pm SEM of n = 4 experiments. In each experiment, each condition was assayed in quadruplicate. *p < 0.05.

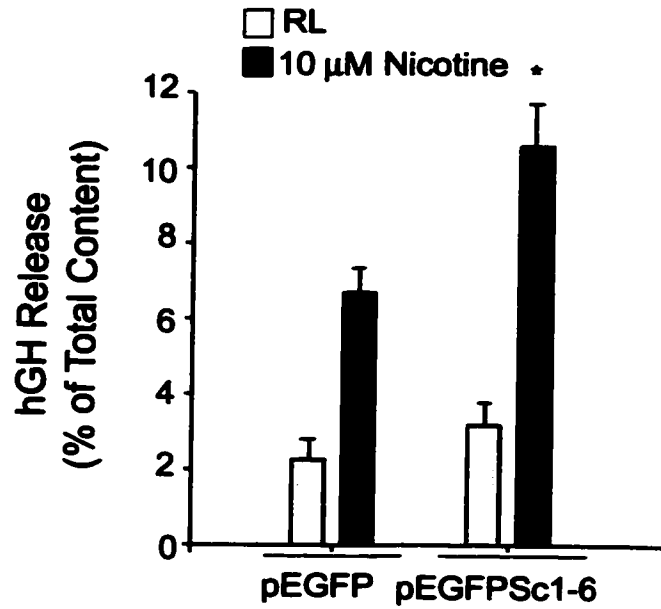


Figure 3.32: The effect of Sc1-6 overexpression on nicotine - evoked chromaffin cell exocytosis. Chromaffin cells highly purified by differential plating (Waymire et al., 1983) were transiently transfected by electroporation using 25 μ g DNA of pEGFP or pEGFPSc1-6 and 25 μ g of pXGH5. Cells were plated at a cell density of 3×10^6 and incubated at 37°C, under an atmosphere of O₂ and 5% CO₂. Twelve h following electroporation, chromaffin cells were exposed to an extensive depletion of intracellular stores by applying 3 pulses of 8 min each of 56 mM K⁺ Locke's solution, repeated at nine minutes intervals. hGH release experiments were performed 48 h after the depletion of intracellular stores (Materials and Methods). Chromaffin cells were rinsed several times with 1 ml of regular Locke's solution and then subsequently incubated for 40sec each with 0.5ml regular Locke's solution, followed by 0.5 ml of Locke's solution containing 10 μ M nicotine. Cells were then lysed in 0.3 ml (3 times 0.1 ml) of 10 mM HEPES (pH 7.4) and 0.2 mM EDTA. hGH content was determined using a radioimmunoassay kit (Nichols Institute, San Juan Capistrano, CA), as described in Materials and Methods. Bars represent the mean \pm SEM of n = 4 experiments. In each experiment, each condition was assayed in quadruplicate. *p < 0.05.

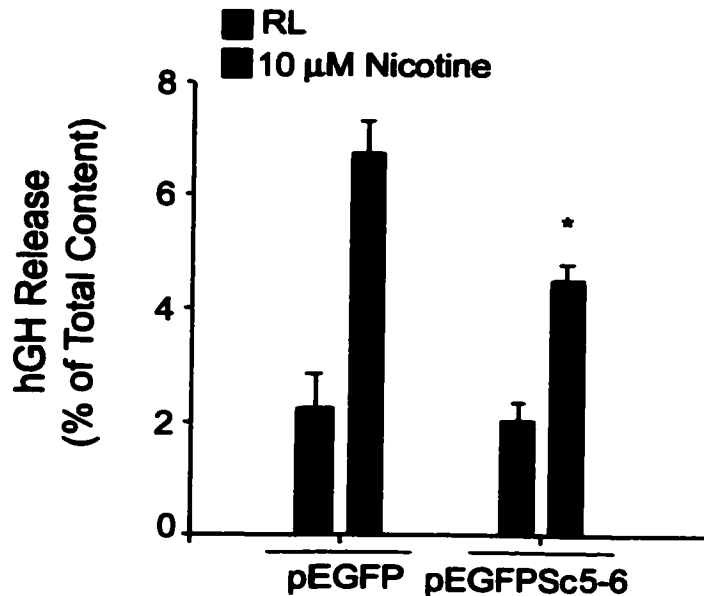


Figure 3.33: The effect of Sc5-6 overexpression on nicotine - evoked chromaffin cell exocytosis.

Chromaffin cells highly purified by differential plating (Waymire et al., 1983) were transiently transfected by electroporation using 25 μg DNA of pEGFP or pEGFPSc5-6 and 25 μg of pXGH5. Cells were plated at a cell density of 3×10^6 and incubated at 37°C, under an atmosphere of O₂ and 5% CO₂. Twelve h following electroporation, chromaffin cells were exposed to an extensive depletion of intracellular stores by applying 3 pulses of 8 min each of 56 mM K⁺ Locke's solution, repeated at nine minutes intervals. hGH release experiments were performed 48 h after the depletion of intracellular stores (Materials and Methods). Chromaffin cells were rinsed several times with 1 ml of regular Locke's solution and then subsequently incubated for 40sec each with 0.5ml regular Locke's solution, followed by 0.5 ml of Locke's solution containing 10 μM nicotine. Cells were then lysed in 0.3 ml (3 times 0.1 ml) of 10 mM HEPES (pH 7.4) and 0.2 mM EDTA. hGH content was determined using a radioimmunoassay kit (Nichols Institute, San Juan Capistrano, CA), as described in Materials and Methods. Bars represent the mean ± SEM of n = 4 experiments. In each experiment, each condition was assayed in quadruplicate.*p < 0.05.

4 - DISCUSSION

4.1. Investigation by transient transfection of the effects of Scinderin or various Scinderin deletion constructs on regulated exocytosis

Techniques have been developed to render the plasma membrane of secretory cells permeable to ions and proteins while maintaining the secretory response to micromolar Ca^{2+} (Wilson and Dunn, 1983). These techniques have made it possible to determine the role of various soluble factors in exocytosis and analyze the steps involved in the secretory pathway (Kelner et al., 1986). However, because permeabilized cells do not reseal readily (Sarafian, 1987; Kelner, 1986), it is not possible to investigate the effects of exogenous expressed proteins on regulated secretion. Furthermore, it has not been possible to investigate the effects on secretion of the overexpression of integral membrane proteins whether derived from the plasma or from the secretory vesicle membranes. To study the role of different scinderin domains in regulated secretion, a bovine chromaffin cell transient transfection system has been used (Hotz et al., 1995). The technique allows for the investigation of the function of soluble or membrane-bound proteins in secretion from either intact or permeabilized cells. A key part of this approach is to co-transfect into chromaffin cells an effector plasmid (pEGFP alone or with different Sc fragments) together with a reporter plasmid encoding human growth hormone (hGH) – pXGH5. It has previously been shown that the rat pheochromocytoma PC12 cell line stably transfected with a plasmid carrying the hGH gene packs the hGH in its secretory granules (Schweitzer and Kelly, 1985; Schweitzer and Paddock, 1990). The same method can be used to insert hGH into chromaffin secretory granules. The hGH was co-purified with the catecholaminergic secretory vesicle fraction following density gradient centrifugation (Schweitzer and Kelly, 1985; Schweitzer and Paddock, 1990).

Primary (non-dividing) bovine chromaffin cells have also been transiently transfected with the hGH gene (Holz, 1995). In these cells, the expressed hGH is stored in chromaffin granules and serves as a reporter for the secretory pathway in the transfected cells (Holz et al, 1993). However, hGH was expressed in a small number of cells (Holz et al, 1993). In experiments done by Holz R. et al. (Holz R. et al., 1995), only 0.1% of the cells were transfected. The transfection rate and the amount of hGH released were measured using a sensitive radioimmunoassay for GH. Although the rate of transfection was small, this system does readily detect secretion. The measurement of catecholamine secretion is predominantly a measure of secretion from nontransfected cells, since they represent the vast majority of the cells on the dish. However, the rate of secretion of transiently expressed hGH is similar to that of endogenous catecholamines. By measuring the effects of expression of the protein of interest on hGH secretion, one can determine the effects of the protein on secretion from the small fraction of transfected cells.

The transient transfection approach is attractive not only because it can be applied to primary cells, but also because (1) experiments can be completed within 1 week instead of the many months required to establish a cell line; (2) the amount of protein expressed per cell can be much greater than in clonal cell lines (Gorman C., et al., 1991), because the cDNA need not be incorporated in the genome (a low efficiency process); (3) copies of two plasmids can enter the same cell, so co-expression of two or more plasmids in the same cell is more likely in transient than in stable transfection (Scangos G., et al. 1981); and (4) secretion can be measured in hundreds or thousands of cells at a time. Scinderin is exclusively detected in tissues with high secretory activity, including brain and chromaffin cells. We have used the transient transfection method approach to investigate

the role of Sc and of various scinderin domains in regulated exocytosis. In this way we have engineered chromaffin cells that overexpress either full-length scinderin (Sc1-6) or one of the scinderin deletion constructs.

4.1.a. Selection of the transient transfection method for chromaffin cells

The need to transfect recombinant DNA molecules into mammalian cells has precipitated the development of many different transfection methods, including calcium phosphate co-precipitation, electroporation, cationic lipid-based transfection and, most recently, the gene gun. Although these methods are effective for transfecting many common cell lines, many other cell types cannot be routinely or efficiently transfected by any of them. Their limitations are even greater when it comes to the transfection of primary cell cultures, which are, in most cases, extremely difficult to transfect by current methods. This constitutes a great challenge, since primary cultures frequently offer major advantages over other cell lines for the biochemical and immunochemical analysis of specific cell functions. Chromaffin cells are non-dividing, primary cells that are quite difficult to transfect. Therefore, the transfection method chosen can strongly influence results. Our primary aim was to develop an efficient method of producing viable transfected cells suitable for release studies. Previous studies with chromaffin cells have reported transfection efficiencies ranging from 0.1% (Holz R. et al., 1993) to 35 % (Wilson S.P. et al., 1995). However, in many cases these results were controversial, mainly due to a lack of systematic analysis. Therefore, we decided to examine and compare four different transfection methods as potential tools for the efficient delivery of DNA. These included two Qiagen lipid-mediated transfection methods (lipofectin and effectene), the calcium phosphate (CaPH) technique, and electroporation. To optimize transfection efficiency, a

number of critical parameters were varied, depending on the method being used.

Lipofectin and effectene are two lipid-mediated transfection methods. Lipofectin is a positively charged liposome that interacts with negatively charged DNA to form a stable complex (Felgner et al., 1987). The fusion of this complex with tissue culture cells results in their uptake and expression of the DNA (Felgner et al., 1987). Effectene is a non-liposomal lipid-mediated gene transfer system in which DNA is strongly condensed by the interaction of negatively charged phosphate groups of the nucleic acid with a specific positively charged enhancer (Ausubel, F., M., et al, 1991). The condensed DNA is then coated with a cationic non-liposomal lipid. This method can be successfully used for the transfection of the rat pheochromocytoma cell line PC12 (manufacturer specifications). Therefore, we decided to try them in chromaffin cells. It has been shown that the lipid: DNA ratio and the overall DNA concentrations used in forming these complexes are extremely important for efficient gene transfer (Wrobel et al., 1995, Chang et al., 1988). Therefore, two different DNA concentrations at two DNA: lipofectin or two DNA: effectene ratios were used, as shown in Table 1 and Table 2 (Materials and Methods). As described in the results chapter, in both cases, increasing the DNA amount resulted in an increase of efficiency of transfection. However, neither of the lipid-mediated gene transfer methods yielded a transfection efficiency higher than 0.5% (compared to a transfection efficiency of 5% for PC12 cells, as described by Choidas et al., 1998). The low level of transfection for chromaffin cells might be due to the fact that they are primary, non-dividing cells that are much more difficult to transfect than cell lines such as PC12.

The calcium phosphate (CaPH) method involves mixing DNA in a phosphate buffer

containing calcium chloride, to form a calcium-phosphate-DNA complex that adheres to the cell membrane and enters the cytoplasm by endocytosis (Graham F., L., et al, 1973). The highest reported rate of the transient transfection of chromaffin cells using the CaPH method was 35%. The experiments described here were performed using the optimal conditions described by Wilson et al. (1995). However, as shown in the results chapter, the efficiency of transfection obtained in our laboratory was much lower than the one reported by Wilson et al. (Wilson et al., 1995). Therefore, we decided to try electroporation as a transient transfection method for chromaffin cells.

Electroporation involves the exposure of cells to a pulsed electric field, which is thought to create pores in the plasma membrane (Kinosita et al., 1977). The basic principles of electroporation have been described by Knight et al. (1981). The pulse delivered is characterized by two pulse parameters, the field strength (kV/cm) and the time constant (τ). The field strength is controlled by setting the voltage (kV) that is pulsed across the cuvette gap (cm). The resistance and capacitance in the complete circuit determine the time constant.

The main advantage of electroporation is its applicability for the transient and stable transfection of all cell types. However, a disadvantage is that it requires approximately five-fold greater quantities of DNA and cells than other available methods. Moreover, a major drawback of electroporation is that it results in a high mortality that can affect 50-70% of cells (Chu et al., 1987). It has been shown that the factors that can lead to a reduction of viability in electroporated cells are DNA breaks, the production of reactive oxygen species and a small effect from fluctuation of calcium levels (Meldrum et al, 1999).

Several studies have been done to determine the optimal electroporation parameters for mammalian cells (Chu et al., 1987; Bodwell et al., 1999). To maximize DNA uptake, the electrical field must be optimized for voltage and duration, in conjunction with DNA concentration, cell number, temperature, and buffer composition (Bodwell et al., 1999). It has been shown that the transfection of mammalian cells by electroporation is more efficient for larger capacitances (1020F vs. 540F) (Chu. et al., 1987). Cell viability appears to depend primarily on the total charge passing through the cell suspension, with a lesser dependence on capacitance (Chu, et al., 1987). Therefore, we tried to determine the optimal voltage and then the optimal DNA concentration for a capacitance of 1020F (Chu. Et al., 1987, Armstrong et al., 1996). The experiments described here indicated that a voltage of 250V produced a lower level of cell viability than 150V. This can be explained by the fact that cell viability depends on the total charge passing through the cell suspension (the total electric charge is equal to the product of the capacitance C and the voltage V). In other words, increasing the total charge passing through the cells, resulted in an increased rate of cell death. However, our experiments show that, notwithstanding the higher mortality rate involved, transfection efficiency was much higher at 250V than at 150V. A possible explanation is that a higher total charge produces larger holes in cell membranes, increasing membrane permeability to larger molecules, so that more cells uptake the DNA. Moreover, our experiments have shown that transfection efficiency is dependent upon DNA concentration. In summary, the electroporation procedure described here was found to be simple, reproducible and highly efficient. Electroporation was more efficient than the calcium phosphate, lipofectin or effectene methods. This can be explained by the fact that electroporation probably

involves a physical interaction between the cell membrane and the applied electric field (Kinosita and Tsong, 1977). Therefore, efficient transfection with this method might prove to be relatively independent of cell type. This represents a significant advantage over the other methods employed here, as they are generally understood to be dependent on cell type. In conclusion, the following transfection conditions were considered optimal with respect to cell viability and transfection efficiency: one pulse of 250 V, 1020 μ F and 50 μ g DNA/ 10⁷ cells (in a volume of 400 μ l), for a time of 34 to 39 msec, in a 0.4 cm diameter cuvette. These parameters were used in all subsequent experiments.

4.1.b. Human Growth hormone is targeted to the regulated secretory pathway in chromaffin cells

Previous experiments done on rat pheochromocytoma-derived neuronal cell line PC12, have shown that hGH can be selectively packed in membrane-bound vesicles that are indistinguishable from the endogenous catecholamine synaptic vesicles (Schweitzer E. et al., 1985). Moreover, it has been shown that in chromaffin cells, hGH is localized predominantly in secretory vesicles in the regulated secretory pathway and that the transiently expressed hGH undergoes Ca²⁺-dependent secretion similarly to endogenous catecholamines (Wick et al., 1993). Our immunofluorescence studies have demonstrated an extensive overlapping in staining, with both markers showing a dot-like staining that corresponds to secretory vesicles. All vesicles stained for hGH were also positive for DBH. On the other hand, not all DBH positive vesicles were positive for hGH. This can be explained by the fact that hGH is synthesized, packed and distributed only in newly synthesized chromaffin vesicles, whereas DBH and catecholamines are present in both newly synthesized vesicles and vesicles present prior to transfection. The perinuclear red

staining observed was due to an accumulation of hGH in the Golgi apparatus. The absence of this red staining in the non-transfected cells demonstrates the specificity of the staining for hGH. Furthermore, our experiments have demonstrated that chromaffin cells stimulated with a depolarizing concentration of K⁺, released up to $6.3 \pm 0.53\%$ of their total hGH content. Previous release experiments done in our laboratories, showed only a 1-3% catecholamine release upon stimulation with 56 mM K⁺ Locke's (Trifaró et al., 1994). A possible explanation is that in our experiments hGH was stored in secretory vesicles synthesized after the dissociation of cells from the medulla, whereas the catecholamines in previous release experiments were stored in older secretory vesicles. The more robust secretion rate observed for hGH may reflect a greater tendency of newly synthesized secretory vesicles to undergo secretion. In any case, our data indicate that transiently expressed hGH is targeted to chromaffin secretory vesicles and undergoes regulated exocytosis.

4.1.c. Extensive high K⁺ depolarization results in an improvement of chromaffin vesicle labeling with hGH and of hGH signal in release experiments

The cellular content and release of hGH was measured using a radioimmunoassay kit. The high sensitivity of this method (0.01 ng of hGH) allowed the precise measurement of 0.9% of the total cellular content. However, because only a small population of cells express hGH, and also because not all chromaffin granules (green) are stained for hGH (red) (Fig. 3.6.), we have attempted to increase the number of secretory vesicles labeled with hGH and consequently, the hGH signal in the release experiments. Previous studies from our laboratory have shown that prolonged stimulation of chromaffin cells brings

about a considerable depletion in their catecholamine content. Ten pulses of six minutes each with a depolarizing concentration (56 mM) of K⁺, each repeated at nine minute intervals, resulted in a practically complete depletion of chromaffin cell catecholamine content. The most significant depletion (above 70% of the total catecholamine content) takes place during the first three pulses. This depletion in catecholamine content was accompanied by changes in the pattern of DBH immunofluorescence. DBH staining disappeared from the perinuclear areas of the cytoplasm and was mainly concentrated in the periphery of the cells. Four days following stimulation, the levels of DBH have been observed to return to control levels (Trifaró et al, 1984). Consequently, it is possible that prolonged depolarization of hGH transiently expressing chromaffin cells would result in the release of the content of most chromaffin vesicles including those synthesized before chromaffin cell dissociation from the adrenal medulla. This would allow vesicle membrane recycling and the synthesis of new vesicles containing both newly synthesized catecholamines and hGH, and, consequently, a better hGH labeling of chromaffin vesicles. This change in our protocol was expected to bring about an improvement in the hGH signal in release experiments. Thus, three pulses of 8 min each applied at 9 minutes intervals, 36 h following transfection, resulted in a significant depletion in the number of chromaffin vesicles. As expected, and in keeping with the previous studies described above, our immunofluorescence studies showed that both DBH and hGH staining disappeared from the perinuclear areas, and they were concentrated mainly in the cell periphery (Fig. 3.8). The present results also indicate that a much better hGH labeling of the vesicle population was obtained when cells were previously depolarized by exposure to high K⁺. Moreover, 48 h following depolarization, our results showed a higher number

of DBH positive vesicles also labeled with hGH, when compared to control cells (Fig. 3.9). For cells previously depolarized, $68.2 \pm 2.1\%$ of the DBH positive vesicles were also positive for hGH, whereas only $50 \pm 2.5\%$ of DBH positive vesicles were labeled with hGH in control cells. Furthermore, there was a 37% increase in depolarization induced hGH release in cells previously challenged with high K^+ . This was due to the better labeling of chromaffin vesicles observed in our immunocytochemical studies, as described above.

4.1.d. Co-expression in chromaffin cells of pXGH5 and pEGFP carrying Sc construct creates a double – labeled system suitable for the study of the effects of this protein on regulated secretion

In order to study the effects of different Sc fragments and domains on regulated secretion, the pEGFP vector carrying the constructs fused in frame with the gene encoding green fluorescent protein (GFP) was transiently expressed into chromaffin cells together with the vector encoding hGH which was used as a reporter for regulated secretion. Living colors constitute excellent reporters for in vivo studies. The GFP-fusion of the constructs can be easily assayed and monitored in – vivo for the intracellular expression and localization of the fusion proteins by inverted microscopy.

As discussed above, electroporation is an efficient method for introducing genes into mammalian cells, and it has proven very efficient for chromaffin cells (Section 4.1.a). However, there are several factors that can lead to a reduction in cell viability in electroporated cells, such as DNA breaks or the production of reactive oxygen species or cell stress (Rosalind et al., 1999). Therefore, it was important to determine if there was a difference in terms of cell viability among cells transfected with different Sc deletion

constructs, compared to those transfected with vector alone or to mock cells. Our experiments showed a different survival of the transfected cells when compared to mock cells (cells electroporated but not transfected). However, when compared to cells transfected with vector alone, cells transfected with any of the Sc deletion construct containing vectors, showed a significantly lower rate of survival than cells transfected with full Sc or vector alone. This could be because the various Sc deletion constructs carry with them different rates of toxicity, and these rates are higher than the toxicity rate of the full scinderin gene.

Our immunofluorescence studies show that hGH is localized in chromaffin vesicles and that the co-expression of other proteins along with hGH does not affect the selective packing of hGH into the regulated secretory pathway. Fluorescence microscopy of the preparations revealed a heterogeneous population of cells that comprises i) cells not expressing any of the two proteins, ii) cells expressing only hGH, iii) cells expressing only GFP-fused Sc constructs, and iv) cells expressing both hGH and GFP-fused Sc fragments. Cells showing green fluorescence were counted under fluorescence microscopy. Our results showed differences in the transfection efficiencies of the various GFP-tagged Sc constructs. Co-transfection efficiency varied from $6.4 \pm 0.51\%$ for cells co-transfected with hGH and GFP-Sc5-6 to $20.47 \pm 1.25\%$ for control cells. One expects exocytosis that is detected by hGH secretion from cells cotransfected with plasmids encoding hGH and GFP-fused Sc construct proteins to be weighted to show secretion from cells that strongly express both proteins. Therefore, in the co-transfected chromaffin cell culture, the sub population of cells expressing both hGH and GFP is the only one relevant for the determination of the role of Sc fragments in regulated secretion.

However, also present is a subpopulation of cells expressing only the hGH. This population can account for a noise in the observed secretion levels. The transfection efficiency was carefully recorded since it represents an important parameter for the normalization of secretion results.

Immunoblots were also performed for hGH, Sc, tubulin and GFP in order to determine the level of protein expression in transfected chromaffin cells. The scinderin antibody raised against recombinant scinderin recognized different Sc truncations, but did not recognize ScABS3. However, this construct was recognized by an antibody raised against GFP. Our results suggest that the Sc constructs have a high level of expression, because the bands corresponding to sc constructs are of the same intensity as, or stronger than, those of endogenous Sc, and only a small fraction of cells were transfected with a Sc construct.

As discussed at the beginning of this section, the GFP-fusion of the constructs can easily be assayed and monitored in-vivo by inverted microscopy for their intracellular expression and localization, and the fate of the fusion proteins. Thus, the localization of GFP and of GFP-fusion constructs was studied using fluorescence microscopy. Control cells (transfected with vector alone) show a cytoplasmic distribution, while cells transfected with GFP- fused Sc1-6 or Sc-deletion constructs, showed both a cytoplasmic and a subplasmalemma distribution. This can be explained by the targeting of the GFP-fused construct to the places where the scinderin deletion construct localizes into the cell. For example, in the case of Sc5-6 the presence of the fusion construct in the cytoplasm is due to the amount of protein expressed in the cells (overexpression).

In summary, our experiments demonstrate that chromaffin cells co-transfected with two

plasmids carrying hGH and GFP-fused Sc or a Sc deletion construct constitute a suitable model for the study of the effects of these proteins on regulated secretion. This hypothesis is supported by the fact that co-expression of an exogenous protein along with hGH does not influence the selective packing and storage of hGH in the regulated secretory pathway. Although only a small population of cells expresses both proteins, the hGH measurement method is sensitive enough to detect as little as 0.01 ng of hGH. In addition, by making extensive use of a depolarization method, we improved the hGH labeling of chromaffin vesicles and obtained a better hGH release signal.

4.2. Scinderin sequence analysis and three dimensional structure prediction by homology modeling using gelsolin as a template for model building.

4.2.a. Molecular structure and active sites of Scinderin

In many eukaryotic cells, actin filaments are noncovalently cross linked in a layer between cytoplasm and cell membrane. This isotropic gel plays an important role in determining cell shape, locomotion, vesicle traffic etc., and is affected by extra cellular signals (Darnell et al., 1990). The cytoplasm of eukaryotic cells contains proteins that can sever actin filaments into short fragments, promoting fast disassembly of the actin network. Severing is a Ca^{2+} -activated, nonenzymatic, nonproteolytic process in which the severing protein binds to an actin subunit in the filament and induces a break with neighbouring subunits (Stossel et al., 1985). In chromaffin cells, filamentous actin (F-actin), mainly localized in the cortical surface, acts as a barrier to the chromaffin vesicles, impeding their free movement and contact with the plasma membrane (Trifaró et al., 1982). But secretion requires the movement of chromaffin vesicles toward the plasma membrane, the fusion of these vesicles with the plasmalemma and extrusion of the

vesicular content to the cell exterior by exocytosis (Viveros et al., 1975; Trifaró et al., 1977). Stimulation of chromaffin cells produces disassembly of the cortical actin network and removal of the barrier, which might impede the free movement of secretory vesicles (Trifaró et al., 1982, 1984, 1989; Cheek and Burgoyne, 1986, 1987). Cytochemical experiments with rhodamine-labeled phalloidin and actin antibodies demonstrated that in resting cells, a filamentous actin network is visualized as a strong cortical fluorescent ring (Lee et al., 1981; Cheek et al., 1986, 1987; Sontag et al., 1988; Trifaró et al., 1989). Upon stimulation there is a fragmentation of the cortical fluorescent ring and areas devoid of fluorescence can be noticed (Cheek and Burgoyne, 1986, 1987; Trifaró et al., 1989). The modifications are accompanied by a decrease in F actin associated with the concomitant increase in G-actin as evaluated by the DNase I inhibition assay (Cheek et al., 1986; Trifaró et al., 1989). F-actin network disassembly has also been observed in depolarized synaptosomes (Bernstein et al., 1985). The cortical F-actin network is not only a barrier to secretion but also controls the access of chromaffin vesicles to the subplasmalemmal area (release-ready vesicle pool) and consequently, the initial rate of exocytosis (Vitale et al., 1995). Most of the dynamic changes in the F-actin network during exocytosis are thought to be the result of activation of F actin severing proteins (Burgoyne et al., 1987; Cheek et al., 1991; Trifaró et al., 1985).

The search for factors that might regulate the dynamics of the actin cytoskeleton resulted in the discovery, in our laboratory, of scinderin (Del Castillo et al., 1990). Nicotine receptor stimulation or K⁺-evoked depolarization of chromaffin cells induces simultaneously cortical F-actin disassembly and redistribution of subplasmalemmal scinderin (Vitale et al., 1991).

Some of scinderin's properties could be demonstrated after purification of small amounts from bovine chromaffin cells (Rodriguez Del Castillo et al., 1990), but the answers to many questions regarding this novel protein were to be found once the scinderin cDNA could be isolated, sequenced and expressed in large amounts followed by purification in order to perform studies on biological systems (secretory cells).

Sequence analysis of scinderin and its close relative, gelsolin (Fig. 4.1), have revealed the interesting fact that scinderin, as well as gelsolin, has six internal repeats of three short sequence motifs (A, B, C) that occur at approximate equal distances in the molecule. Two smaller actin filament severing proteins, severin from *Dictyosteliurn discoideum* (André et al., 1988) and fragmin from *Physarurn polycephalum* (Ampé et al., 1987) also contain homologies to scinderin. Thus, they both have about half the molecular mass of scinderin and, as with gelsolin (Way et al., 1988), the homologies in sequence are high in the N-terminal half; also, the A, B, C motifs are to be found three times in severin and fragmin. After the alignment of motifs A, B and C, gelsolin, and scinderin both reveal six domains (1 to 6) with strong similarities between domains 1 and 4, 2 and 5, 3 and 6 (Fig.4.1). This data suggested that both of these proteins might have derived by gene duplication from an ancestral actin filament-severing protein (which was similar to the N-terminal half of these molecules) that looked a lot like severin or fragmin. It has also been suggested that this family of actin filament-severing proteins may have evolved by tandem gene triplication with a predicted 14 kDa monomer unit of 120-130 amino acid residues (Way et al., 1988), such as (approximately) domain 1 of gelsolin. However, chymotrypsin digestion of gelsolin and scinderin carried out under identical conditions produced a distinct 16 kDa fragment from gelsolin only (Rodriguez Del Castillo et al., 1990).

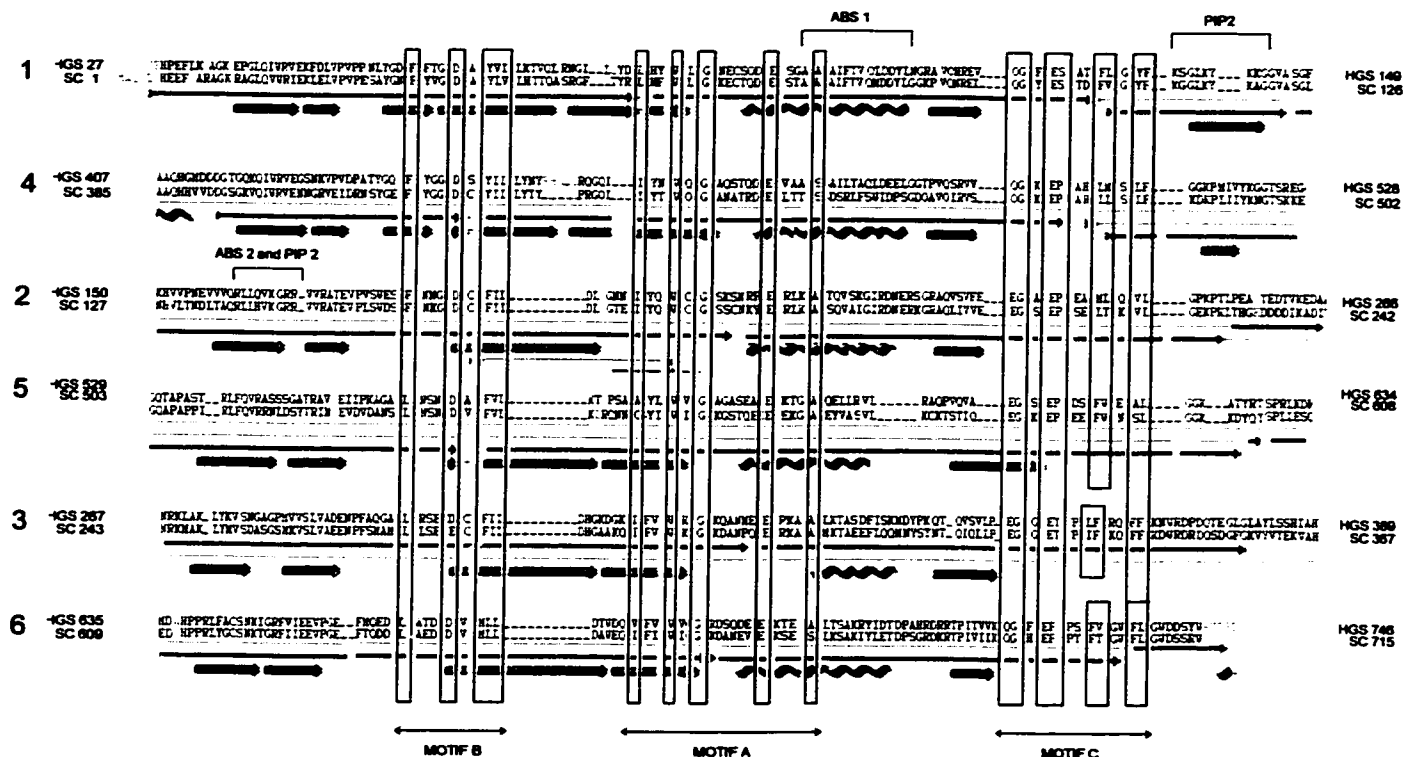


Figure 4.1. Sequence alignment and domain organization of human plasma gelsolin and bovine scinderin.

Alignment is based on pairwise analysis of all combinations of sequences as performed by Way and Weeds (1988) for gelsolin. Identities are outlined in red. Highly conserved motifs (B, A, and C) are shown in boxes. Gelsolin's secondary structure is indicated. Proteins are abbreviated as follows: HGS = human plasma gelsolin; SC = bovine scinderin; The numbers at either end indicate the positions of amino acid residues. The large numbers at the left side indicate the domain number (1-6) for the two proteins. Each motif is found once in a domain of each protein and it is repeated five additional times along the protein (Taken from Trifaró and Garcia, 1995).

The smaller fragment obtained from scinderin under these conditions had a molecular mass of 32 kDa (Rodriguez Del Castillo et al., 1990). Amino acid sequence analysis of three cyanobromide peptides of the 40 kDa Sc fragment has shown (once the whole sequence was available) that they are pieces of the N-terminal half of the protein.

4.2.b. Actin binding sites of Scinderin

Earlier data from our laboratory have shown that two molecules of actin bind one molecule of scinderin and this interaction is Ca⁺-dependent (Trifaró et al., 1992).

Furthermore, the two main fragments (40 and 38 kDa) obtained by the limited proteolytic digestion of Sc also interacted with actin, in a Ca²⁺-dependent manner, yielding protein complexes of molar ratios 1:1 (Del Castillo et al., 1990). These results suggested that each Sc fragment contains at least one actin and one Ca²⁺-binding site.

Comparison of the sequences of scinderin with those of gelsolin and villin showed the presence of two actin-binding sequences with high homology, in domains 1 and 2 respectively (Fig. 4.2.a). This suggests that the type of interaction (recently described by crystallographic studies) between gelsolin domains 1 and 2 and actin regarding the mechanisms of filament severing (McLaughlin et al., 1993) might be similar for scinderin and villin.

In other words, the filament-severing activity of scinderin might reside in the first two Domains, since it has been demonstrated for gelsolin that in addition to domain 1, another stretch of a few amino acid residues from domain 2 (second actin-binding site, Fig.4.2.b) is necessary for full severing activity (Way et al., 1988, Pope et al., 1991).

a	GELSOLIN	100	AAAIFTVQLDDYL	112
	SCINDERIN	77	AAAIFTVQMDDYL	89
	VILIN	76	AAAIYTTQMDEYL	88
b	GELSOLIN	161	RLFQVKGRR	169
	SCINDERIN	138	RLLHVKGRR	146
	VILIN	137	RLLHVKGKK	145

Figure 4.2. Comparison of amino acid sequences of two Sc regions with corresponding sequences of known actin-binding domains of gelsolin and villin. Two stretches of amino acid sequences of Scinderin from position 77 to 89 and from 138 to 146 show a high degree of homology with two (A and B) actin-binding domains previously described for human plasma gelsolin (Kwiatovski et al., 1986) and chicken intestinal brush border villin (Bazari et al., 1988). Aspartate 86 of scinderin corresponds to similar residues in positions 109 and 85 of gelsolin and villin, respectively. Aspartate 109 has been shown to be one of the Ca²⁺-binding sites of gelsolin (McLaughlin et al., 1993). The numbers on either side indicate the position of amino acid residues.

Moreover, it has been showed that the NH₂ terminal region of gelsolin domain 2 and the α 2 – helical segmnt in the COOH terminus (aa198-aa227) cooperate to form the F-actin binding site of gelsolin, and that both sequences are necessary to obtain full binding and severing.

It is possible, therefore, that severing activity requires interaction between more domains. Isoleucine residue 103 in gelsolin's first actin binding site also seems to be important for the interaction with sub domains 1 and 3 of actin (McLaughlin et al., 1993). Scinderin and villin have an isoleucine in the same position (residues 80 and 79 respectively) within their actin-binding sites (Fig.4.2.a). Previous work from our laboratory has also shown that the C-terminal half of scinderin binds monomeric actin in a Ca⁺-dependent manner (Trifaró et al., 1992), the same way as does the C-terminal half of gelsolin (Pope et al.,1991). It was recently suggested that one Ca²⁺ ion is intermolecularly bound between D109 of gelsolin and E167 of actin, with the rest of coordination links coming from domain 1 of gelsolin (crystallographic study, McLaughlin et al., 1993). Comparison of the amino acid sequence of the actin—binding sites of scinderin and gelsolin indicate that D86 of scinderin corresponds to D109 of gelsolin (Marcu et al., 1998). A second Ca²⁺ site has also been identified in domain 1 of gelsolin (McLaughlin et al., 1993). This site is an intramolecular pocket with binding coming from G65, D66, E97 and V145 and having the seven binding sites free for interaction with a phospholipid head group, as suggested for the annexins (Huber et al., 1990). Scinderin domain 1, also, has the same conserved amino acid sequence (G44, D66, E75, V122) with the first two amino acids in motif B and the third in motif A of domain 1 as in gelsolin (Marcu et al, 1998). Therefore, it is quite possible that scinderin will display the same spatial arrangement for the binding of

Ca²⁺.

Published evidence indicates that binding *in vitro* of domain 1 of gelsolin to actin is Ca²⁺-independent (Chaponnier et al., 1986; Bryan et al., 1989), whereas in the case of the N-terminal half of scinderin, the presence of Ca²⁺ is required for binding to actin (Trifaró et al., 1992). From this point of view, scinderin resembles villin rather than gelsolin.

Previous published work has demonstrated the presence and functional properties of three actin-binding sequences in domains 1 and 2 and 5 of scinderin (Marcu et al., 1994, 1998; Zhang et al., 1996). The high homology of the first two actin-binding sites in gelsolin, villin and scinderin would suggest that the type of interaction described for domains 1 and 2 of gelsolin with actin (McLaughlin et al., 1993) might be similar for scinderin and villin. However, it should be pointed out that published evidence indicates that the *in vitro* binding of domain 1 of gelsolin to actin seems to be Ca²⁺-independent (Chaponnier et al., 1986; Bryan, 1988), whereas in the case of scinderin, this binding requires the presence of Ca²⁺ (Trifaró et al., 1992). In this regard, scinderin resembles villin rather than gelsolin.

The first 5 amino acids in the sequence (RLFQVRRNL) of the third actin binding site which correspond to amino acids in position 511-519 of scinderin are the same as those present in positions 161— 165 which corresponds to the second actin-binding site (RLFQVKGRR) of gelsolin's segment 2. The site (aa511-519) present in Sc5-6 is able to bind actin monomers, a property similar to gelsolin S4-6 (Way et al., 1989). However, the actin-binding site in this part of gelsolin has been localized to segment 4 (Pope et al., 1995). The results of different types of experiments indicate that segment 4 of scinderin has no actin binding properties (Marcu et al, 1998). Moreover, and contrary to what has

been described for gelsolin S4-6 though similar to gelsolin S-2 (Way et al., 1989), the binding of actin to Sc5-6 is Ca^{2+} —independent (Marcu et al. 1998).

Previous experiments from our laboratory have demonstrated that intact native scinderin interacts with actin in a Ca^{2+} -dependent manner and is eluted from actin Sepharose 4B affinity columns with EGTA buffers (Marcu et al., 1994; Trifaró et al., 1989;), suggesting a homology between these two proteins. Therefore, it is quite possible that the third actin-binding site of scinderin is hidden and it is only exposed upon binding of Ca^{2+} and/or actin to other scinderin sites with the consequent changes in the configuration of the protein.

Approaches to structure prediction leverage the fact that proteins with similar sequences have similar structures, and thus similar functions. Homology modeling is an approach that aligns the sequence of a novel protein with those of proteins whose 3-D structure is known. The structure of the protein whose sequence is most homologous is used as a template for model building. As discussed above, the amino acid sequence indicates that bovine chromaffin cell scinderin shares 63% and 53% homology respectively with gelsolin and villin, two other F-actin severing proteins. Models of gelsolin structure and function based upon analyses of proteolytically-derived or bacterially-expressed fragments have been refined by determination of the crystallographic structure of full length gelsolin in submicromolar free Ca^{2+} (Leslie D. Burtnick et al., 1997). As expected, the conserved residues in each of the six domains define the basic domain structure, whereas actin binding and other functions involve residues that vary between the domains (Leslie D. Burtnick et al., 1997). Viewed in the context of the primary structure, domains 1-6 of gelsolin may be considered as beads on a string. However, in

the crystallographic model, gelsolin's six domains condense into a globular structure. Fig. 4.3 shows a set of panels with the three dimensional structure of gelsolin. Every panel has one of gelsolin's domains highlighted. Domain 6 is centrally placed in the structure of gelsolin, having multiple interactions with the first three segments. The structural analysis of the inhibited form of gelsolin (Ca^{2+} free) has provided evidence for a noncovalent interaction between the C-terminal part of domain six and domain 2, which renders all of its three actin-binding sites inaccessible (Leslie D. Burtnick et al., 1997). The C-terminal part of gelsolin involved in this interaction is showed in blue in Fig. 4.4.a and b. Conserved positively charged residues in domain 2 at Arg 207, Lys218 and Arg225 interact electrostatically with conserved negatively charged residues Asp744, Asp 747, and Glu 752 in the C-terminal helix (Fig. 4.4.b) (Leslie D. Burtnick et al., 1997). It has been shown that the absence of the helix (aa738 to aa 755) (Fig. 4.4.a, blue) greatly alters the Ca^{2+} sensitivity of gelsolin, but it does not create a calcium-insensitive molecule (Lueck et al., 2000).

It has been proposed that the effector of the remaining Ca affinity sites may reside very near the C-terminus with the domain six. Thus, the deletion of another 5 aminoacids (732-755) shown in Fig. 4.4.a in bold characters, results in a total loss of calcium regulation, but not in the loss of the severing and nucleating activity of gelsolin (Lueck et al., 2000; Kwiatkowski et al., 1989). In the calcium-free gelsolin crystal, these aminoacids are in close association with stretches of domains 4 and 6 (Burtnick et al., 1997). These residues are identical in scinderin and gelsolin as shown in Fig. 4.4.a.

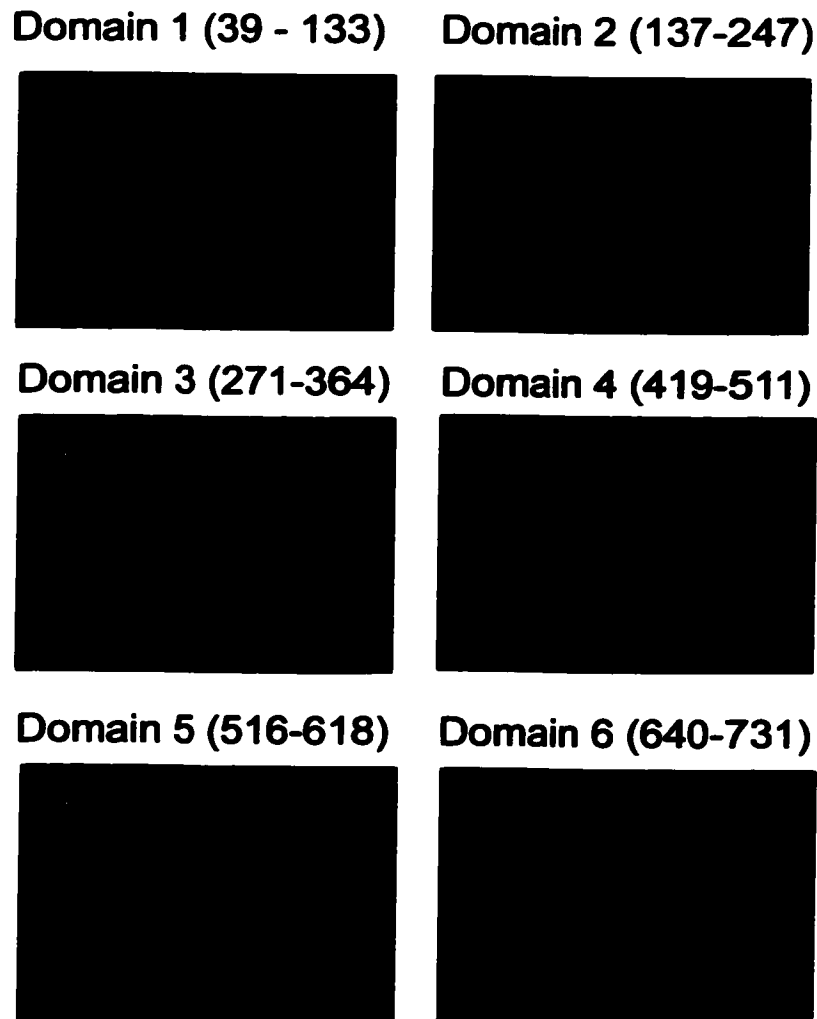


Figure 4.3. Three-dimensional structure and domain arrangement of calcium free gelsolin.

The three-dimensional structure of Ca²⁺-free gelsolin (Burtnick et al., 1997) was obtained from NCBI's Entrez database of experimentally determined three-dimensional biomolecular structures and viewed with Cn3D, a helper application for the web browser. Each panel contains one of gelsolin's domains highlighted (yellow). Domain six is centrally placed in the structure of gelsolin making connections with domains 2, 3, and 4. The C-terminal latch helix of gelsolin involved in a non-covalent interaction with domain 2 (upper right panel) is shown in blue.

a

SC	700	PTFTGW FLGW DSSRW	715
HGS	723	FEPPSFV GWFLGW DDDYWSVD	755

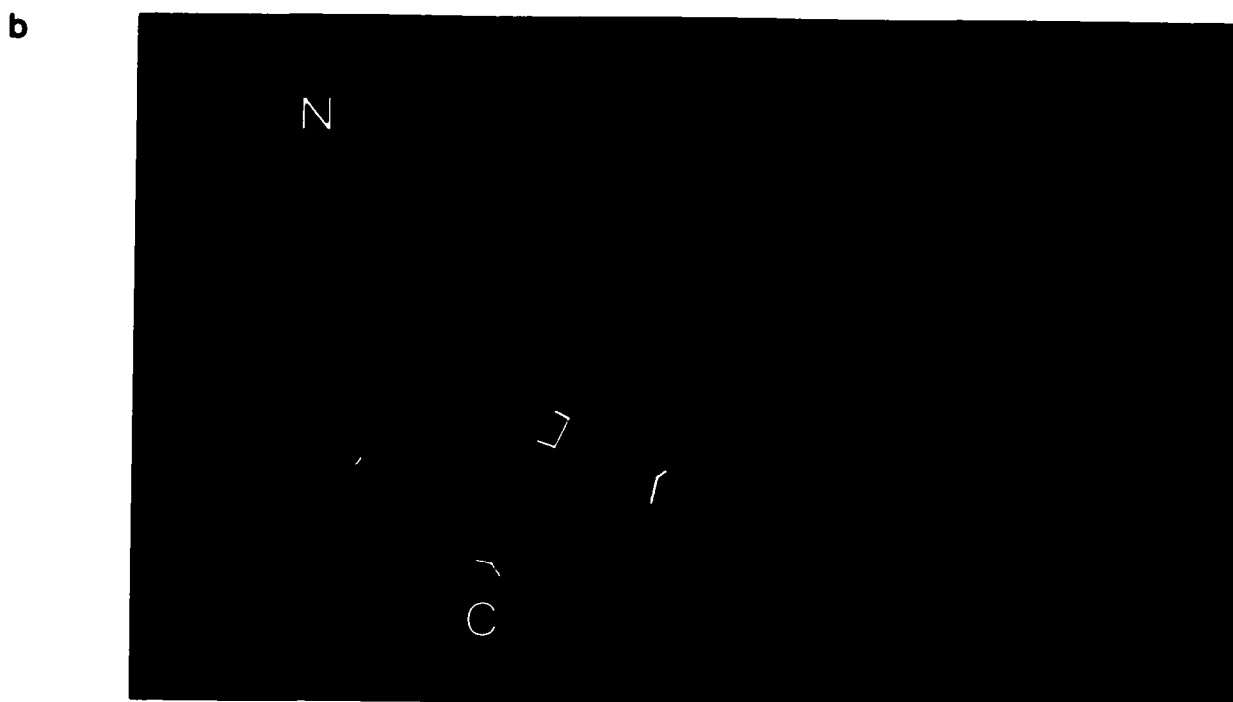


Figure 4.4. Homology of Scinderin and gelsolin in a region necessary for calcium regulation.

Intra-molecular interactions between the C-terminal part of gelsolin and the first three domains. The sequences of the C-termini of gelsolin and adseverin are listed in panel a. The C-terminal latch helix is shaded in blue, and the residues identified as being necessary to maintain calcium regulation are identified in boldface type. These residues are identical in scinderin and gelsolin (a) (Taken from Lueck et al., 2000). In the wireframe diagram (b) of the calcium-free gelsolin crystal, the C-terminal helix is identified in blue. These aminoacids are in close association with stretches of domains 4 and 6 (Burtnick et al., 1997). Conserved positively charged residues in domain 2 interact with conserved negatively charged residues in the C-terminal helix of gelsolin: Asp669, Asp670 with Arg168, Arg169 (white); Arg207 with Asp744 (green); Lys218 with Asp747 (blue) and Arg225 with Glu752 (yellow).

Some other intramolecular interactions within gelsolin's molecule, revealed in the crystallographic structure of full length gelsolin, include the conserved Asp669, Asp670 just prior to the start of strand C in domain six, with Arg168 and Arg169 at the edge of the core β sheet of the second domain, in the putative actin filament binding site (Burtnick et al., 1997) (fig. 4.4.b, white).

The identity in sequence between gelsolin and scinderin in regions necessary for calcium regulation, and the similarity of scinderin and the helix-deficient gelsolin construct (lacking aa732-aa755), suggest that Sc's 6th domain may also be centrally situated in the molecule, making connections with domains 2,3 and 4. Moreover, it is possible that these two proteins undergo similar structural changes upon calcium binding.

The conformation of the protein compact in EGTA, with the carboxy-terminal peptide overlying an actin-binding helix of domain 2, suggests that a major structural change occurs with activation.

4.2.c. PIP2- binding sites of Scinderin

Our previous molecular cloning experiments (Marcu et al., 1994) and sequence analysis have described two PIP2 binding sites in scinderin and additional experiments have demonstrated the ability of PIP2 liposomes to bind scinderin in a Ca^{2+} - and pH-dependent manner (Rodriguez Del Castillo et al., 1992,b ; Marcu et al., 1994). The two PIP2 binding sites of scinderin show the consensus sequence R(X)XXXKXRR, characteristic of PIP2 binding sites of phospholipase C (Marcu et al., 1994). Furthermore, one of the PIP2 binding sites of scinderin overlaps with its second actin binding site (Marcu et al., 1994) and this might account for the inhibitory effect of PIP2 on scinderin F-actin severing activity (Maekawa and Sakai., 1990) and the inhibition of

the recombinant scinderin effects on catecholamine release. On the other hand, Sc-PIP2BP, a scinderin-derived PIP2-binding peptide, blocked both the binding of PIP2 liposomes to scinderin and the PIP2 inhibition of scinderin effects (Zhang et al., 1996). The effects of PIP2 on F-actin disassembly and Ca²⁺-induced exocytosis are mediated through the interaction between scinderin and the intact phospholipids of the membrane (Zhang et al., 1996).

A large amount of data indicate that phospholipids of the membrane (mainly PIP2) modulate the activity of many actin regulatory proteins, as gelsolin and scinderin (Janmey et al., 1987; Lassing et al., 1988; Maekawa et al., 1990; Rodriguez Del Castillo et al., 1992, *b*). Additional work from our laboratory has shown that Sc also binds to PS and PIP2 in a Ca²⁺, and pH—dependent manner (Rodriguez Del Castillo et al., 1992). Amino acid sequence analysis revealed the presence in scinderin, in the C-terminal of domain 1 and N-terminal of domain 2, of sequences with high homology to those known to bind PIP2 in gelsolin, in the same positions (Marcu et al., 1994). There is a consensus sequence for the PIP2 binding sites in all these actin filament-severing proteins and this sequence can also be found in several phospholipase C isozymes where it is known as the “X Box” (Rhee et al., 1989; Janmey et al., 1992; Yu et al., 1992).

4.3. Role of Scinderin in the control of F-actin disassembly and chromaffin cell exocytosis

Adrenal medullary chromaffin cells are an excellent system for the study of the mechanism of secretion; these cells can be maintained in primary culture and the influences on catecholamine secretion can be rigidly controlled (Trifaró et al., 1980; Kumakura et al., 1986). All cell types are capable of transporting proteins to the extra

cellular space via a vesicle-mediated constitutive secretory pathway (Tartakoff, 1978). Neural, endocrine and exocrine cells additionally possess a regulated secretory export pathway of hormones, neurotransmitters and enzymes (Tartakoff, 1978). For these systems, the main intracellular signal that triggers secretion is an increase in cytoplasmic Ca^{2+} (Douglas et al., 1961, 1982). The proteins that participate in Ca^{2+} -dependent exocytosis are still to be fully identified. Vesicle movement and fusion in the early steps of the secretion seem to involve a multitude of cytosolic and extrinsic membrane proteins; exocytosis itself might be even more complex (Rothman et al., 1992)

After obtaining the scinderin and various scinderin deletion constructs, they were cloned in pEGFP vector, in frame with the green fluorescent protein (GFP) and overexpressed in chromaffin cells as described in Materials and Methods. This was followed by the stimulation of chromaffin cells with either a depolarizing concentration of K^{+} or with 10 μM nicotine. The purpose of these experiments was to further understand the role of scinderin in secretion.

4.3.a. Effect of full Scinderin (Sc1-6) or of Sc1-2 deletion construct overexpression on high K^{+} - or nicotine – induced hGH release from chromaffin cells

Previous experiments in our laboratory used permeabilized chromaffin or human platelets (Zhang L et al., 1996; Marcu, M. et al., 1996) to study the function of recombinant full scinderin and various recombinant scinderin truncations. When digitonin permeabilized cells were incubated with full length recombinant scinderin and stimulated by 10 μM Ca^{2+} , the release of catecholamine increased in a concentration dependent manner (Zhang et al., 1996). Similarly, serotonin release from platelets was increased by

recombinant scinderin (Marcu et al., 1996; Rodriguez del Castillo, 1990). The potentiation of Ca^{2+} -evoked catecholamine release was due to an enhanced F-actin severing activity of scinderin as demonstrated by an increase in the number of cells displaying cortical F-actin disassembly (Zhang et al., 1996). Furthermore, the severing activity of recombinant full scinderin was determined by measuring F-actin gel low shear apparent viscosity using a ball viscosimeter (Marcu et al., 1998). The viscosity of actin gels was effectively decreased by the presence of recombinant Sc (Marcu et al., 1998). The hypothesis that scinderin controls F-actin disassembly and exocytosis is strengthened by the experiments with chromaffin cells overexpressing full length Sc. The results described here, show that chromaffin cells overexpressing full scinderin (Sc1-6) display a significant increase in hGH secretion upon high K^{+} - evoked depolarization, when compared to cells transfected with pEGFP vector alone (control). The potentiation of the high K^{+} - evoked depolarization by Sc1-6 overexpression was due to the enhanced F-actin severing activity of scinderin, as demonstrated by an increase in the number of cells displaying cortical F-actin disassembly in cells overexpressing Sc1-6. Similarly, the nicotine-induced hGH release from cells overexpressing Sc1-6 was greater than for control cells, and this was due to an increase in the number of cells displaying cortical F-actin disassembly compared to control cells. These experiments demonstrate that cortical F-actin disassembly and chromaffin cell exocytosis upon high K^{+} depolarization or nicotine receptor stimulation are mediated by scinderin activation.

Previous experiments in our laboratory have shown that when digitonin permeabilized platelets were incubated with recombinant Sc1-4,6 (a recombinant protein that is devoid of domain 5, the domain that comprises scinderin's nucleating activity) and stimulated

with 10 μM Ca^{2+} , the release of serotonin increased in a concentration-dependent manner (Marcu, M. et al., 1996). An additional proof in favor of F-actin disassembly mediating the response of recombinant scinderin, was the fact that increases in both neurotransmitter release and F-actin disassembly in chromaffin cells were inhibited by two recombinant peptides (ScABP1, ScABP2) with sequences corresponding to two actin binding sites of scinderin (Zhang L et al., 1996). Similarly, increases of serotonin release induced by recombinant full Sc or recombinant Sc1-4,6 was inhibited by ScABP1, ScABP2. Furthermore, the viscosity of actin gels was effectively decreased by the presence of recombinant Sc1-4,6 (Marcu, M. et al., 1998). Two of the actin binding sites of scinderin are in domains S1 and S2 of the molecule (Marcu M., et al., 1994). These are the F-actin severing domains of the protein and should be the domains responsible for the scinderin potentiation of Ca^{2+} induced release of catecholamines. This hypothesis is strengthened by the experiments presented in this thesis with chromaffin cells overexpressing Sc1-2. The results presented here show an increase in the high K^{+} -induced hGH release when compared to control cells. This potentiation of the hGH release was due to an enhanced F-actin disassembly as demonstrated by the increased number of cells displaying cortical F-actin disassembly.

4.3.b. Effect of Sc56, Sc5, ScL5 or ScABS3 deletion constructs overexpression on high K^{+} - or nicotine – induced hGH release from chromaffin cells

As described above, previous work done in our laboratory has identified and characterized a third actin binding site in domain 5 of Sc (Marcu et al., 1998). The Sc5-6 fragment of scinderin not only binds monomers of actin, but also, and similar to gelsolin

S4-6 (Way et al., 1989), is capable of nucleating actin assembly in a polymerization assay (Marcu et al. 1998). In this case Sc5-6 was as effective as recombinant full-length scinderin (r-Sc). However, ScL5-6 was ineffective in promoting nucleation (Marcu et al. 1998).

Viscosimetric analysis of actin gels showed that the decrease in viscosity produced by r-Sc was completely blocked in the presence of either recombinant Sc5-6 or peptide Sc-ABP3 (with amino acid sequence corresponding to the third actin-binding site) (Marcu et al. 1998). Moreover, in the presence of recombinant ScL5-6 (peptide containing the last 2 domains of Sc, but lacking the third actin binding site sequence), the ability of recombinant full scinderin to decrease the viscosity of actin gels was not affected. Similarly to the experiments described above, the ability of recombinant Sc to potentiate serotonin release in the presence of recombinant Sc5-6, ScABP3, and ScL5-6 was tested. When both recombinant Sc and Sc5-6 were present together in the incubation medium, the potentiation effect r-Sc of the Ca²⁺ induced release of serotonin was blocked by Sc5-6. Similarly, the potentiation effect r-Sc of the Ca²⁺ induced release of serotonin was blocked by ScABP3. On the other hand, ScL56 failed to block the potentiation effect r-Sc of the Ca²⁺ induced release of serotonin. These experiments suggest that scinderin, in addition to binding actin on sites present in domains 1 and 2, must bind actin on a third site in domain 5 to sever and nucleate actin effectively. An additional proof to support this hypothesis is provided by the experiments described in this thesis, where different Sc deletion constructs were overexpressed in chromaffin cells.

Thus, chromaffin cells overexpressing Sc5-6, Sc5 or only the third actin binding site (ScABS3) showed a decrease in hGH secretion upon high K⁺ - evoked depolarization

(Fig. 3.30, 3.32, 3.34), when compared to control cells (transfected with pEGFP vector alone). The inhibition of hGH release was due to an inhibition of F-actin disassembly as demonstrated by a decreased number of transfected cells displaying cortical F-actin disassembly (Fig. 3.20,e; 3.22,e and 3.24,e). Similarly, chromaffin cells overexpressing Sc5-6 showed a decreased nicotine-induced hGH release (Fig. 3.36) due to an inhibition of cortical F-actin disassembly (Fig. 3.26,e). Moreover, overexpression of ScL5 in chromaffin cells did not result in a significant difference in K⁺- induced hGH release (Fig. 3.33); and similarly, the number of transfected cells showing cortical F-actin disassembly was not different from that of control cells. These results demonstrate that the third actin-binding site of Sc is involved in the nucleation and polymerization of actin.

In summary, our results suggest that Sc controls the cortical F-actin network disassembly during exocytosis. Moreover, our results demonstrate that the F-actin severing domains of the protein are the first two domains corresponding to the two actin binding-sites of the protein. Furthermore, as described above, cells overexpressing ScABS3 or Sc constructs that comprise the third actin-binding site displayed a decreased stimulation-induced cortical F-actin disassembly and hGH secretion whereas cells overexpressing ScL5 (lacking the third actin binding site) did not show a significant difference when compared to control cells. This suggests the possibility that scinderin may act as a molecular switch during the secretory cycle. In conclusion, the experimental evidence discussed above indicates that the cortical F-actin network constitutes a barrier to the movement of secretory vesicles to release sites, and it must be locally disassembled to allow the translocation of the vesicles to the plasma membrane. Disassembly of cortical F-actin is

brought about by activation of Scinderin, a Ca^{2+} - dependent F-actin-severing protein present in secretory tissues.

**5 - SUMMARY OF CONTRIBUTIONS TO ORIGINAL
KNOWLEDGE**

1. A transient transfection method with high and reproducible transfection efficiency was developed for chromaffin cells. Our experiments demonstrate that this method allows the transient transfection of the cells with two different genes with co-transfection efficiency up to 90%.
2. Using a hGH reporter system for the regulated chromaffin secretory pathway, we developed a method to improve the hGH labeling of the chromaffin vesicles from the ready-to-release pool. This contributes to an increased hGH signal upon stimulation, providing a more precise methodology for the study of scinderin's role in regulated secretion.
3. Large amounts of Sc were transiently expressed in chromaffin cells. Sc overexpression in chromaffin cells permitted the study of its mechanism of action and its relevance in neurosecretion. The experiments discussed here clearly demonstrate that scinderin Sc controls the cortical F-actin network disassembly during exocytosis and is an important component of the exocytotic machinery.
4. A large number of Sc deletion constructs were also derived and overexpressed in chromaffin cells allowing the more revealing study of scinderin's mechanism of action. Our results show that during secretion the first two domains (actin binding sites 1 and 2) of scinderin are involved in F-actin severing. The last two domains (actin binding site 3) are responsible for actin nucleation and polymerization.
5. A structural analysis of scinderin was performed, based on the crystallographic model of the inhibited form (Ca²⁺-free) of gelsolin, taking into account the high degree of homology between the two proteins in regions necessary for actin regulation and their identity in sequence in regions necessary for calcium binding.

These observations allowed a better understanding of Sc function and its relation to other Ca^{2+} -dependent actin-severing proteins such as gelsolin and villin.

6 - REFERENCES

- Ampe, C., Vandekerchove, J. (1987). "The F-actin capping proteins of *Physarum polycephalum*: cap42 (a) is a very similar if not identical to fragmin and is structurally and functionally very homologous to gelsolin; cap42(b) is *Physarum* actin." EMBO J. 6: 4149-4157.
- Andre, E., Lottspeich, F., Schleicher, M., Noegel, A. (1988). "Severin, gelsolin and villin share a homologous sequence in regions presumed to contain F-actin severing domains." J. Biol. Chem. 263: 722-728.
- Armstrong, J., Thompson, N., Squire, J., H., Smith, J., Hayes, B., Solari, R. (1996). "Identification of a novel member of the Rab8 family from the rat basophilic leukaemia cell line, RBL.2H3." J. Cell Sci. 109: 1265-1274.
- Aunis, D., and Perrin, D. (1984). "Chromaffin granule membrane F-actin interactions and spectrin-like protein of subcellular organelles: a possible relationship." J. Neurochem 42: 1558-1565.
- Ausubel, F., M., Brent, R., Kingston, R., E., Moore, D., D., Seidman, J., G., Smith, J., A., Struhl, K., (1991). Current protocols in molecular biology. New York, Wiley interscience, New York.
- Bader, M.-F., Trifaró, J.-M., Langley, O., K., Thierse, D., and Aunis, D (1986). "Secretory cell actin-binding proteins: identification of a gelsolin-like protein in chromaffin cells." J. Cell. Biol. 102: 636-646.
- Baines, A. J., and Bennett, V (1985). "Synapsin I is a spectrin - like protein immunologically related to erythrocyte protein 4.1." Nature 315: 410-418.
- Baker, P., F., and Knight, D., E. (1981). "Calcium control of exocytosis and endocytosis in bovine chromaffin cells." Philos. Trans. R. Soc. Lond. 296: 83-103.
- Banks, P., and Helle, K. (1965). "The release of proteins from the stimulated adrenal medulla." Biochem. J. 97: 40-48.
- Benchimol, S., and Cantin, M. (1977). "Ultrastructural cytochemistry of the human adrenal medulla." Histochemistry 54: 9-14.
- Bennet, V. (1990). "Brain spectrin, a membrane associated protein related in structure and function to erythrocyte spectrin." Physiol. Rev. 70: 1029-1065.
- Blaschko, H., and Welsch A., D. (1953). "Localization of adrenaline in cytoplasmic particles of the bovine adrenal medulla." Arch. Exp. Pathol. Pharmacol. 219: 17-22.

- Blondel, O., Bell, G., I., Seino, S. (1995). "Inositol 1,4,5-triphosphate receptors, secretory granules and secretion in endocrine and neuroendocrine cells." TINS 18: 157-161.
- Bodwell, J., Swift, F., Richardson, J. (1999). "Long duration electroporation for achieving high level expression of glucocorticoid receptors in mammalian cell lines." J. of Steroid Biochem. and Mol. Biol. 68: 77-82.
- Bradford, M., M. (1976). "A rapid and sensitive method for the quantitation of microgram quantities of protein utilizing the principle of protein-dye binding." Anal Biochem 72: 248-254.
- Bretscher, A., and Weber, K (1980). "Villin: the major microfilament associated protein of the intestine microvillus." Proc. Natl. Acad. Sci USA 76: 2321-2325.
- Brooks, J., C. (1977). "The isolated bovine adrenomedullary chromaffin cell: a model of neuronal excitation-secretion." Endocrinology 101: 1369-1378.
- Bryan, J. (1988). "Gelsolin has 3 actin binding sites." J. Cell Biol. 106: 1553-1562.
- Burgoyne, R., D., and Cheek, T., R. (1987). "Reorganization of peripheral actin filaments as a prelude to exocytosis." Biosci. Rep. 7: 281-288.
- Burgoyne, R., D. (1991). "Control of exocytosis in adrenal chromaffin cells." Biochem. Biophys. Acta 1071: 174-202.
- Burgoyne, R., D., Cheek, T., R., and Norman, K., M. (1986). "Identification of a secretory granule-binding protein as caldesmon." Nature 319: 68-73.
- Burgoyne, R., D., Morgan, A., and O'Sullivan, A., J. (1989). "The control of cytoskeletal actin and exocytosis in intact and permeabilized adrenal chromaffin cells: role of calcium and protein kinase C." Cell. Signaling 1: 323-334.
- Burridge, K., Feramisco, J., R. (1988). "No-muscle α -actinins are calcium actin-binding proteins." Nature 294: 565-567.
- Burtnick, L., D., Koepf, E., K., Grimes, J., Jones, E., y., Stuart, D., I., McLaughlin, P., J., Robinson, R., C. (1997). "The crystal structure of plasma gelsolin: implications for actin severing, capping, and nucleation." Cell: 661-670.
- Carmichael, S., W. (1982). Secretory mechanisms in adrenal medulla. St. Albans, Eden Press.
- Chang, A., C., and Brenner, D., G. (1988). Focus 10: 66.

- Chaponnier, C., Janmey, P., Yin, H. (1986). "The actin filament severing domain of plasma gelsolin." J. Cell Biol. 103: 1473-1481.
- Cheek, T., R., and Burgoyne, R., D. (1991). Cytoskeleton in secretion and neurotransmitter release. The neuronal cytoskeleton. R. Burgoyne, D.: pp. 309-329.
- Cheek, T., R., and Burgoyne, R., D. (1986). "Nicotine-evoked disassembly of cortical actin filaments in adrenal chromaffin cells." FEBS letters 207: 110-114.
- Cheek, T., R., and Burgoyne, R., D. (1987). "cAMP inhibits both nicotine-induced actin disassembly and catecholamine secretion from bovine adrenal chromaffin cells." J. Biol. Chem. 262: 11663-11666.
- Cheek, T., R., Jackson, T., R., O'Sullivan, A., J., Moreton, R., B., and Burgoyne, R., D. (1989). "Simultaneous measurements of cytosolic calcium and secretion in single bovine adrenal chromaffin cells by fluorescent imaging of Fura-2 in co-cultured cells." J. Cell Biol. 109: 1219-1227.
- Chomczynski, P., Sacchi, N. (1987). "Single-step method of RNA isolation by acid guanidinium thiocyanate-phenol-chloroform extraction." Anal. Biochem. 162: 156-159.
- Chu, G., Hayakawa H, Berg P. (1987). "Electroporation for the efficient transfection of mammalian cells with DNA." Nucleic Acids Res 11: 1311-1326.
- Chu, G., Sharp, P.,A. (1981). "SV40 DNA transfection of cells in suspension: analysis of efficiency of transcription and translation of T-antigen." Gene 13: 197-202.
- Coupland, R., E., (1989). "The natural history of chromaffin cell." Arch. Histol. Cytol. 52(331-342).
- Craig, S., W., and Pollard, T., D. (1982). "Actin-binding proteins." TIBS 75: 88-92.
- Darnell, J., Lodish, H., Baltimore, D., (1990). Molecular cell biology, Scientific american books.
- DeCamili, P., and Greengard, P (1986). "Synapsin I: a synaptic vesicle - associated neuronal phosphoprotein." Biochem. Pharmacol. 35: 4349-4354.
- DeQuatro, V. (1979). Anatomy and biochemistry of the sympathetic nervous system. Endocrinology. J. In DeGroot L. New York. 2: 1241.
- Doucet, J.-P., Trifaro, J.-M. (1988). "A discontinuous and highly porous sodium dodecyl sulfate-polyacrylamide slab gel system of high resolution." Anal Biochem 168: 265-271.

- Douglas, W., W., and Rubin, R. P. (1961). "The role of calcium in the secretory response of the adrenal medulla to acetylcholine." J. Physiol. (London) 159: 40-48.
- Douglas, W., W., Kanno, T., and Sampson, S., R. (1967). "Effects of acetylcholine and other medullary secretagogues and antagonists on the membrane potentials of adrenal chromaffin cells: an analysis employing techniques of tissue culture." J. Physiol. London 188: 107-120.
- Douglas, W., W., Nemeth, E., F. (1982). "On the calcium receptor activating exocytosis." J. Physiol. (London) 323: 229-234.
- Dunn, L., A., Holz, R., W. (1982). "Catecholamine secretion by digitonin treated adrenal medullary chromaffin cells." J. Biol. Chem. 258: 4989-4993.
- Eberhard, D., A., and Holz, R., W. (1987). "Colinergic stimulation of inositol phosphate formation in bovine adrenal chromaffin cells: distinct nicotinic and muscarinic mechanisms." J. Neurochem. 49: 1634-1643.
- Eranko, O. (1955). "Distribution of the fluorescent islets, adrenaline and noradrenaline in the adrenal medulla of the hamster." Acta. Endocrinol. 18: 174-182.
- exocytosis." J. Biol. Chem. 262: 16671-16676.
- Faultich, H., Zobeley, S., Rinnerthaler, G., Small, J., V. (1988). "Fluorescent phallotoxins as probes for filamentous actin." J. Muscle Res. Cell Motil. 9: 370-383.
- Felgner, P., L., Gadek, T., R., Holm, M., Roman, R., Chan, H., W., Wenz, M., Northrop, J., P., Ringold, G., M., Danielsen, M. (1987). "Lipofection: a highly efficient, lipid-mediated DNA-transfection procedure." Proc Natl Acad Sci U S A 84: 7413-7417.
- Fujita, T. (1977). "Concept of paraneurons." Arch. Histol. Jpn. 40: 1-12.
- Glanz, J. (1997). "Force carrying web pervades living cells." Science 276: 678-679.
- Gorman, C., E., Gies, D., R., and McCray, G. (1991). DNA Protein Eng. Tech. 2: 3-10.
- Graham, F. L. a. A. J. V. D. E. (1973). "A new technique for the assay of infectivity of human adenovirus 5 DNA." Virology 52: 456-467.
- Greengard, p., Valtorta, F., Czernik, A., J., and Benfenati, F. (1993). "Synaptic vesicle phosphoproteins and regulation of synaptic function." Science 259: 780-785.
- Gumbiner, B., Kelly, R., B., (1982). "Two distinct intracellular pathways transport secretory and membrane glycoproteins to the surface of pituitary tumor cells." Cell 28: 51-62.
- Guyton C., A. (1987). Basic neuroscience. Philadelphia.

- Haycock, J., Greengard, P., and Browning, M., D. (1988). "Cholinergic regulation of protein III phosphorylation in bovine adrenal chromaffin cells." J. Neurosci. 8: 3233-3239.
- Herlant, M. (1964). "The cells of the adenohypophysis and their functional significance." Int. Rev. Cytol. 17: 299-382.
- Hillarp, N., A., and Hofcelt, B. (1953). "Evidence of adrenaline and noradrenaline in separate adrenal medullary cells." Acta. Physiol. Scand. 30: 55-68.
- Hirokawa, N. (1991). Molecular architecture and dynamics of the neuronal cytoskeleton.
The neuronal cytoskeleton. R. Burgoyne, D.: p. 5-74.
- Hochman, J., and Perlman, R., L. (1976). "Catecholamine secretion by isolated adrenal cells." Biochem. Biophys. Acta 421: 168-175.
- Holz, W., R., Senter, R., A., Uhler, M., D. (1995). "Investigation by transient transfection of the effects on regulated exocytosis of Rab3a." Methods in enzymology 257: 221-231.
- Huber, R., Schneider, M., Mayr, J., Romisch, J., Paques, E., P. (1990). "The calcium binding sites in human annexin V by crystal structure analysis at 2.0 Å resolution." FEBS letters 275: 15-24.
- Huxley, H., E., (1963). "Electron microscope studies on the structure of natural and synthetic protein filaments from striate muscle." J. Mol. Biol. 7: 281-308.
- Ito, S., Mochizuki, O., N., Hori, K., Ozaki, K., Myiakawa, A., Negishi, M. (1991). "Characterization of prostaglandin E-2 induced calcium mobilization in single bovine adrenal chromaffin cells by digital image microscopy." J. neurochem. 56: 531-540.
- Janmey, P. A., Stossel, T., P. (1987). "Modulation of gelsolin function by phosphatidylinositol 4,5-biphosphate." Nature 325: 3714-3723.
- Janmey, P., A., Lamb, J., Allen, P., G., Matsudaira, P., T. (1992). "Phosphoinositide binding peptides derived from the sequences of gelsolin and villin." J. Biol. Chem. 267: 11818-11823.
- Jokush, B., M., Burger, M., M., Daprada., M., Richard., J., G., Chaponnier, C., Gabbiani, G. (1977). "Alpha-actinin attached to membranes of secretory vesicles." Nature 270: 628-629.
- Keese W.K., P., T., L., Coupland R., E. (1988). "The innervation of the adrenal gland." J. Anatomy 157: 33-41.

- Kelly, R., B. (1993). "Storage and release of neurotransmitters." Cell 72: 43-53.
- Kelner, K., Morita K, Rossen JS, Pollard HB. (1986). "Restricted diffusion of tyrosine hydroxylase and phenylethanolamine N-methyltransferase from digitonin-permeabilized adrenal chromaffin cells." Proc Natl Acad Sci U S A 83: 2998-3002.
- Kinosita, K. J., Tsong TY. (1977). "Voltage-induced pore formation and hemolysis of human erythrocytes." Bioch. Biophys. Acta 471: 227-242.
- Knight, D., E., and Baker, P., F., (1982). "Calcium dependence of catecholamine release from bovine adrenal chromaffin cells after exposure to intense electric fields." J. Membr. Biol. 68: 107-140.
- Kobayashi S., a. C. R., E. (1977). "Two populations of microvesicles in the SGC cells of the mouse adrenal medulla." Arch. Histol. Jpn. 40: 251-259.
- Kohn, A. (1902). "Das chromaffine Gewebe." Ergebnisse Anat. Entwickl. 12: 253-267.
- Kumakura, K., Ohara, M., Sato, G. (1986). "Real-time monitoring of the secretory function of adrenal chromaffin cells." J. Neurochem 46: 1851-1858.
- Kwiatkowski, D., Janmey, P. A., Yin, H., L. (1989). "Identification of critical functional and regulatory domains in gelsolin."
- Landsberg, L., Young, J., B. (1980). Catecholamines and the adrenal medulla. Philadelphia.
- Lassing, I., Lindberg, U. (1988). "Specific interactions between phosphatidylinositol 4,5- biphosphate and profilactin." Nature 314: 472-474.
- Lazarides, E., Lindberg U. (1974). "Actin is the naturally occurring inhibitor of DNase I." Proc. Natl. Acad. Sci USA 71: 4742-4746.
- Lee, R., W., H., and Trifaró, J.-M. (1981). "Characterization of anti-actin antibodies and their use in immunocytochemical studies on the localization of actin in adrenal chromaffin cells." Neuroscience 6: 2087-2108.
- Lee, W., M., Galbraith, R., M. (1992). "The extracellular actin scavenger system and actin toxicity." new Engl. J. Med. 326: 1335-1341.
- Lelkes, P., i., Friedman, J., E., Rosenheck, K., Oplatka, A. (1986). "Destabilization of actin filaments as a requirement for the secretion of catecholamines from permeabilized chromaffin cells." FEBS letters 208: 357-363.

- Lesczynskyn, D., J., Jankovski, J., A., Viveros, O., H., Diliberto, E., M., Neur, J., A., Wightman, R., M. (1990). "Nicotinic receptor mediated chromaffin cell secretion from individual chromaffin cells." J. Biol. Chem. 265: 14736-14737.
- Llinas, R., Sugimori, M, and Silver, R. (1992). "Microdomains of high calcium concentration in a presynaptic terminal." Science 256: 677-679.
- Lopez, M., G., Villarroya M., Lara, B., Sierra, M., R., Albillos, A., Garcia, G., A., Gandia, L. (1994). "Q and L-type Ca²⁺ channels dominate the control of secretion ion bovine chromaffin cells." FEBS Letters 349: 331-337.
- Lueck, A., Yin, H., L., Kwiatkowski, D., J. and Allen, P. G (2000). "Calcium regulation of gelsolin and adseverin: a natural test for the helix latch hypothesis." Biochemistry 39: 5274-5279.
- Maekawa, S., and Sakai, S., (1990). "Inhibition of actin regulatory activity of the 74 kDa protein from bovine adrenal medulla (adseverin) by some phospholipid." J. Biol. Chem. 265: 10940-10942.
- Marcu, G., M., Zhang, L., Elzagallaai, A., Trifaró, J.-M. (1998). "Localization by segmental deletion analysis and functional characterization of a third actin binding site in domain 5 of scinderin." J. Biol. Chem. 273: 3661-3668.
- Marcu, G., M., Zhang, L.,Rodriguez del Castillo, A., Trifaró, J.-M. (1994). "Molecular cloning and functional expression of chromaffin cell scinderin indicates that it belongs to the family of Calcium-dependent F-actin severing proteins." Mol. Cell. Biochem. 141: 153-165.
- Marcu, M., G., Zhang, L., Staudt, K., and Trifaró, J.-M. (1996). "Recombinant scinderin, an F-actin severing protein, increases calcium-induced release of serotonin from permeabilized platelets, an effect blocked by two scinderin-derived actin binding peptides and phosphatidylinositol 4,5-biphosphate." Blood 78: 20-24.
- Maruyama, K., Ebashi, S (1965). "F-actinin, a new structural protein from striated muscle. II Action of actin." J. biochem. 58: 13-19.
- Matsudaira, P., and Janmey, P. (1988). "Pieces in the actin-severing protein puzzle." Cell 54: 139-140.
- McLaughlin, P. J., Gooch, J., T., Mannherz, H., H., Weeds, A., G. (1993). "Structure of gelsolin segment I-actin complex and the mechanism of filament severing." Nature 364: 685-692.
- Meldrum, R., A., Bowl, M., Ong, S. B., Richardson, S. (1999). "Optimization of electroporation for biochemical experiments in live cells." Bioch. Biophys. Res. Commun. 256: 235-239.

- Nagel, D. (1886). "Über die struktur der nebennieren." Arch. Anat. Physiol. Wissen Med Verlag., Berlin, p.63.
- Nathan, M., Mertz, L., and Fox, D. (1995). "Optimizing Long RT-PCR." Focus 17: 78.
- Navone, F., Digioia, D., Nonomura, Y., (1994). "Differential expression of bovine adseverin in adrenal gland revealed by in situ hybridiztion." J. Biol. Chem. 269: 5890-5896.
- Neher, E., and Marty, A. (1982). "Discrete changes in the cell membrane capacitance observed under conditions of enhanced secretion in bovine adrenal chromaffin cells." Proc. Natl. Acad. Sci USA 79: 6712-6716.
- Neher, E., and Zucker, R., S. (1993). "Multiple calcium-dependent processes related to secretion in bovine chromaffin cells." Neuron 10: 21-30.
- Nordmann, J., J. (1984). "Combined stereological and assay analysis of storage and release of catecholamines in the adrenal medulla of the rat." J. Neurochem 42(434-440).
- O'Sullivan, A., J., Cheek, T., R., Moreton, R., B., Berridge, M., J., Burgoyne, R., D. (1988). "Localization and heterogeneity of agonist-induced changes in cytosolic calcium in bovine adrenal chromaffin cells from video imaging of fura-2." EMBO J. 8: 401-411.
- Pearse, A. G. E. (1969). "The cytochemistry and ultrastructure of polypeptide hormone binding cells of the APUD series and the embryologic, physiologic and pathologic implications of the concept." J. Histochem. Cytochem 17: 303-313.
- Perrin, D., and Aunis, D. (1985). "Reorganization of α -fodrin induced by stimulation of secretory cells." Nature 315: 589-592.
- Pope, B., Way, M., Weeds, A., G. (1991). "Two of the three actin binding domains of gelsolin bind to the same subdomain of actin." FEBS letters 280: 70-74.
- Potter, H. (1992). Protocols for using electroporation to stably or transiently transfect mammalian cells. Guide to electroporation and electrofusion. D. Chang, C., Chassy, J., A., Sanders, A., E., Sowers, A., E. San Diego, Academic press Inc.: 457-463.
- Prentice F., D., and Wood J., G. (1985). "Adrenergic innervation of cat adrenal medulla." Anat. Rec. 181: 689-703.
- Pringault, E., Arpin, M., Garcia, A., Finidori, J., and Louvard, D. (1986). "A human villin cDNA clone to investigate the differentiation of intestinal and kidney cells in vivo and in culture." EMBO J. 5: 3119-3124.

- Ravazzola, M., Halban, P., A., Orci, L. (1996). "Inositol 1,4,5-triphosphate receptor subtype 3 in pancreatic islet cell secretory granules revisited." Proc. Natl. Acad. Sci USA 93: 2745-2748.
- Rhee, S., G., Suh, P., G., Ryu, S., H., and Sang, Y., L. (1989). "Studies of inositol phospholipid-specific Phospholipase C." Science 244: 546-550.
- Rodriguez Del Castillo, A., Lemaire, S., Tchakarov, L., Jeyapragasan, M., Doucet, J., P., Vitale, M., L., and Trifaró, J., M. (1990). "Chromaffin cell scinderin: a novel calcium-dependent actin-filament severing protein." EMBO (Eur. Mol. Biol. Organ.) J. 9: 43-52.
- Rodriguez Del Castillo, A., Vitale, M., L., Tchakarov, L. and Trifaró J.-M. (1992). "Calcium and pH determine the interaction of chromaffin cell scinderin with phosphatidylserine and phosphatidylinositol 4,5-biphosphate and its cellular distribution during nicotinic-receptor stimulation and protein kinase C activation." J. Cell. Biol. 119: 797-810.
- Rodriguez Del Castillo, A., Vitale, M., L., Tchakarov, L. and Trifaró J.-M. (1992). "Human platelets contain scinderin, a calcium dependent actin filament-severing protein." Thromb. haemost. 67: 248-251.
- Rothman, J., E., and Orci, L. (1992). "Molecular dissection of the secretory pathway." Nature 355: 409-415.
- Runger-Brandle, E., Gabbiani, G., (1983). "Role of cytoskeletal and cytocontractile elements in pathologic processes." Amer. J. Pathol. 110: 361-383.
- Sambrook, J., Fritsch, E.F., Maniatis, T. (1989). Molecular Cloning: A Laboratory Manual, Cold Spring Harbor.
- Sanes, J. R. J. N. J. (1986). "Use of a recombinant retrovirus to study post-implantation cell lineage in mouse embryos." EMBO J. 5: 3133-3142.
- Sanger, F., S. Nicklen, and A.R. Coulson. (1977). "DNA sequencing with chain-terminating inhibitors." Proc. Natl. Acad. Sci 73: 3418.
- Sarafian, T. A. D. B. M. (1986). "Loss of proteins from digitonin-permeabilized adrenal chromaffin cells essential for
- Scangos, G., Ruddle FH (1981). "Mechanisms and applications of DNA-mediated gene transfer in mammalian cells - a review." Gene 14: 1-10.
- Schafer, T., Karli, U., O., Gratwohl, E., K., Schweizer, E., F., and Burger, M., M. (1987). "Digitonin-permeabilized cells are exocytosis competent." J. Neurochem 49: 1696-1707.

- Schweitzer, E., Kelly RB (1985). "Selective packaging of human growth hormone into synaptic vesicles in a rat neuronal (PC12) cell line." J. Cell. Biol. 101: 667-676.
- Searle, P., F., Stuart, G., W., and Palmiter, R., D. (1985). "Building a metal-responsive promoter with synthetic elements." Mol. Cell Biol. 5: 1480-1488.
- Selden, R., F., Burke Howie, K., Rowe, M., E., Goodman, H., M., and Moore, D., D. (1986). "Human growth hormone as a reporter gene in regulation studies employing transient gene expression." Mol. Cell Biol. 6: 3173-3179.
- Smith, D., B., and Johnson, K., S., (1988). "Single-step purification of polypeptides expressed in E. coli as fusions with glutathione S-transferase." Gene 67: 31-40.
- Sobue, K. (1988). "Caldesmon regulates myosin in smooth and non-muscle tissues." J. Cell. Biochem. 37: 317-321.
- Sontag, J., M., Aunis, D., Bader, M.-F. (1988). "Peripheral actin filaments control calcium-mediated catecholamine release from streptolysin O-permeabilized chromaffin cells." Eur. J. Cell Biol. 46: 316-326.
- Stossel, T., P., Chaponnier, C., Exxel, R., Hartwig, J., H., Janmey, P., A., Kwiatkowski, D., J., Lind., S., E., Smith, D., B., Southwick, F., S., and Yin, H., L. (1985). "Non-muscle actin binding proteins." Ann. Rev. Cell Biol. 1(353-402).
- Tartakoff, A., m., Vassali, P., Detraz, M. (1978). "Comparative studies of intracellular transport of secretory proteins." J. Cell Biol. 79: 694-705.
- Tchakarov, L., Vitale, M., L., Jeyapragasan, M., Rodriguez Del Castillo, A., and Trifaró, J.-M. (1990). "Expression of scinderin, an actin filament-severing protein in different tissues." FEBS letters 268: 209-212.
- Tellam, R., L., Morton, D., J., Clarke, F., M. (1989). "A common theme in the amino acid sequences of actin and many actin-binding proteins." TIBS 14: 130-133.
- Trifaró, J.-M. (1977). "Common mechanisms of hormone secretion." Annu. Rev. Pharmacol. Toxicol. 17: 27-47.
- Trifaró, J.-M., and Lee, R., H., W. (1980). "Morphological characteristics and stimulus secretion coupling in bovine adrenal chromaffine cell cultures." Neuroscience 5: 1533-1546.
- Trifaró, J.-M., and Poisner, A., M. (1982). Common properties in the mechanisms of synthesis, processing and storage of secretory products. The secretory process. A. Poisner, M., and Trifaró, J.-M. New York, Elsevier/North Holland. 1: pp. 387-407.

- Trifaró, J.-M., and Vitale, M., L. (1993). "Cytoskeleton dynamics during neurotransmitter release." TINS 16: 466-471.
- Trifaró, J.-M., Bader, M.-F., and Doucet j.-P. (1985). "Chromaffin cell cytoskeleton: its possible role in secretion." Can. J. Biochem. Cell Biol. 63: 661-669.
- Trifaró, J.-M., Duerr, A., C., Pinto, J., E., B. (1976). "Membranes of the adrenal medulla: a comparison between the membranes of the Golgi apparatus and chromaffin granules." Mol. Pharmacol. 12: 536-545.
- Trifaró, J.-M., Kenigsberg, R., L., Côté, A., Lee, R., W., H., and hikita, R. (1984). "Adrenal paraneuron contractile proteins and stimulus - secretion coupling." Can. J. Physiol. Pharmacol. 62: 493-501.
- Trifaró, J.-M., Novas, M., L., Fournier, S., Rodriguez Del Castillo, A (1989). Cellular and molecular mechanisms in hormone and neurotransmitter secretion. Recent advances in pharmacology and therapeutics. M. VVelasco, Israel, A., Romero, E., Silva, H., Elsevier Publishing: 15-19.
- Trifaró, J.-M., Rodriguez del Castillo, A., Vitale, M., L (1992). "Dynamic changes in chromaffin cell cytoskeleton as prelude to exocytosis." Mol. Neurobiol. 6: 339-346.
- Trifaró, J.-M., Rosé, S., D., Marcu, M., G. (2000). "Scinderin, a calcium-dependent actin filament severing protein that controls cortical actin network dynamics during secretion." Neurochem. Res. 25: 133-144.
- Trifaró, J.-M., Zhang, L., Marcu, M., G. (1998). Molecular and cellular mechanisms in neurotransmitter release. Pain Mechanism and Management. S. Ayrapetyan, N., Apkarian, A., V, IOS Press.
- Unsiker, K. (1976). Comparative ultrastructural aslects of adrenal chromaffin cells in reptiles. Amsterdam, Elsevier Scientific Press.
- Vitale, M., L., Rodriguez Del Castillo, A, and Trifaró, J.-M. (1992). "Loss of calcium-dependent retention of scinderin in digitonin-permeabilized chromaffin cells: correlation with calcium-evoked catecholamine release." J. Neurochem 59: 1717-1728.
- Vitale. M., L., Rodriguez Del Castillo, a., Tchakarov, L., and Trifaró, J.-M. (1992). "Loss and calcium dependent retention of scinderin in digitonin-permeabilized chromaffin cells: corelation with calcium-evoked catecholamine release." J. Neurochem 59: 1717-1728.
- Vitale, M., L., Rodriguez del Castillo, A., Tchakarov, L., and Trifaró, J.-M., (1991). "Cortical filamentous actin disassembly and scinderin redistribution during chromaffin cell stimulation precede exocytosis, a phenomenon not exhibit by gelsolin." J. Cell Biol. 113: 1057-1067.

- Vitale, M., L., Seward, E., P., and Trifaró, J.-M., (1995). "Chromaffin cell cortical actin network dynamics control the size of the release-ready vesicle pool and the initial rate of exocytosis." Neuron 14: 353-363.
- Viveros, D., H., Argueros, L., kirshner, N. (1968). "Release of catecholamines and dopamine α -oxidase from the adrenal medulla." Life. Sci. 7: 609-614.
- Way, M., Gooch, J., Pope, B., and Weeds, A (1989). "Expression of human plasma gelsolin in *E. coli* and dissection of actin binding sites by segmental deletion mutagenesis." J. Cell Biol. 109: 593-605.
- Way, M., Weeds, A (1988). "Nucleotide sequence of pig plasma gelsolin. Comparison of protein sequence with human gelsolin and other actin severing proteins shows strong homologies and evidence for large internal repeats." J. Mol. Biol. 203: 1127-1133.
- Waymire, J., C., Bennett, W.,F., Boehme. R., Hankins, L., Gilmer-Waymire, K., Haycock, J.,W. (1983). "Bovine adrenal chromaffin cells: high-yield purification and viability in suspension culture." Journal of Neuroscience Methods 7: 329-351.
- Westfall, B., Sitaraman, K., Beringer, M. and Mertz, L. (1994). "ELONGASE® Reagents for Amplification of Long DNA Templates." FOCUS 17: 62.
- Wick, P., F., Senter, R., A., Parsels, L., A., Uhler, M., D., Holz, W (1993). "Transient transfection studies of secretion in bovine chromaffin cells and PC12 cells." J. Biol. Chem. 268: 10983-10989.
- Wigler, M., Pellicer A, Silverstein S, Axel R. (1978). "Biochemical transfer of single-copy eucaryotic genes using total cellular DNA as donor." Cell 14: 725-731.
- Wilson, S., P., and Kirshner, N. (1983). "Calcium-evoked secretion from digitonin-permeabilized adrenal medullary chromaffin cells." J. Biol. Chem. 258: 4994-5000.
- Wilson, S., P., Liu, F., Wilson, R., E., and Housley, P., R. (1995). "Optimization of calcium phosphate transfection for bovine chromaffin cells: relationship to calcium phosphate precipitate formation." Anal. Biochem. 226: 212-220.
- Wong, T., K., Neumann, E. (1982). "Electric field mediated gene transfer." Biochem. Biophys. Res. Commun. 107: 584-7.
- Yeasting, R., A. (1986). Selected morphological aspects of human suprarenal glands. The adrenal gland. P. Mulrow, J. New York, Elsevier: p.418.
- Yin, H., Albrecht, J., H, and Fattoum, A. (1981). "Identification of gelsolin, a calcium-dependent regulatory protein of actin gel-sol transformation and its intracellular distribution in a variety of cells and tissues." J. Cell Biol. 19: 901-906.

Yin, H., and Stossel, T., P. (1979). "Control of cytoplasmic actin gel-sol transformation by gelsolin, a calcium-dependent regulatory protein." Nature 281: 583-586.

Yin, H., L., Iida, K., Janmey, P., A., (1988). "Identification of a polyphosphoinositide-modulated domain of gelsolin which binds to the sides of actin filaments." J. Cell Biol. 106: 805-812.

Yoo, S.-H., and Albanesi, J., P. (1990). "Inositol 1,4,5,-triphosphate - triggered Ca²⁺ release from bovine chromaffin adrenal medullary secretory vesicles." J. Biol. Chem. 265: 13446-13448.

Yu, F., X., and Albanesi, J., P. (1992). "Inositol 1,4,5-triphosphate-triggered calcium release from bovine chromaffin medullary secretory vesicles." J. Biol. Chem. 265: 13446-13448.

Zhang L., M., M., G., Nau-Staudt, K., and Trifaró, J.-M. (1996). "Recombinant scinderin enhances exocytosis, an effect blocked by two scinderin-derived actin-binding peptides and PIP 2." Neuron 17: 287-296.

Zucker, R., S., (1996). "Exocytosis: a molecular and physiological perspective." Neuron 17: 1049-1055.